Analysis/Development of a Crash Sensing Algorithm

Using Multiple Accelerometers

by

Fon-Jui Tsai

Submitted to the Department of Electrical Engineering and Computer Science

in Partial Fulfillment of the Requirements for the Degrees of

Bachelor of Science in Electrical Engineering and Computer Science

and Master of Engineering in Electrical Engineering and Computer Science

at the Massachusetts Institute of Technology

May 23, 1997

[June 1997]

Author_____
Department of Electrical Engineering and Computer Science
May 23, 1997

Certified by_____
Martin Schmidt
Thesis Supervisor

Accepted by_____
Authur C. Smith
Chairman, Department Committee on Graduate Theses

Analysis/Development of a Crash Sensing Algorithm

Using Multiple Accelerometers

by

Fon-Jui Tsai

Submitted to the

Department of Electrical Engineering and Computer Science

May 23, 1997

in Partial Fulfillment of the Requirements for the Degrees of
Bachelor of Science in Electrical Engineering and Computer Science
and Master of Engineering in Electrical Engineering and Computer Science

ABSTRACT

Single-point, multi-directional crash sensing is a relatively new concept in collision detection, and there remain many question which today's research and study have not been able to answer. The objective of the thesis is to analyze and understand the benefits of using multiple accelerometers placed in multiple directions and, furthermore, to measure the effectiveness and the applicability of the multi-axes crash sensing algorithm. The results indicate that the ability to detect high speed angle collisions is greatly enhanced when lateral and vertical signals are used. The study also finds that the additional information provided by lateral and vertical signals only slightly enhance the ability to detect severe pole collisions. In addition, the lateral and the vertical information alone cannot successfully categorize the collisions; the longitudinal signals must be used to filter the rough road and other long-duration events.

Thesis Supervisor: Martin Schmidt
Title: Associate Professor of Electrical Engineering

Table of Contents

Chapter 1

1. ABSTRACT

Single-point, multi-directional crash sensing is a relatively new concept in collision detection, and there remain many question which today's research and study have not been able to answer. The objective of the thesis is to analyze and understand the benefits of using multiple accelerometers placed in multiple directions and, furthermore, to measure the effectiveness and the applicability of the multi-axes crash sensing algorithm. The results indicate that the ability to detect high speed angle collisions is greatly enhanced when lateral and vertical signals are used. The study also finds that the additional information provided by lateral and vertical signals only slightly enhance the ability to detect severe pole collisions. In addition, the lateral and the vertical information alone cannot successfully categorize the collisions; the longitudinal signals must be used to filter the rough road and other long-duration events.

Chapter 2

2. OBJECTIVE

Currently in the SIR (Supplementary Inflatable Restraint, i.e. the airbag) algorithm, the severity of the crash and the deployment of the airbag are determined by calculations and analysis of a single accelerometer aligned in the front-rear directions (referred to as the longitudinal direction hereafter). However, some European and Japanese car makers are experimenting and, in some cases, already using multiple accelerometer inputs to determine the severity of the crash. The objective of this project is to investigate the benefits of using multiple accelerometers in the crash sensing, and furthermore, develop a feasible implementation and algorithm which utilize multiple accelerometer inputs. This project is to focus on cases in which several accelerometers are packed closely in space such that they can be approximated to originate from a single point. However, the orientation of these accelerometers corresponds to the longitudinal, the lateral, the vertical, or other arbitrary axis relative to the vehicle. The scope of the thesis includes analyzing raw crash data, creating a functional algorithm, generating a algorithm model which is tested through extensive simulation.

Chapter 3

3. BACKGROUND

3.1. Industry Standards in Airbag Technology

Supplementary Inflatable Restraint (SIR) systems, or airbags, are becoming standard equipment on most cars and light trucks sold today. In the past, the predominant crash sensing system was a multi-point sensing system in which the deployment decision is based on crash sensors placed at strategic locations in the vehicle. However, the industry trend has since been toward a single-point crash sensing system[1].

The inflatable restraint system design considerations can be divided into three areas: vehicle system, electronic diagnostic module, and crash sensors.

3.1.1. System

In a deployment event, the inflatable restraint system functions in less than 100 milliseconds[2]. The effectiveness of the system is determined by the rate and the state of the deployment at given time during the crash event. The inflatable restraint system which includes the inflator and bag assembly, diagnostic module, crash and safing sensors, is designed to perform with respect to other subsystems of the vehicle, such as the vehicle structure, steering control system, instrument panel, seat belts, and the seats. The inter-relationship between these subsystems must be considered in order to optimally protect the occupant in a collision[3].

3.1.2. Electronic Diagnostic Module

The diagnostics module and sensors play a critical role in the overall effectiveness of the SIR. The module must be well designed in the sensing technology to ensure the accuracy of the deployment, as well as in robustness in order to sustain long life under severe environmental conditions. In addition, to ensure the safety critical nature of the system, a diagnostic module is used to continuously monitor the firing circuits and provides driver warning. Furthermore, a redundant energy source is crucial since the battery may be cut off in a severe collision[4].

3.1.3. Sensors

The system considerations in the design of a crash sensor include the number of sensors needed and the operational logic in the sensing system. In addition, the locations and the directions of these sensors are significant Essentially, the goal of an ideal sensing design and algorithm is to maximize the ability to differentiate deploy crash events from the non-deploy crash events while still providing timely

deployment. In addition, the sensor design must be flexible to allow transferring from one vehicle platform to another[5]. It is the sensing considerations which are explored in this thesis.

3.2. Efforts in Using Multiple Accelerometers

In most of the vehicles equipped with the airbags today, the crash sensing algorithm uses only the longitudinal signals to determine the severity of the crashes[6]. Although some car makers are experimenting with using multiple accelerometers in multiple directions, the concepts are still relatively new.

Toyota Motors of Japan has patented the concept of using the longitudinal and the lateral acceleration vectors to determine the angle of the collision. The actuation of the airbag is determined by comparing the magnitude of the crash signals to a set of predetermined thresholds based on the calculated angle of impact. Because the angle of impact cannot be accurately determined, the calculation categorizes the angle into one of the 10 groups: ±15°, ±30°, ±45°, ±60°, and ±75°. The thresholds used for comparison are stored in a large look-up table[7].

Daewoo Electronics extended the above idea to incorporate the vertical signal in the crash sensing algorithm. Specifically, the algorithm proposed by Daewoo is aimed at discriminating between oblique (angle), frontal barrier, and center pole collision. The deployment decision is based on the thresholds placed on the velocity signals in all three directions. Daewoo claims that the angle collisions can be easily detected with the lateral velocity signal. Furthermore, the vertical velocity can be used to effectively detect the pole collisions[8].

Lastly, algorithm engineers from Schrobenhausen, Germany also believed in a crash sensing by determining the angle of the impact. In a patent filed jointly by several engineers, the proposed method of determining the angle is to use dual accelerometers placed at $\pm\theta$ from the longitudinal axis or the direction of travel. By resolving these two vectors using cosine law, the angle of the collision can be better determined. The magnitude of the resolved vector is compared to the variable threshold which is based on the calculated angle[9].

While these patents outline the crash sensing concepts, very little detail is disclosed. Part of the objective of this thesis is to duplicate the experimentation and the results described in these patents.

3.3. Current Single-Axis Crash Sensing Algorithm

The analysis of the single-axis crash sensing algorithm is based on a current production version developed by a large automotive electronics firm. The algorithm arrives at the deployment decision based on calculations and analysis of the vehicle's longitudinal acceleration, velocity, and displacement. Prior to discussing the algorithm with multiple accelerometer inputs, it is essential to explore and understand the functionality of the basic single-axis algorithm which uses only the longitudinal accelerometer input.

The deployment logic of the current production algorithm is based on the idea of classifying the severity of the crashes into different categories. Each of these categories represents a crash scenario in which the airbag must deploy. For example, a category, or a "mode" as they are sometimes referred to, may be used to catch the high severity events on time and act as back-up mode of deployment for less severe deployment events. Moreover, other modes can be set to discriminate threshold, angle, and offset barrier events. Lastly, another mode can be designed to detect events that are of longer duration, and the examples include poles, some angle, and lower speed threshold frontal events.

The basis of the algorithm details how the collisions are classified into separate categories. Specifically, the collisions are classified based on the behavior of the longitudinal acceleration. There are different traits associated with the acceleration signals of different types of crashes, and these traits are best identified using the threshold tests. A threshold test is exactly what the name suggests: a certain flag is set when the signal exceeds a preset level. Of course, the behavior of the acceleration signal is not the only criteria tested. The velocity (integration the acceleration) and the displacement (integration of the velocity) are two other measures which can provide valuable information. Consequently, many threshold tests are used to evaluate and classify the collisions, and in most cases, a collection of threshold tests have

to pass in order for the algorithm to conclude if the severity of the collision requires the deployment of the airbag.

Until now, the word "threshold" has been used loosely to mean a preset level which, when it is crossed, can correctly categorize the severity of the crashes. These thresholds are either based on or derived from the acceleration, the velocity, and the displacement of the vehicle in a crash. First of all, the fundamental thresholds are the acceleration, the velocity, and the displacement, which are compared against the acceleration, the velocity, and the displacement of the vehicle. Next set of thresholds examines the behaviors of the acceleration, the velocity, and the displacement. Lastly, some thresholds are time-dependent. Specifically, these threshold tests require that the signal crosses a preset level for a finite period of time. These time-dependent threshold tests can be used to separate cases which the signal has crossed the thresholds briefly due to noise or other factors and fall below the thresholds immediately after. In conclusion, the categories, or the modes, of collisions are no more than a combination of different threshold tests. When a set of threshold tests is exceeded, the collision can then be categorized into respective modes.

The deploy logic of the current crash-detection algorithm can be summarized in the following logic diagram.

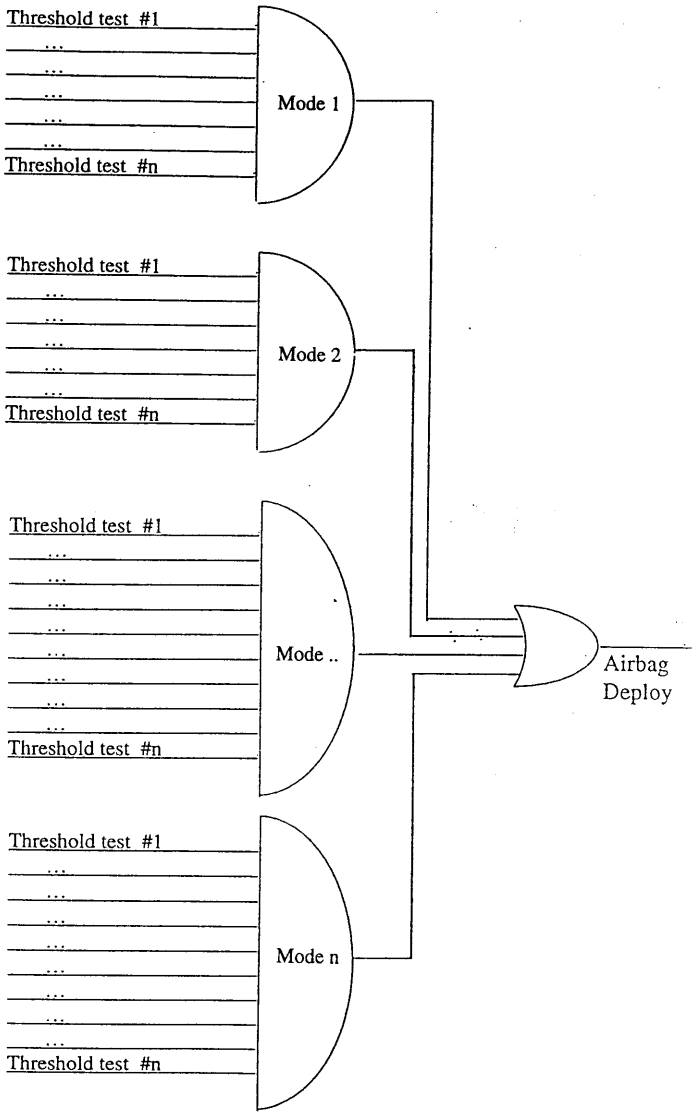

Deployment Logic of the Current Production Algorithm

Figure 1: Deploy Logic of the Single-Axis Algorithm

A possible limitation of the current production algorithm is that only the longitudinal signals are used in the decision making process. This may be adequate for the moment, but some European and Japanese car makers are beginning to experiment with the idea of incorporating accelerometer inputs in both the lateral and the vertical axis into the crash sensing algorithm. Furthermore, Daewoo Electronics

Co. has recently patented the idea that it is possible to accurately categorize the different types of crashes using tri-axial accelerometer inputs[10]. Realizing the potential in this methodology, this thesis is to investigate the benefits and the shortcomings of using multiple-axis acceleration inputs in crash sensing.

Chapter 4

4. SCOPE

The idea of the single-point, multiple-axis crash sensing algorithm is certainly not unheard of in the airbag industry. Research has been done in this area by almost all the major leaders in the automobile industry, and in fact, there are several existing patents focusing on this methodology[11]. As a whole, however, the development of the single-point, multiple-accelerometer algorithm is still relatively new, and there remains room for expansion. The following lists some of the algorithms which have previously been considered but not fully explored. Furthermore, the following also includes the new approaches to the algorithm which are examined in detail. The study of these algorithms and the results discovered constitutes the main bulk of the thesis.

4.1. Independent Threshold Method Contrasted with Correlation Method

The first step of the algorithm analysis is to examine the lateral signals, and in the course of study, try to establish the correlation between the longitudinal and the lateral signals. From the previous studies and experiences, the current production algorithm exploits the information contained in the longitudinal signals. Using this knowledge as the foundation, the lateral signals can be used to facilitate the current algorithm by strengthening the areas which are weak in the current algorithm. A specific area may be the angle collisions. Because the vehicle makes contact with the barrier at an offset angle, the longitudinal acceleration of the vehicle is weaker. However, the lateral signal may be able to provide additional information. Following is a comparison of the lateral velocity between a 30-mph frontal collision and a 30-mph angle collision (the car collides with the barrier at a 30° angle).

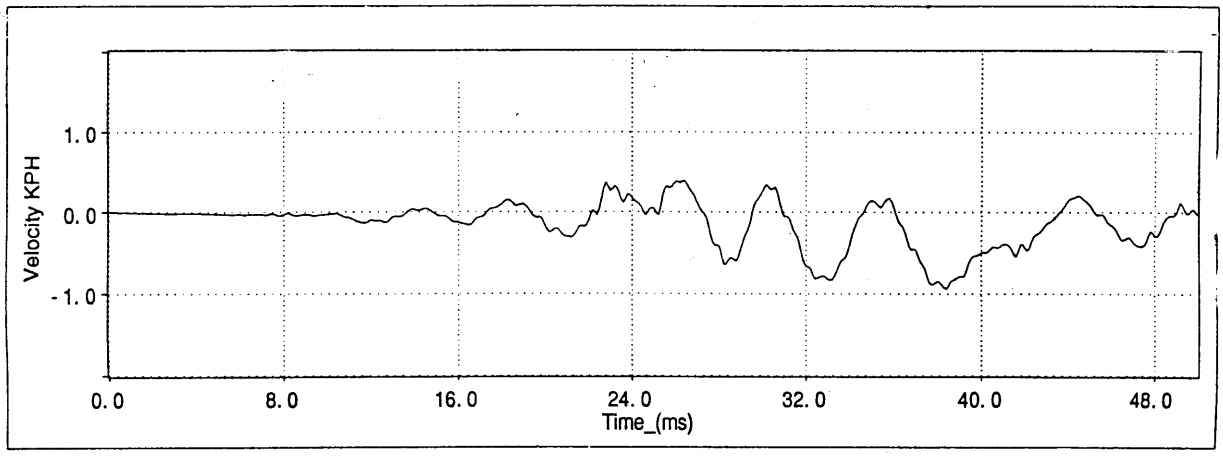

Lateral velocity of a 30 MPH frontal collision

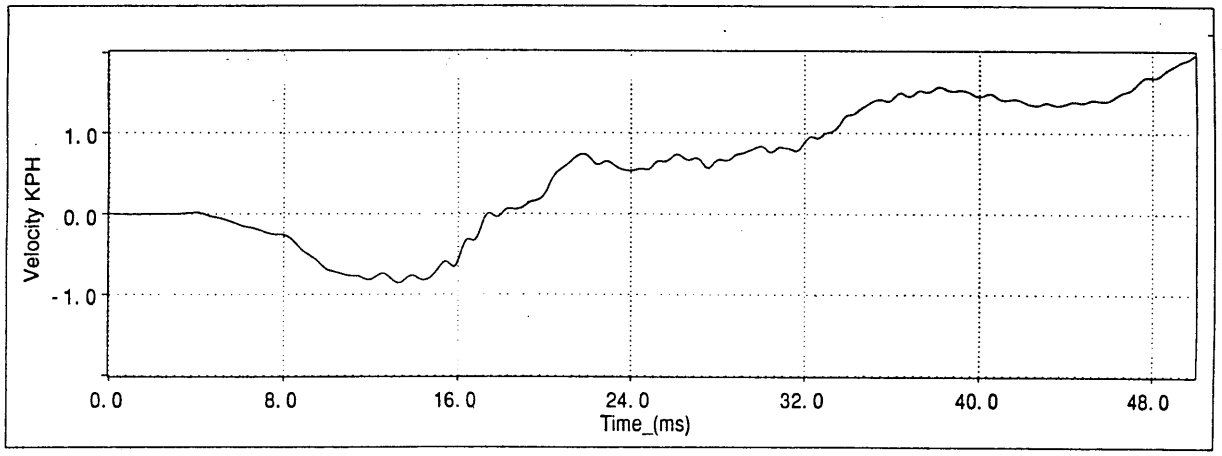

Lateral velocity of a 30 MPH angle collision (barrier offset at 30 degrees)

Figure 2: Lateral Velocity - 30-mph Frontal Collision vs. 30-mph Angle Collision

The initial glance suggests that these signals are discernible, but there are several aspects which must be studied in depth. First of all, are the above signals representative of all the other crashes of the similar type? Second, is the "dip" in the velocity as shown in the bottom graph a characteristic of all the 30 MPH angle collisions, and what does this dip represent? Furthermore, do the magnitudes of the lateral signals remain essentially unchanged across vehicle platforms? Last and the most important of all, is there a correlation between the longitudinal and the lateral signals? The answers to these questions can essentially lead to two possible algorithms. First, if the longitudinal and the lateral signals are not correlated, the two signals can be examined separately to arrive at the deployment decision. Specifically, two sets of thresholds are used for the longitudinal and the lateral signals, and the airbag is deployed

when both sets of thresholds are exceeded. However, if there is indeed a correlation between the longitudinal and the lateral signals, an algorithm can derive the deployment decision by manipulating both the longitudinal and the lateral signals. One such approach is to use the magnitude of one signal to adjust the thresholds and the decision making process of the other signal[12]. For example, let us assume that the longitudinal and the lateral signals are found to be inversely proportional to each other, an increase in the lateral signal allows the longitudinal thresholds to be lowered proportionally. These two algorithms are the ideal starting points because they will establish the foundation of the multiple accelerometer, multiple-axis sensing algorithm.

The second algorithm described above provides some interesting issues to explore. If there is indeed a correlation between the longitudinal and the lateral signals, can the angle of the collision be accurately determined? If the angle of the collision cannot be accurately determined, can this angle be roughly estimated? Lastly, if the angle can be determined, either accurately derived or roughly estimated, how can this information be used most effectively?

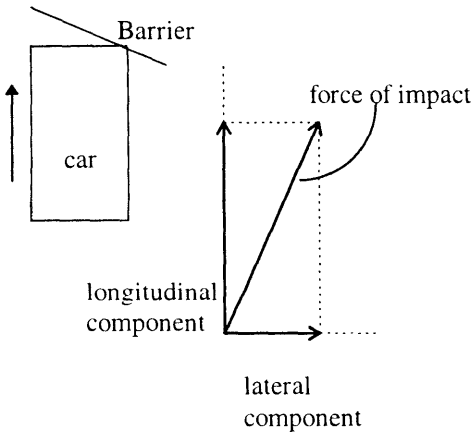

Figure 3: Forces of an Angle Collision

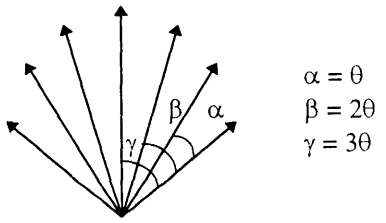

Figure 4: Categories of the Impact Angle

Figure 3 above suggests that if the impact of the collision is at an offset angle, this impact force can be resolved into the longitudinal and the lateral components. Naturally, this is a rough estimate of the

forces involved in an actual collision. For example, this force diagram assumes that the shear force between the vehicle and the barrier is small and thus can be ignored. Assuming this rough characterization is accurate, is it possible that the angle of collision can be resolved by geometrically manipulating the longitudinal and the lateral signals. If so, how accurately can the angle be determined? Furthermore, if the angle can only be estimated, is it possible to categorize the ranges of the angle such as shown in figure 4?

While the lateral signals may provide useful information in the cases of angle collisions, the vertical signals may also provide fresh insights. In a recently published patent, Daewoo claims that the vertical signals can be used to detect a pole collision[13]. Therefore, part of this thesis is to be devoted to determining if the vertical signals can be used to enhance the algorithm. However, if the algorithm does incorporate the vertical signals, the robustness of the algorithm must be thoroughly tested against the rough road tests† .

4.2. Rotated-Axis Method

Thus far, the algorithms assume that the orientations of the accelerometers corresponds to the tri-axial orientations of the vehicle. The next step is to explore the possibility of placing the accelerometers at arbitrary orientations. Following is one such example.

† Rough road tests are standard tests which the vehicle with limited or no shocks is subjected to treacherous off-road conditions, and these conditions include the potholes, chatterbumps, railroad crossing, and the vertical drops.

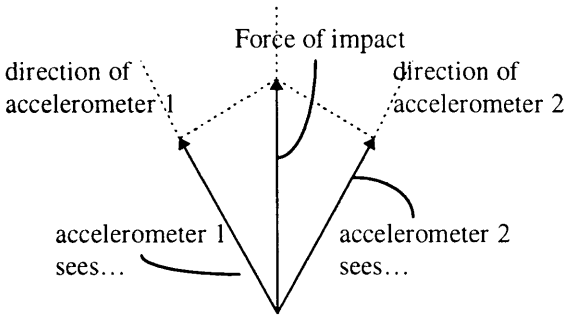

Figure 5: Offset Accelerometers - Long. Force

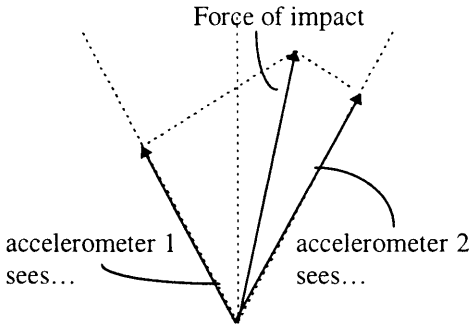

Figure 6: Offset Accelerometers - Offset Force

In the above case, two accelerometers are placed at the same offset angle from the longitudinal axis. If the force of impact is along the longitudinal axis of the vehicle, both accelerometers must have the same reading (figure 5). This may seem redundant and wasteful at first, but if the force of impact is at an offset angle relative to the longitudinal axis, the reading of one accelerometer is greater than the other. The analysis is carried out using the data from the accelerometer with higher readings. The advantage of this algorithm is that it has the potential to represent the magnitude of the crash signal more accurately than if the accelerometer is placed along the longitudinal axis (figure 7). Due to the noisy nature of the acceleration signal, the overall effects of the noise can be lessened if the magnitude of the signal is the greatest. However, this is only true when the arbitrary angle corresponds closely to the angle of impact. As in the case portrayed in figure 8, the acceleration signals from the offset accelerometers are actually worse representations of the actual crash signals. In addition to examining the signals from these two accelerometers separately, there may be methods which these signals can be resolved to provide more information.

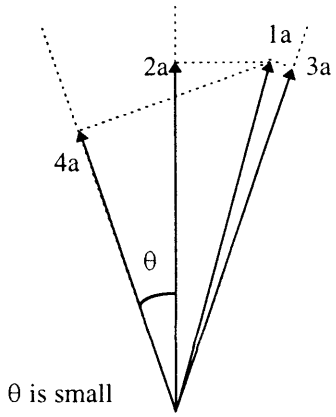

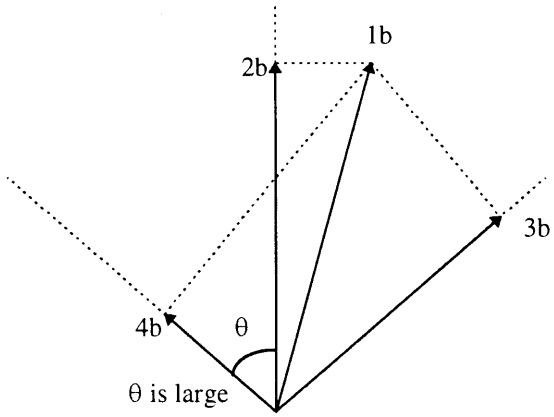

1a = force of impact = 1b
2a = longitudinal component = 2b
3a = accelerometer #2 component = 3b
4a = accelerometer #1 component = 4b

Figure 7: Offset Forces Evaluated by Offset Accelerometers - θ is small

Figure 8: Offset Force Evaluated by Offset Accelerometers - θ is large

Chapter 5

5. PROCEDURE

5.1. Examine the Raw Crash Data

5.1.1. Primary characteristics

The primary characteristics are criteria used to assess the severity of the collisions. These are the essential characterizations in the decision process of the deployment of the airbag.

5.1.1.1. *Acceleration*

Acceleration is the primary crash signal since all others measures (velocity, displacement, etc.) are derived from it. The acceleration signals are collected by placing three accelerometers in longitudinal, lateral, and vertical directions near where the crash sensing module is located, and the focus of the analysis is on the lateral and the vertical accelerations. Using electronic sensors, the acceleration is sampled and digitized at high enough frequency to not affect the analysis.

There are several criteria one can use to analyze the acceleration signal. First of all, the slope of the acceleration can be used to detect unusually large changes in the acceleration signal. The jerk, or the delta acceleration, is calculated by taking the acceleration from the current time and subtract from it the previous acceleration value. However, the instantaneous jerk may not have much practical value because of the oscillatory nature of the acceleration signal. The alternative is to calculate jerk by taking the difference in the acceleration of two points which are separated by some time. The technique used to filter the jerk signal is discussed in the later section.

In addition, the magnitude of the acceleration can be used to classify the severity of the crash. By establishing a minimum acceleration threshold, the severity is based on whether the acceleration exceeds a certain G threshold.

Lastly, the oscillation of the acceleration signal may provide valuable information. In a severe collision, the acceleration signal shows a significant oscillatory motion or characteristics. While some of the oscillation is filtered out through the initial low-pass filtering, it remains an important criteria which must not be ignored.

5.1.1.2. *Velocity*

Velocity is derived by integrating the acceleration signal. The velocity is the integration of the raw acceleration signal and not the filtered acceleration signal which was calculated and used only for analysis purpose.

The criteria used to analyze velocity is similar to those used to analyze the acceleration. First of all, the magnitude of the velocity is a useful criteria to determine the severity of the collision. It is

important to note that the velocity threshold must be absolute because, in some cases, the velocity can either be positive or negative. For example, in an angle collision, the vehicle is just as likely to crash into a barrier from the left side as from the right side, and therefore the magnitude of the lateral velocity tends to either positive or negative to reflect the direction of the impact. In addition, there may be characteristics which are most pronounced in the velocity domain. The lateral velocities of the high-speed full frontal collision and that of the high-speed angle collision are very good examples. The lateral acceleration of a high-speed full frontal collision has a tendency to be oscillatory with the magnitude of the filtered signal varying from -10 G to +10 G. On the contrary, the lateral acceleration of the high-speed angle collision is less oscillatory with the magnitude varying from -5 G to +5 G. However, once the acceleration signals are integrated, a very clear distinction can be drawn. The high-speed frontal collision shows a lateral velocity which is much weaker and oscillates along the x-axis. The high-speed angle collision, however, has a strong lateral velocity which reflects the direction of the impact. This is a characteristic not visible in the acceleration signals of the collisions.

5.1.1.3. *Displacement*

The displacement is obtained by integrating the velocity signal. Because the displacement is the double integration of the original acceleration signal, some sharper features may be lost in the signals. Therefore, the overall significance of the displacement signal may be limited. In general, the displacement signals are smoother and reacts to disturbances (sharp drops or increases and peaks in the acceleration signal) slowly. Therefore, the displacement is usually used to analyze the overall magnitude of the collisions and not for distinct pattern recognition and comparison. Furthermore, studies have shown that in a high severity collision, the relative displacement of the vehicle is a good approximation of the motion of the driver's body under the free-body assumptions[14].

5.1.1.4. *Averaged Slope*

The slope of a signal is a good indication of how the signal is changing over time. It may seem unnecessary to calculate the slope since the slope of the velocity is the *acceleration,* and the slope of the

displacement is the *velocity*, two criteria which have been discussed and examined. One reason is that the slope of the acceleration, also known as jerk, must be explicitly calculated. Since the acceleration is the original raw signal, how it changes over time can provide very useful information. However, the instantaneous slope signal is very noisy and oscillatory (figure 9).

Because the instantaneous slope is noisy, filtering techniques can be applied. One such technique is to generate the slope signal by convolving the instantaneous slope signal with a "box car". In other words, the current slope value is the average of the previous n samples. As n increases, the signal becomes smoother. However, at the same time, some degree of precision is lost as n increases. In addition, instead of finding the instantaneous slope values and perform the average, a more efficient approach is to calculate the slope value by finding the difference between the current value of the signal and that which is n samples back. However, this operation requires memory space of size n. Following is an example which includes the original signal of data, the instantaneous slope, and the filtered slope where n is equal to five.

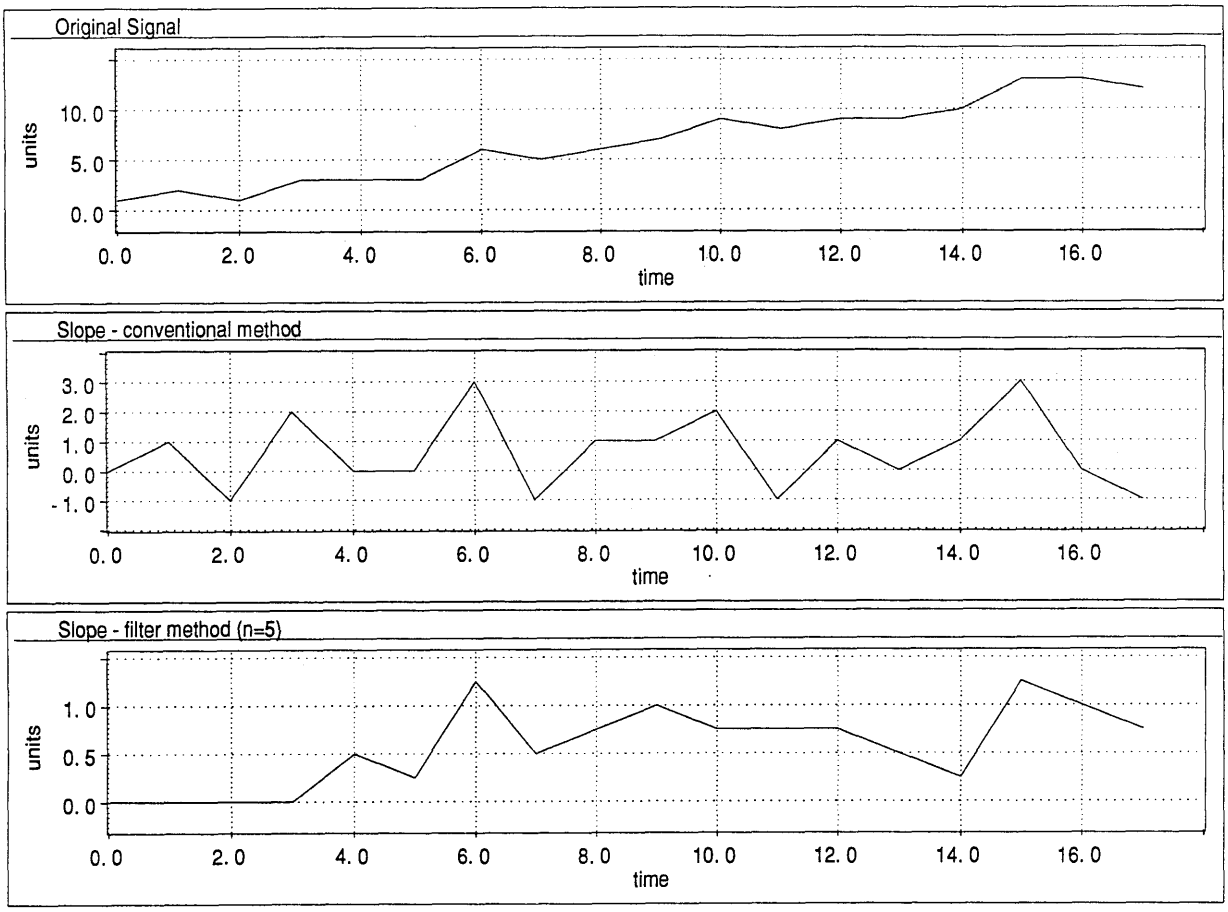

Figure 9: Methods of Calculating Slope

5.1.1.5. *Energy Indicator*

Energy is a more complicated criteria for two reasons: it encompasses a wide scope, and the optimal method to calculate the energy is difficult to determine. The conventional definition of the amount of energy of a moving object is

$$KineticEnergy = \frac{1}{2}mv^2$$

The definition claims that the kinetic energy of a moving vehicle is proportional to the square of the velocity of the vehicle. As the speed increases, the kinetic energy grows with respect to v^2. This may not be the most ideal definition of energy because it depends heavily on the measure of velocity. Since the magnitude of the velocity signal is small in the initial stage of the crash, this velocity-dependent energy measurement may not be an ideal discriminating criteria.

Another energy indicator is the rectified energy. The rectified energy is defined below.

$$\text{Re}\,ctifiedEnergy = \int |OriginalSignal|$$

The rectified energy is derived by integrating the rectified signal which is the absolute value of the original signal. Specifically, the rectified energy can be represented by the integrated rectified acceleration and the integrated rectified velocity. These measures are defined below.

$$Integrated\ \text{Re}\,ctifiedAcceleration = \int |OriginalAcceleration|$$
$$Integrated\ \text{Re}\,ctifiedVelocity = \int |OriginalVelocity|$$

The integrated rectified acceleration is the integration of the absolute acceleration signal and the integrated rectified velocity is the integration of the absolute velocity signal. These measures are useful when the acceleration signal tends to zero over a long period of time. For example, when the movement of the vehicle, regardless of the direction, consists mostly of the "back-and-forth" motion, the velocity and displacement tends to zero over time. Consequently, the kinetic energy dissipated is low in the initial stage of the crash. However, the strength of this "back-and-forth" motion may be a key in determining the severity of the collision. This consideration can not be clearly represented using the original definition of the kinetic energy. However, by using the new approach and first rectifying the acceleration or the velocity signal, portions of the original signal, which by normal integration would have been canceled, can now enforce each other. This is shown more clearly in the figure below (figure 10).

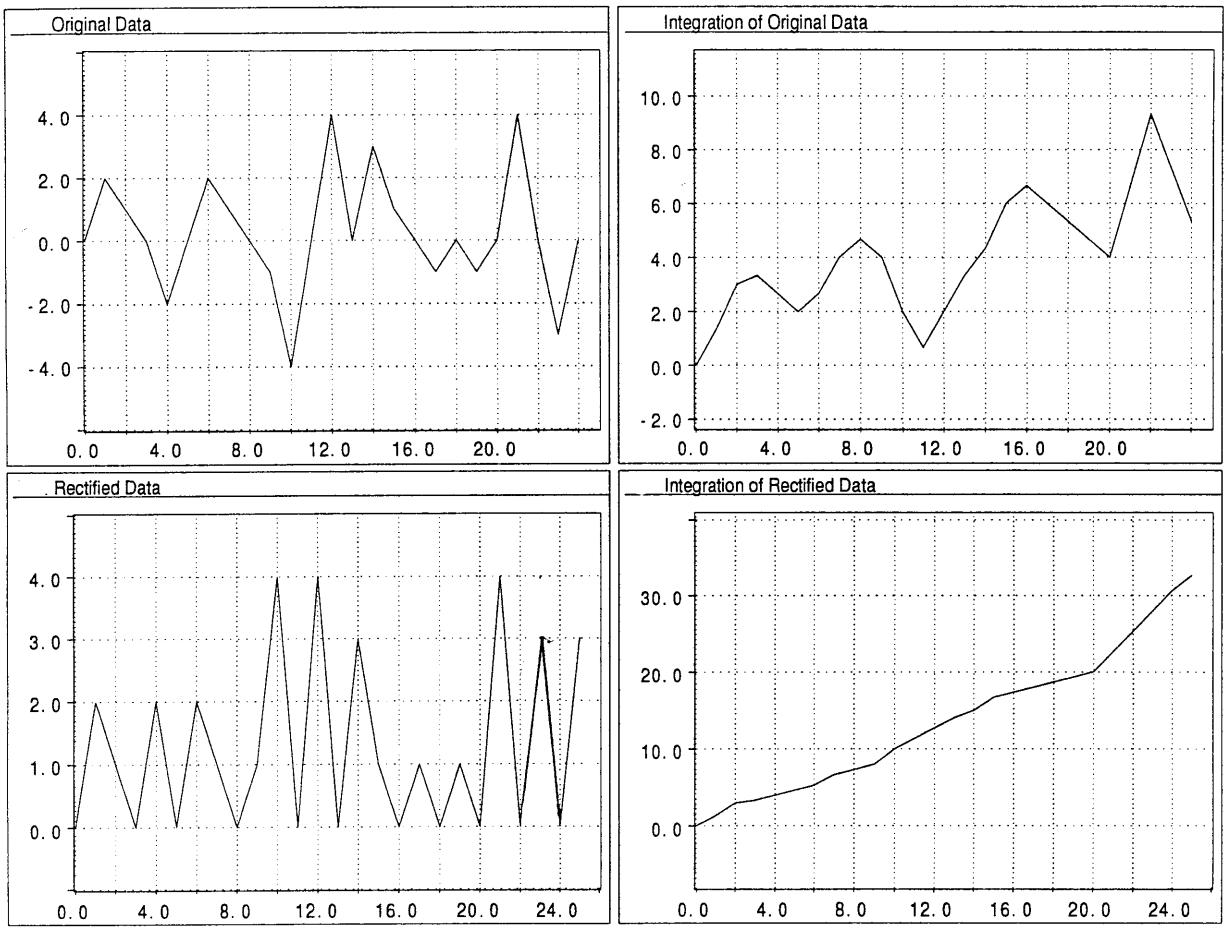

Figure 10: Rectified Energy Calculation – Justification for Using the Rectified Signal

In addition to examining the rectified energy measure in longitudinal, lateral, and vertical directions separately, another criteria is to combine the rectified energy measures from some or all directions. Furthermore, there are several ways to combine the rectified energy measures from different directions. For example, it may be useful to combine the three rectified energy components using a variable ratio. The ratio depends on the relationship between the different rectified energy components.

5.1.2. Secondary characteristics

Secondary characteristics are criteria used to monitor the progress of the collision. While the primary characteristics are used to measure the severity of the collision and to classify the types of collisions, the secondary characteristics are used to monitor the progression of the collision. These are characteristics used to determine if the collision exists and, if the collision is detected, evaluate and monitor the progression of the collision.

5.1.2.1. *Algorithm Enable*

Algorithm Enable is a frequently overlooked criteria. With the enable signal, the algorithm knows when the collision has begun. It is a challenging criterion to satisfy because of the implications. For example, if the enabling thresholds are set low, the algorithm is more likely to detect the start of a collision. However, the algorithm may be enabled by typical rough road events, mild disturbances (i.e. external forces applied on the vehicle such as the door slamming), or the inherent noise in the signal. In contrast, if the thresholds are set high, it serves as a natural filter to the non-deployment events. At the same time, the probability is higher that the start of the collision is not detected on time, or it may not be detected at all.

Detecting the start of the collision is important for thresholds which are time-dependent. Although it is undesirable to use time-dependent variables because of the complications and the possible lack of repeatability, it is unavoidable in some cases. In determining the severity of the collision, there are criteria which are effective during a certain time interval after the collision has started. This may be because the thresholds hold true only during a certain period of time after the collision has begun. Furthermore, assuming that decay is not introduced into the signal, most upward-sloping signals will cross a fixed threshold when given enough time. Therefore, the accuracy of when the thresholds start and stop is crucial. Finally, there may be cases where the initial period immediately after impact contains useful information. In such cases, detecting the start of the collision accurately is critical.

The enable signal can be asserted by using the acceleration signal. If the acceleration exceeds a certain level, the algorithm is to be enabled. The question is in which direction should the acceleration be used to assess and enable the algorithm? In the original algorithm, only the longitudinal acceleration signal is available for evaluation. Given the lateral and the vertical acceleration signals, can they be used to help assess when the collision has begun? In addition to the acceleration, are there other available criteria which can help better determine the start of a collision? The answers to these questions defines the algorithm.

5.1.2.2. *Collision Progression*

Once the collision has been detected, one of the following two scenarios will happen: the triggering conditions of the airbag are met and the airbag is deployed, or the triggering conditions are not met and the algorithm resets to the initial state. Therefore, there must be a criteria used to monitor if the collision is still in progress.

This collision progression marker can be set using several criteria. First of all, a minimum acceleration threshold can be used to monitor the severity of the crash signal. If the acceleration falls below a threshold consistently, it is implied that the collision is either a non-deploy event or that the algorithm was enabled unnecessarily. Instead of only keeping track of the present acceleration level, there is a danger in resetting the algorithm when the acceleration signal has a region of very low acceleration. Therefore, the history of the signal may also play a role in the collision progression marker.

Another possible scenario which makes the collision progression marker a crucial factor is in the detection of the collisions which are near the threshold level. In most of these collisions, the collision progression marker must prevent the algorithm from resetting due to the low acceleration input. If the reset does take place, the more severe section of the later acceleration signal may likely enable the algorithm again. By this time, the time dependent threshold can no longer accurately determine the start of the collision and the thresholds are no longer applicable. This problem is commonly known as the shift in the enable, and tracking the progression of a collision becomes a very difficult process.

5.2. Construction of the Algorithm

Once all the criteria are gathered, an algorithm is built using these criteria as the fundamental building blocks. The algorithm will be tested using simulation tools.

The essential skeleton of the algorithm is as the following:

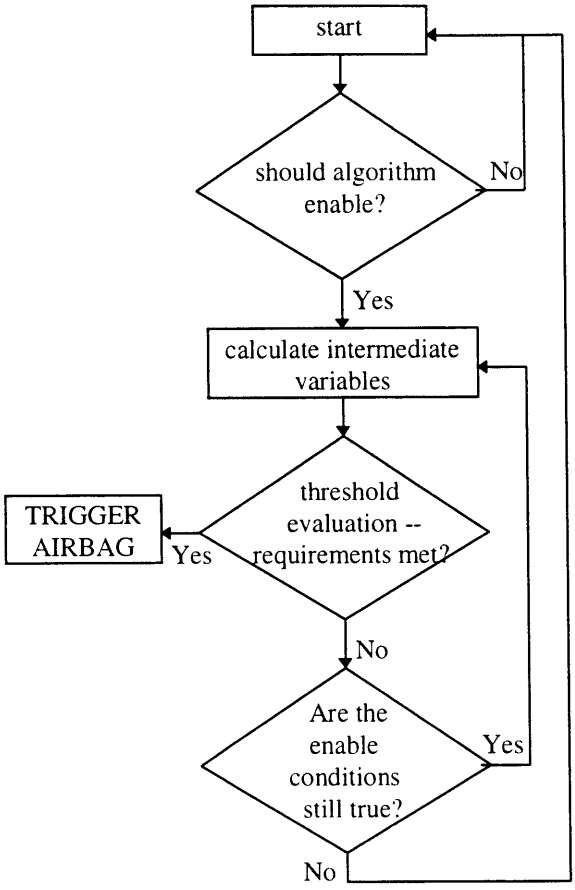

Figure 11: Flow Chart of the Algorithm

The algorithm first calculates and checks the enable signal. This is an indication of whether the a collision is occurring. If the enable signal is not asserted, the algorithm repeats the process by capturing and evaluating the next point. Once the collision has been detected, the algorithm is enabled and the main loop of evaluations starts.

Next, the intermediate values are calculated. These values include velocity, displacement, slope, energy, and more. There are other additional criteria including the rough road measures, the collision progression marker, and any other criteria which are used to assess the severity of the collision. Furthermore, these criteria are calculated in all three directions, unless there are cases in which these

criteria are unnecessary. For criteria such as the combined rectified energy, it becomes necessary to first calculate variables in each direction and combined using a fixed ratio.

Once all the intermediate values are calculated, they are compared against a set of calibrated thresholds. These thresholds are specially calibrated based on the platform of the vehicle. Since there may be 10-20 different criteria used, there are a few ways to derive the deployment decision based on these multiple criteria. First of all, the deployment decision can be based on crossing *all* of the thresholds simultaneously. This is a very stringent condition which is aimed at eliminating unnecessary deployment of the airbag. However, there is always the possibility that not all of the criteria are met, even in a severe collision. Furthermore, in order to ensure all the criteria are met in a deploy event, the thresholds of the criteria have to be set at low levels. The thresholds must be kept low or else there is a risk that one of the thresholds is not crossed. Therefore, another approach is to allow the deployment decision to be based on only a fixed number of criteria which must cross the respective thresholds simultaneously. For example, instead of requiring all n thresholds are exceeded simultaneously, the deployment is valid if only $(n-1)$ separate thresholds are crossed. This allows more leeway in calibrating the thresholds. However, as fewer thresholds are required to deploy the airbag, the repeatability and the validity of the algorithm begins to suffer. Another variation of this approach is to arbitrarily weigh the criteria used in the decision process. In other words, each criteria is assigned a number reflecting it's importance. At the end of the evaluation, the importance values of all the criteria which crossed the thresholds are added. The deployment decision will be based on the value of this final "score". This new extension serves one very important purpose. It introduces intelligence by allowing the algorithm to pick and choose which criteria are needed for the deployment decision. However, there are also drawbacks. Certain criteria may be *essential* for the deployment decision, and therefore these criteria must be given very high weight such that the deployment is not possible unless these criteria are met.

Once the evaluation process is complete, the algorithm either asserts a deploy signal or it returns the control to the top of the algorithm and evaluates the next point. However, before the algorithm evaluates the next point, it first must check to see if the collision is still in progress. The collision progression measure is used to determine if the collision is still in progress. If the measure indicates that

the collision is still in progress, the algorithm fetches the next point and recalculate the intermediate variables. If the collision progression measure falls below the threshold, the control is returned to the top of the algorithm where it begins to look for the algorithm enable condition.

5.3. Performance Evaluation

5.3.1. Crash data

The crash data used for the evaluation is acceleration data from the actual vehicle crashes done at the vehicle test facility. In these controlled crashes, accelerometers are mounted on various locations of the vehicle to record the acceleration signals. For simplicity, the evaluation will be based on the acceleration signal collected from the accelerometers mounted near where the crash sensing module is placed. Furthermore, the crash data is obtained from a single platform of vehicle for reasons of consistency.

The categories of the crashes used for this evaluation are the following:

Full-frontal collisions:

- the vehicle is crashed into a non-deformable flat barrier at zero-offset and zero angle
- various speed: 9mph, 12mph, 15mph, 30 mph, and 35 mph.

Angle collision:

- the vehicle is crashed into a non-deformable flat barrier which is placed such that the angle formed between the flat surface of the barrier and the bumper of the vehicle is at ±30°.
- various speed: 12 mph, 15 mph, 30 mph.

Pole collisions:

- the vehicle is crashed into non-deformable, cylindrical, high (telephone pole) and low (fire hydrant) pole at zero or percentage offset.
- various speed: 9 mph, 15 mph, 18 mph, 21 mph, 25 mph, 30 mph.

Rough road events:

- uneven terrain: chatterbumps, potholes, bumps,
- exterior events: hammer blow, door slam

The crash data is the raw acceleration read by the accelerometer. For each crash, the acceleration of the vehicle is recorded starting from the bumper contact (in some cases, however, the data is collected prior to the bumper contact) and continues to record for approximately 200-250 millisecond.

5.3.2. Procedure

The evaluation is done using a simulation tool. The tool simulates how the crash sensing module behaves when given the crash data collected from actual vehicle crashes done at the vehicle test facility.

Specifically, the tool is designed with a blackbox approach such that the end-user only needs to specify the input crash file. The results of the simulation are series of table and graphs. These tables and graphs show the activities of the algorithm by recording the time of all the events. The events include the enabling of the algorithm, the crossing of thresholds (both exceeding and falling below), and the time and the condition of trigger, if the deployment decision has been reached. In addition, the values of the intermediate variable (velocity, displacement, slope, etc.) throughout the entire evaluation interval are recorded. This information is helpful for optimizing the algorithm.

The original simulation tool was modified in order to accommodate the analysis of this project. The major change was in the input phase. Instead of using only the longitudinal acceleration signal, the input mechanism of the simulation tool had to be expanded to accept the lateral and the vertical acceleration signals. Furthermore, the structure of the evaluation stage was expanded because new criteria had been added. Lastly, there were peripheral functions such as data collection and representation which must be modified for compatibility.

The results of the simulation details the performance of the algorithm. By examining the conditions and the timeliness of the deployment, the overall effectiveness and efficiency of the algorithm can be estimated.

5.3.3. Performance Requirements

5.3.3.1. *Customer Requirements*

The first step of the performance evaluation is to examine if all the customer requirements are met. These requirements are further broken down into two parts: the accuracy of the deployment decision, and in the case of a deploy events, the timeliness of the deployment. The requirements are derived from the injury criteria established by the National Highway and Transportation Safety Authority[16]. In other words, the automotive manufacturers establish and adjust the requirements of each individual vehicle platform specifically to satisfy these injury requirements. The requirements for the vehicle platform under analysis, which are discussed in the next section, are used as the benchmarks for the evaluation.

There are several generalizations about the severity and the timing thresholds for the deployment of the airbag. First of all, the severity thresholds (the velocity which the airbag should be deployed) varies depending on the type of the collision. In the case of the full-frontal collisions of the vehicle under study, the velocity threshold for deployment is between 12 to 15 mph. The angle collision has a higher deployment threshold at 20 mph. The pole collisions, which are difficult to detect, has a severity deployment threshold at 18 to 21 mph.

In addition, the typical deployment requirements are given in the following table.

Crash type & velocity	deploy requirements	goal time requirements
Frontal - 9 mph	no deploy	N/A
15 mph	deploy	50 ms
30 mph	deploy	24 ms
35 mph	deploy	18 ms
Angle - 15 mph	no deploy	N/A
20 mph	deploy	44 ms
30 mph	deploy	36 ms
Pole - 14 mph	no deploy	N/A
18 mph	deploy	75 ms
21 mph	deploy	75 ms
25 mph	deploy	56 ms
30 mph	deploy	43 ms

5.3.3.2. *Comparison to the Single-Axis Algorithm*

In addition to satisfying the customer requirements, the benefits of the new multi-axes algorithm cannot be shown unless the performance is compared against that of the single-axis algorithm. The criteria for comparison are discussed in the next section.

5.3.4. Criteria for Performance Evaluation

The following are the criteria used to evaluate the performance of the three-directional algorithm with respect to the single-directional algorithm. In general, these criteria are used to evaluate the effectiveness and efficiency of any crash sensing algorithm.

5.3.4.1. *Accuracy*

Accuracy refers to whether the algorithm has accurately distinguished the deploy events from the non-deploy events. This is the first pass of the evaluation process aimed at knowing if the algorithm has successfully identified the crashes which are near deployment thresholds. Once the accuracy of the algorithm is established, the performance of the deploy events are examined more carefully.

5.3.4.2. *Timeliness*

Timeliness refers to the time required for the algorithm to arrive at the deployment decision. Timeliness is not necessarily judged by how fast the deployment decision is made. The reason for that is because the airbag should not be deployed much *earlier* than needed. First of all, the airbag is designed to inflate and deflate very quickly. After the airbag has fully inflated, the force of the body impacting the airbag should allow it to deflate quickly in order for the airbag to absorb the momentum of the moving body. If the airbag is inflated prematurely, it could have started to deflate by the time of the body contact. Therefore, while it is necessary to deploy the airbag within the time threshold, it is not necessary to make the decision as soon as possible[17].

The timeliness is judged by whether the deployment decision is made within the required time. However, to reach the deployment decision quickly is not necessarily useless. First of all, it increases the margin for errors. For example, if the deployment decision can be made very quickly, it is more likely that the similar collisions are also detected on time. Second, if the decision has been arrived too quickly, an arbitrary delay can be imposed on the deployment signal. During the delay, the algorithm can *reconfirm* the decision by continuing to evaluate the data until the end of the delay when the deployment signal is asserted. If the evaluation of the data during the delay strongly suggests a non-deploy event, the deployment can be suppressed.

5.3.4.3. *Robustness*

Robustness ties in both the accuracy and the timeliness of the algorithm. It measures the performance of the algorithm if the original crash signals are altered. The crash signals are altered by multiplying the acceleration by a scale factor between 0.1 and 1.5.

Although changing the crash signal by multiplying it by a scale factor does not guarantee that the accuracy of the crash signal is preserved, it does, however, offer a new set of crash signals which carries some validity. For example, the crash signal of a 30 mph collision is multiplied by factors 0.9 and 1.1. It is true that these may not be the signals observed if the vehicle was crashed into the barrier at 27 mph and 33 mph, respectively, but they serve as estimations. One must keep in mind that the validity of the altered signal diminishes as the scale factor deviates farther away from 1.

To test the performance, the original crash signals are multiplied by factors from 0.1 to 1.5 with increments of 0.1. Using simulation, these scaled signals are evaluated by the algorithm, and the accuracy and timeliness results are recorded. The evaluation is performed on the three-directional algorithm as well as the single-directional, controlled algorithm. The results are then compared.

Chapter 6

6. ANALYSIS/DISCUSSION

6.1. Correlation Method

Undoubtedly, the correlation methods relies heavily on the relationship between the signals from the different directions. If there are clear and consistent relationships between the signals, the correlation method allows one to make predictions about the unknown signals based on the known signals. However, the validity of the predictions depends heavily on the consistency of the relationships.

In this section, the analysis is aimed at establishing the relationships between the longitudinal, lateral, and vertical signals. Specifically, the analysis is focused on three groups of collisions, the frontal,

the angle, and the pole collisions. The goal of the method is to use the lateral and the vertical signals (the secondary signals) to assist the decision making processing which is based on the longitudinal signal (the primary signal).

6.1.1. Longitudinal *versus* Lateral

The focus of this analysis is to establish a relationship between the longitudinal and the lateral signals. One area where this relationship may be the strongest is the angle collision. Intuitively, the angle collisions have a significant lateral acceleration.

One method to establish the relationship is to analyze the angle of the collision. The algorithm can accurately determine the angle of the collision only if the relationship between the longitudinal and the lateral is valid (Figure 12). To test this hypothesis, the longitudinal and the lateral velocity signals of a 30° angle collision are used to derive the angle of the impact force.

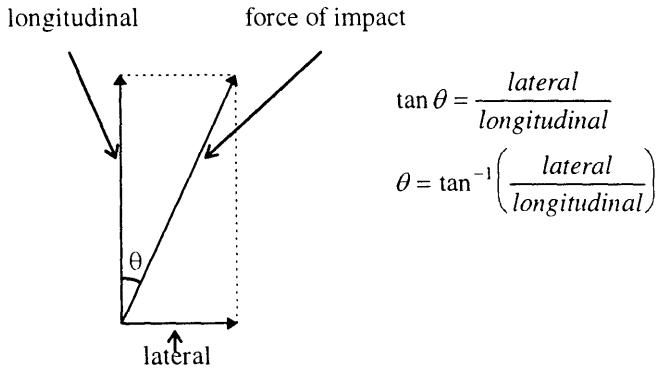

Figure 12: Calculation of the angle of impact

However, without the need to carry out any calculation, this method cannot accurately determine the angle of collision. The top graph is the lateral velocity of a frontal collision and the bottom graph is the lateral velocity of the 30° angle collision.

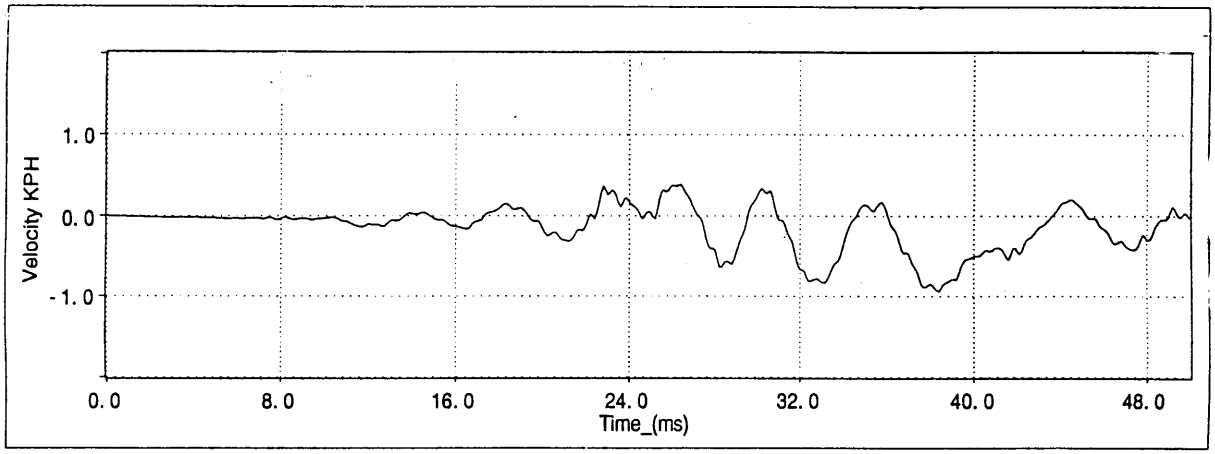

Lateral velocity of a 30 MPH frontal collision

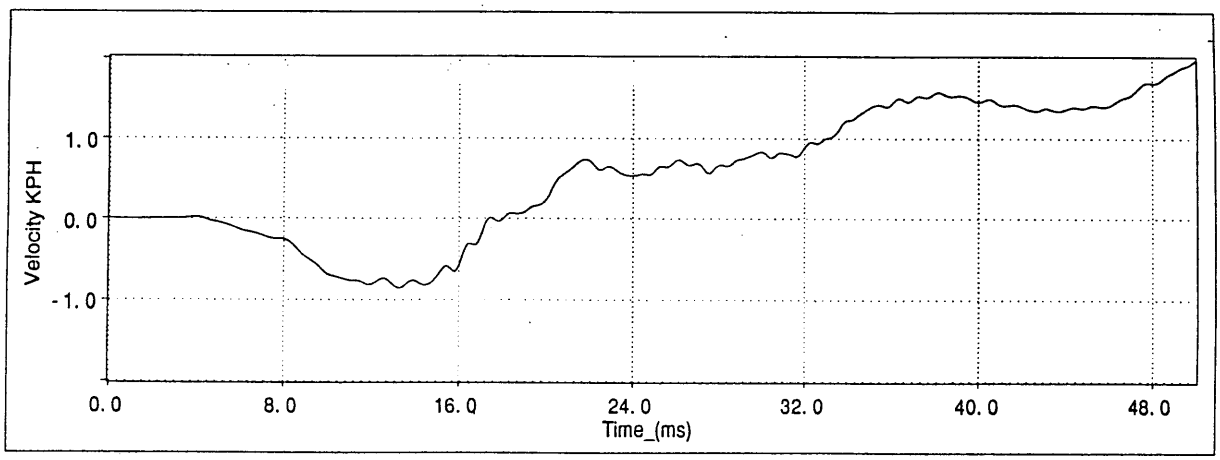

Lateral velocity of a 30 MPH angle collision (barrier offset at 30 degrees)

Figure 18: Lateral Velocity - Frontal vs. Angle Collisions

The lateral velocity signal reveals a dip in the initial 15-20 milliseconds. Because of the change in the polarity of the velocity, the polarity of the angle of impact reverses. In addition, the calculated angle of impact is not accurate. At 15 millisecond into the collision, the longitudinal velocity is roughly 6 times larger than the lateral velocity, and the resolved angle is only approximately 14 degrees. The magnitude of the lateral velocity then begins to decrease which causes the angle to also decrease until the

sign of the angle is eventually reversed. At this time, the algorithm is required to reach the deployment decision. Because the calculated angle varies significantly up until the required time of deployment, the angle of the collision cannot be accurately determined by the required triggering time. Of the 10 high severity angle collisions analyzed, all shared the similar inconsistency.

Why did this method fail? Some speculations suggest that the energy transfer may not be consistent because of the structural components of the vehicle. By the time the impacting force has propagated through the vehicle to the accelerometer, the direction and the magnitude may have been dampened or altered. Another possible source causing the changes may be from the deformation. It is likely that the deformation of the main chassis also absorbs and alters the magnitude and the direction of the impacting force[18].

6.1.2. Longitudinal *versus* Vertical

Because the net displacement in the vertical direction is zero, it leads to the natural conclusion that the collision cannot have an impact vector which lies in the longitudinal-vertical plane. Therefore, instead of focusing on the direction of the impact, the analysis is based on the magnitude of the signals.

The plots of longitudinal and vertical velocity signals of frontal, angle, and pole collisions can be found in Appendix A. Plots 1, 4, and 7 are the longitudinal velocity signals of the frontal, angle, and pole collisions, respectively; plots 3, 6, and 9 are the vertical velocity signals of the frontal, angle, and pole collisions, respectively. The velocity signals are chosen because of the intuition it provides and the ease to convert to either the acceleration or displacement signals.

The plots found in Appendix A consist of collisions of the same type at various speed. The focus of this analysis is only based on high speed collision, namely the 30-mph collisions. Consequently, the magnitude of the severity in all these collisions are the same. A quick look at the longitudinal velocities during the early part of the crashes when the discrimination against non-deploy events needs to be done reveals significant differences among the frontal, angle, and pole collisions. The longitudinal velocity of the frontal collision is clearly larger than those of the angle and the pole collisions in the first 20 to 50 milliseconds. The correlation method would suggest that the discrepancies may be compensated by the

vertical signals. However, a closer look at the vertical velocities of the respective collisions does not show that the differences in the longitudinal signals can be compensated. In the case of comparing the frontal to the angle collisions, the vertical velocity of the angle collision appears to be weaker than that of the frontal collision. Not only is the maximum velocity greater for the frontal collision, the area under the vertical velocity curve is also larger than that of the angle collision. Furthermore, the longitudinal velocity of the pole collision is even weaker than that of the angle collision, and instead of compensating for this weakness, the vertical velocity is small compared to both the frontal and the angle collisions.

The conclusion of the simple analysis above reveals that for the collisions of the same degree of severity, the vertical signal does not compensate the differences in the longitudinal signals. Instead, the vertical signals are proportional to the magnitude of the longitudinal signals. Therefore, using the vertical signals to compensate the longitudinal signals is not feasible.

6.1.3. Feasibility of the Algorithm

The analysis above shows very limited relationships between the longitudinal signals and both lateral and vertical signals. Although very specific correlation may exist between the variable, they are not global characterizations. For example, if a very specific, well-behaved relationship between the longitudinal and the lateral signals of the angle collision is discovered, the algorithm must first establish that the collision at hand is an angle collision before the correlation can be used. Consequently, the time required to establish the identity of the collision may be too long for the algorithm to be effective.

Without the predictable and reliable relationships between the variables, the correlation method is not feasible.

6.2. Rotated Axis Method

Rotated-axis method suggests that it may be possible to enhance the performance of the crash sensing algorithm if multiple accelerometers are placed at offset angles. If the method does suggest improvement in the performance, the question is what angle the accelerometers should be placed at.

6.2.1. Patents

There are several patents which describe crash detection methods using dual accelerometers placed at offset angle from the longitudinal axis or the direction of travel, one of which discusses how the crashes can be classified by using dual accelerometers placed at ±45° from the longitudinal axis[19]. The detection method relies on resolving the angle of the collision and deriving a threshold level based on the calculated angle of impact.

The analysis from the previous section concludes that the angle of collision cannot be accurately determined using longitudinal and lateral signals. Therefore, the question becomes: can the acceleration signals of the rotated-axis accelerometers provide a more accurate determination of the angle of impact? Following is the method used to determine the angle of impact described by the patent.

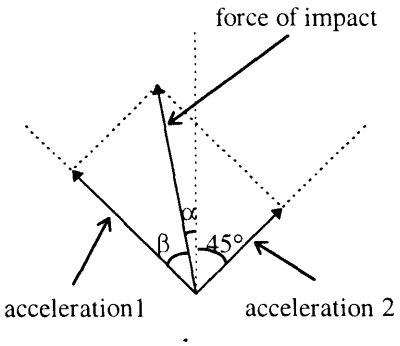

$$\tan\beta = \frac{acceleration2}{acceleraton1}$$

$$\beta = \tan^{-1}\left(\frac{acceleration2}{acceleration1}\right)$$

$$\alpha = 45° - \beta$$

Figure 14: Using Accelerometers placed at ±45° to Calculate the Angle of Collision

The algorithm calculates the angle of impact by finding the inverse tangent of the quotient between two raw acceleration signals. However, the validity of this approach is low because the raw acceleration signals are very noisy. When this approach was duplicated using the available raw crash data, the calculated angle varied inconsistently between 0 and 90 degrees.

6.2.2. Analysis

The results of the method described by the patent was not only difficult to duplicate, it did not contain additional information which was not available using longitudinal and lateral acceleration signals. The patented method relied on resolving the two acceleration signals to determine the angle and the magnitude of the impact force. Once the angle and the magnitude of the crash are known, the thresholds for crash detection are adjusted accordingly. However, despite the fact that acceleration signals are noisy and the angle of impact cannot be accurately determined, there is no reason to believe that the results achieved by the offset accelerometers cannot be achieved by using the longitudinal-lateral pair of accelerometers. Using the longitudinal-lateral pair of acceleration signals, the cosine law can also be used to determine the impact vector.

One benefit of the using a pair of accelerometers placed at $\pm\theta$ degrees instead of the longitudinal-lateral pair is when the noise-to-signal ratio is large. To minimize the effects of this ratio, the magnitude of the original signal should be as large as possible. Therefore, placing the accelerometers in the direction of the impact may maximize the magnitude of the crash signal. However, the energy transfer must be consistent throughout the vehicle such that in an angle collision, the angle of impact can be recovered by resolving the signals of the accelerometers. In other words, it may be possible that due to the structural deformation or the inconsistent energy transfer that the angle seen by the accelerometers is not the same angle as the angle of impact[20]. In addition, to place the accelerometers at an offset angle to better detect the angle collisions inevitably sacrifices the effectiveness in detecting the full frontal collisions. If the accelerometers are placed at $\pm 45°$ with respect to the longitudinal axis, a frontal collision would therefore be recognized only with approximately 70% of the signal amplitude. Consequently, the threshold must

also be lowered by 70%. Assuming that the magnitude of the noise remains constant, the noise-to-threshold ratio becomes larger.

One can also argue that the rotated-axis method improves reliability of the algorithm[21]. Because each of the two accelerometers placed at ±45° with respect to the longitudinal axis contains both longitudinal and lateral information, the crash sensing unit can be functional even if only one accelerometer is present. However, the complexity increases if the crash sensing algorithm must be functional with both single *and* dual accelerometers. Furthermore, the robustness of the algorithm is seriously damaged if only one accelerometer remains, and inevitably, the crash sensing unit must be replaced immediately.

The rotated-axis method cannot better determine the angle of impact of a collision. However, it provides addition lateral information which is not available in the single-directional sensing strategy. One can further conclude that the while the rotated-axis method generates the lateral information which can be treated as an independent component and analyzed separately, the same information can be obtained using accelerometers placed along longitudinal and lateral axis of the vehicle. In conclusion, the rotates-axis method does not provide additional information which is not available using the independent threshold method with the longitudinal-lateral pair of accelerometers. The independent threshold method is discussed in the following section.

6.3. Independent Threshold Method

Because the above two methods are not feasible or practical, the focus of the thesis is on the independent threshold method discussed here. The results and the evaluation are based solely on this algorithmic approach.

6.3.1. Threshold Requirements

The independent threshold approach requires that separate thresholds are used for the acceleration signals from longitudinal, lateral, and vertical directions. Consequently, the deployment decision is drawn from the logic function based on all of these thresholds. Although in most cases, the thresholds are completely limited to the criteria in one specific direction, there are also thresholds, such as the combined rectified energy of the crash, which are derived from multi-directional signals. The specific criteria/thresholds tested are discussed in this section.

6.3.1.1. *Longitudinal Requirements*

The longitudinal criteria are not the focus of the algorithm. In the studies of the conventional crash sensing algorithms using only the longitudinal signal, the properties of the longitudinal signals are well defined and utilized. Therefore, the longitudinal thresholds used in the new algorithm are derived from some of these well-defined characterizations.

The main purpose of evaluating the longitudinal criteria is to establish the baseline crash conditions. Specifically, instead of sensing and identifying the crash, the longitudinal criteria are used only to detect the presence of a crash and estimate severity of the crash. In other words, although the longitudinal criteria are used in the algorithm, they do not contribute directly to the calculation of the severity of the collision. Therefore, the emphasis of the longitudinal threshold testing is to identify and reject the non-deploy events.

To identify the non-deploy events, the thresholds must be able to identify the low speed frontal, angle, and pole collisions as well as the rough road events. Special attention will be given to the collisions which the severity, implied by the impact velocity of the vehicle, are close to the deployment thresholds. These crashes will be used as the benchmarks for the calibration of the criteria thresholds.

The thresholds of these criteria are derived from previously established calibration data. First, the calibration data reveals the threshold levels of these criteria. Second, the thresholds are compared against the actual longitudinal crash data. In this step, the longitudinal crash data are drawn from all the

crash scenarios including full frontal collisions, angle collisions, pole collisions, and rough road events. Third, the new longitudinal thresholds are established. The new thresholds are derived by lowering the original thresholds by an arbitrary amount. Since the original thresholds *must* reject the non-deploy events, they are designed to accurately distinguish the deploy and the non-deploy events. Because the new algorithm does not need to make such clear distinction using only the longitudinal thresholds, the thresholds can be less stringent. Besides the apparent reason that the severity decision is not made based on the longitudinal criteria, it is *necessary* to lower the importance of the longitudinal thresholds. In order to understand and compare the benefits of the lateral and the vertical signals, it is necessary to let the longitudinal criteria carry the least weight in the severity decision. With the low weighing of the longitudinal criteria, the final deployment decision is based primarily on the lateral and the vertical signal. In addition, the amount which the original thresholds are lowered by is arbitrary for the reasons of robustness. Instead of reducing all the thresholds uniformly by a percentage amount, each and every criteria are examined such that all deploy events are clearly above the thresholds.

The longitudinal criteria can be viewed at as a first pass through the crash data. The collisions which cross the longitudinal thresholds include all the deploy events and some non-deploy events. The purpose of this level of threshold testing is to isolate all the crash events which are near the deployment thresholds, both above and below.

6.3.1.2. *Lateral Requirements*

Intuitively, the lateral signal provides valuable information in separating the angle collisions from the others. When colliding with the barrier at an offset angle, the force exerted on the vehicle contains a relatively large lateral (relative to the vehicle) component. In the discussion of the correlation method, the lateral velocity was shown not to be useful in determining the angle of the impact. However, distinct characterizations of the lateral signal may provide discriminating evidences. Therefore, the analysis of this section is focused on the angle collisions, and the question to consider is how the lateral signal can best be used to characterize the angle collisions. However, the analysis also extends to other areas where the lateral signals may be useful.

6. 3.1.2.1. *Acceleration*

The most important characterization of the lateral acceleration is that magnitude does not tend toward positive or negative. This characterization is true because in most collisions which require the deployment of the frontal airbag, the lateral displacement of the vehicle is small. The generalization holds true even in the offset frontal or the angle collisions. Since the vehicle usually does not have a net displacement in the lateral direction, the integrated sum of the acceleration, or velocity, is small.

In the case of the full frontal collision, the raw magnitude of the acceleration is large. However, the signal oscillates with a relatively consistent frequency along the x-axis, and because of the cancellation due to oscillation of the signal, the integrated sum of the acceleration is small. In the case of the angle collision, the raw magnitude of the acceleration is smaller, but the signal is mostly of either positive or negative because of the lateral displacement. Therefore, a threshold placed on the magnitude of the acceleration cannot accurately differentiate the frontal and the angle collisions. A more sophisticated method which takes into account the direction of the signal is discussed in the rectified energy section.

6.3.1.2.2. *Velocity*

Lateral velocity represents the lateral motion of the vehicle, and the direction and the severity of the crash signal provides valuable information. The lateral velocity is calculated by integrating the lateral acceleration signal.

Following is a comparison of the lateral velocity of angle and frontal collisions, both with the same impact velocity. The top plot is the lateral velocity of a 30-mph, full-frontal collision, and the bottom plot is the lateral velocity of a 30-mph, 30° angle-barrier collision. Since both collisions require the deployment of the airbag, it is not necessary to distinguish one from the other. However, these two velocity signals contains some of the basic characterizations of the frontal and angle collisions. The

understanding of these characterizations may help the algorithm perform accurate classification of the crashes and, eventually, improve the deployment decision process.

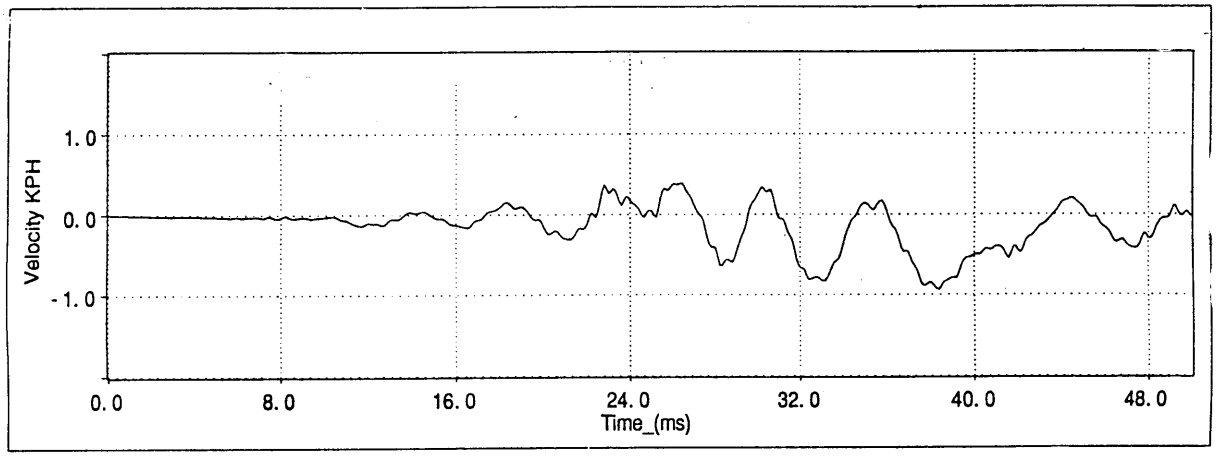

Lateral velocity of a 30 MPH frontal collision

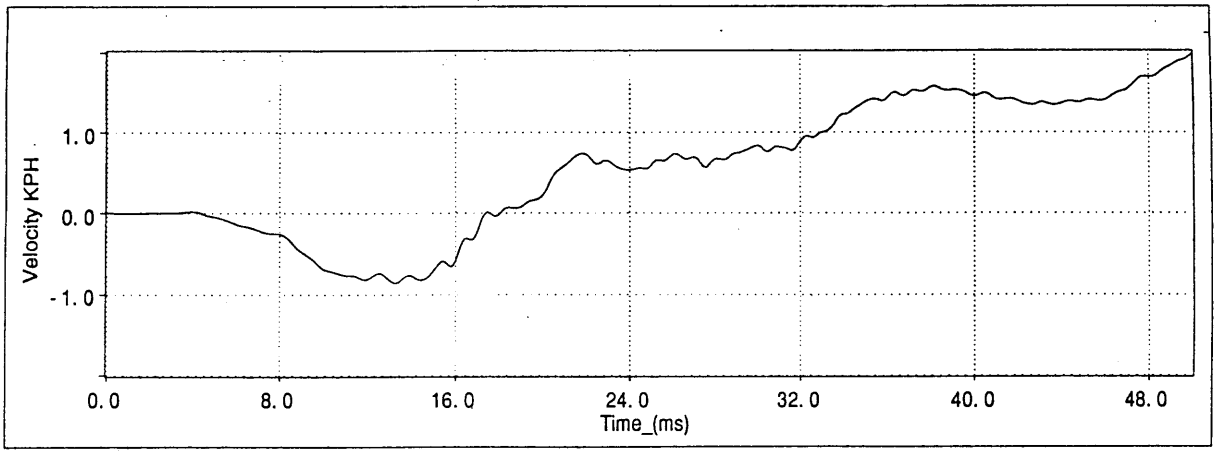

Lateral velocity of a 30 MPH angle collision (barrier offset at 30 degrees)

Figure 15: Lateral Velocity - High Speed Frontal vs. High Speed Angle

The lateral velocity of the angle collision has a characteristic "dip", a local minimum, in the first 15-20 ms. This dip is unusual for several reasons. First, from the available data, the initial 10 to 20 milliseconds of most collisions are often very weak as indicated by the lack of activities in the acceleration. Second, the magnitude of the dip is very small. Given that the lateral displacement of the accelerometer represented by the dip is approximately only 1 millimeter, the overall lateral displacement of the vehicle must not be more than a few millimeters. Such limited movement cannot be observed by

the naked eyes, and film analysis have failed to show the evidence for this lateral movement. Lastly, the direction of the dip is puzzling. After the dip has peaked, the signal continues to gain magnitude in the direction opposite of the dip. This last point is explored more extensively in the following section.

6.3.1.2.2.1. *Causes of the "dip"*

The presence of the dip suggests the vehicle experiences a slight, short burst of energy in the lateral direction immediate after the bumper contact. The analysis of the source and the direction of this burst may provide insights into the nature of the collision and establish the characterization of the angle collisions. The following is the previously seen plot of the 30-mph, 30° angle-barrier collision.

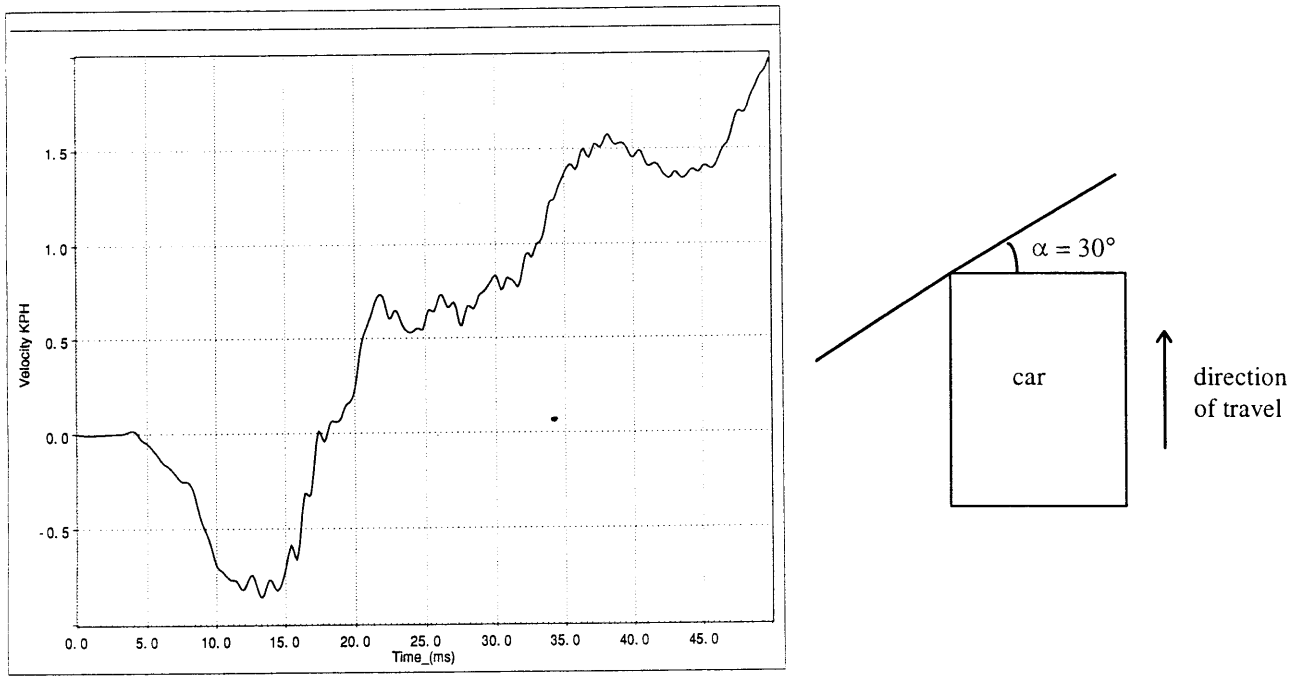

Lateral Velocity of a 30 mph 30° Angle Collision

Figure 16: Lateral Velocity of an Angle Collision

The plot indicates the direction of the final settling velocity is opposite from the direction of the dip. Exactly which direction is the dip with respect to the vehicle? By convention, the lateral velocity is positive when the vehicle is moving to the *left* and negative if it is moving to the *right*. Therefore, in the above 30-mph, 30° left front impact collision, the final velocity shows that the final resting position is to the right of the point of impact. This behavior confirms the logical assumption that upon impact, the barrier exerts a force from the left of the vehicle which pushes the vehicle to the right. Of course, this simple assumption does not take into account the friction force between the vehicle and the barrier when the vehicle is sliding along the barrier, and it also does not consider the friction between the tires and the ground. In actuality, various crash tests captured on film shows that a vehicle in an angle barrier impact

either slides along the barrier or shows no lateral displacement. The later case, which the vehicle "sticks" to the barrier, suggests that the lateral force exerted by the barrier is compensated by the deformation and the friction forces between the vehicle and the outside elements.

From the analysis above, the direction of the dip in the velocity, which is opposite to the overall direction of lateral movement, is an exception. The dip shows that the vehicle is moving to the left, or toward the barrier, in the initial stage of impact. To gain a better understanding of this phenomenon, the longitudinal and the lateral velocity from various locations of the vehicle are collected.

The following graph shows a composite of lateral and the longitudinal velocities collected at various locations of the vehicle.

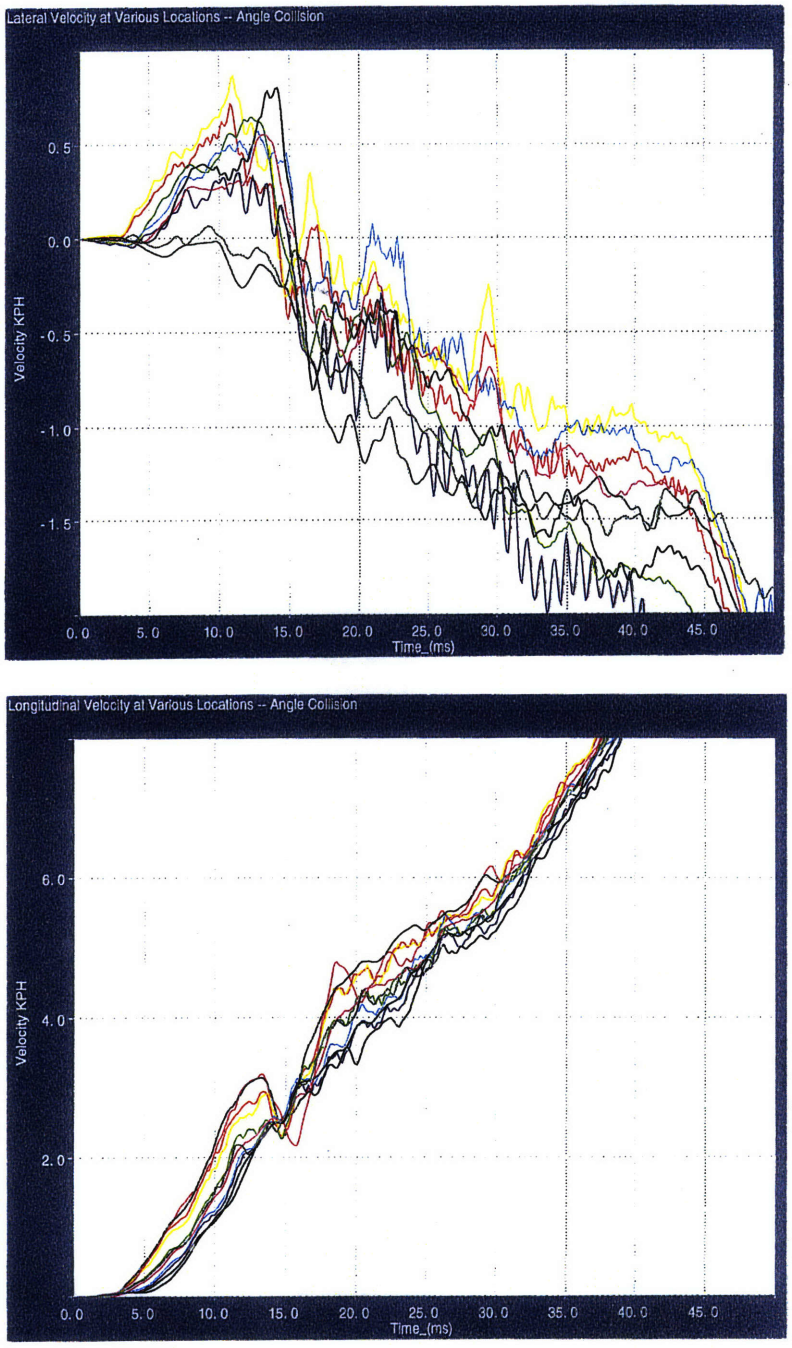

Figure 17: Composite of the Lateral and Longitudinal Velocities at Various Locations

These two graphs clearly indicate that at different locations of the vehicle, the direction and the severity of the signals are different. These inconsistencies suggest that different locations of the vehicle are not moving uniformly in a collision. Because the above plots contain too many signals to analyze, figure 18 shows a series of plots which are groups of signals which are arranged by the locations of the accelerometers. The positions shown can be referenced in figure 19.

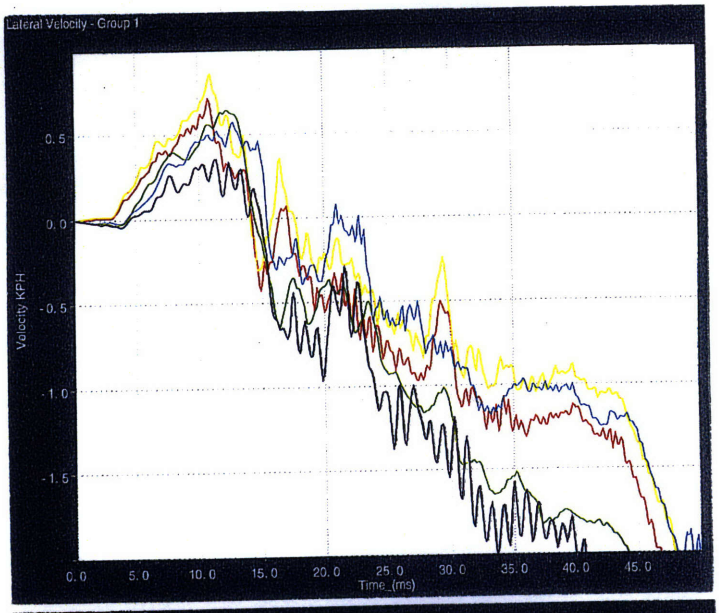

Red - Position 1
Yellow - Position 2
Green - Position 3
Light Blue - Position 4
Dark Blue - Position 5

Figure 18.a: Lateral Velocity Group 1

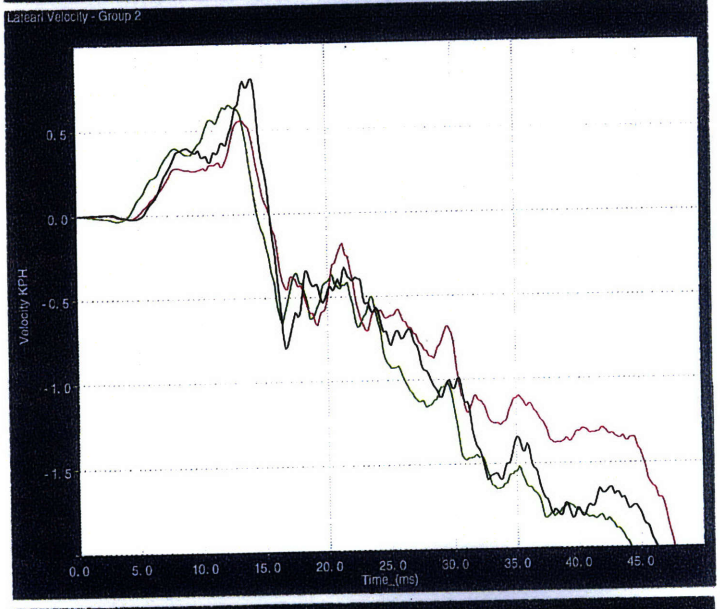

Green - Position 3
Pink - Position 6
DarkBrown - Position 9

Figure 18.b: Lateral Velocity Group 2

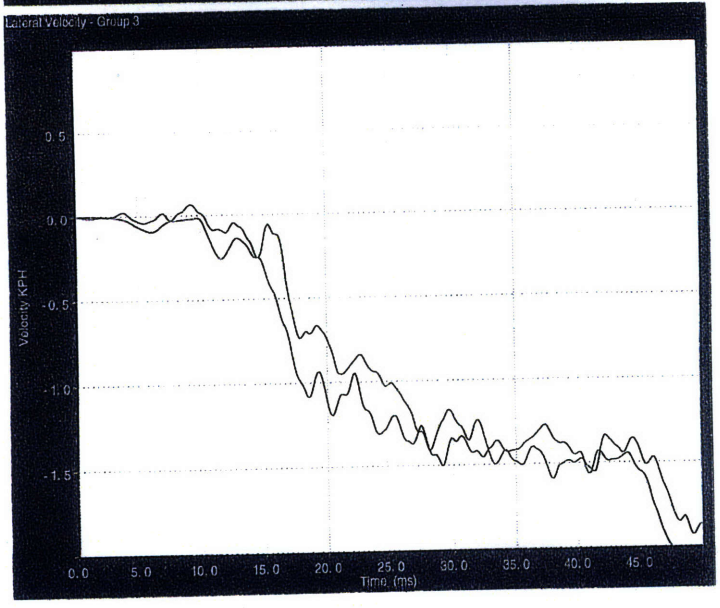

Moss - Position 10
Indigo - Position 11

Figure 18.c: Lateral Velocity Group 3

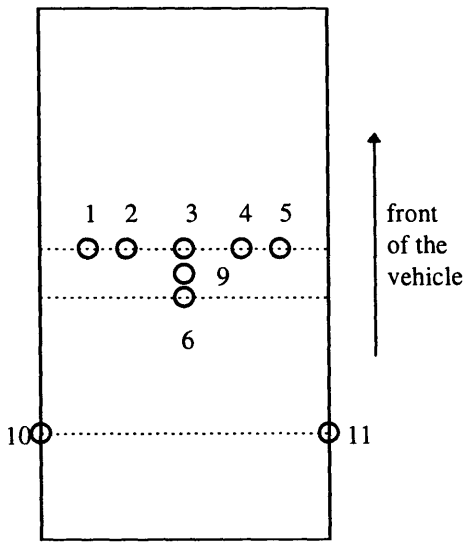

Figure 19: Locations of the Accelerometers

These three plots are the breakdowns of the lateral velocity signals from earlier. The groups are based on the locations of the accelerometers. Group 1 contains the lateral velocity signal taken from different locations along the #2-Bar (horizontal beam running across the car). In these crash signals, the magnitude of the lateral signals vary considerably in the region of the dip. From the graph, it seems that the left side of the vehicle is moving slightly faster than the right side in the lateral direction. However, this direction of the movement is consistently toward the left.

Group 2 contains the lateral velocity signals taken from along the center line of the vehicle. However, these accelerometers are placed relatively close to the center of the vehicle. Although the variations among these three signals are slight, the overall trend suggests that within this region, the accelerometers near the front are subjected to larger lateral force than the ones located near the rear.

Group 3 contains the lateral velocity signals taken from the left and right rear rockers of the vehicle. From these locations, the dip in the lateral velocity is no longer present. In fact, the right rocker begins to move to the right almost immediately after the initial bumper contact.

The fluctuation in the lateral velocity does not lead to any solid conclusion. To gain a better insight into the motion of the vehicle in this stage of the collision, the longitudinal component must also be taken into consideration. By resolving both the longitudinal and the lateral velocity into a directional vector for all the different locations which the data has been collected from, the resulting vectors may better demonstrate the motion of the vehicle. the following are plots of the longitudinal velocity signals which are also grouped by the relative positions of the accelerometers.

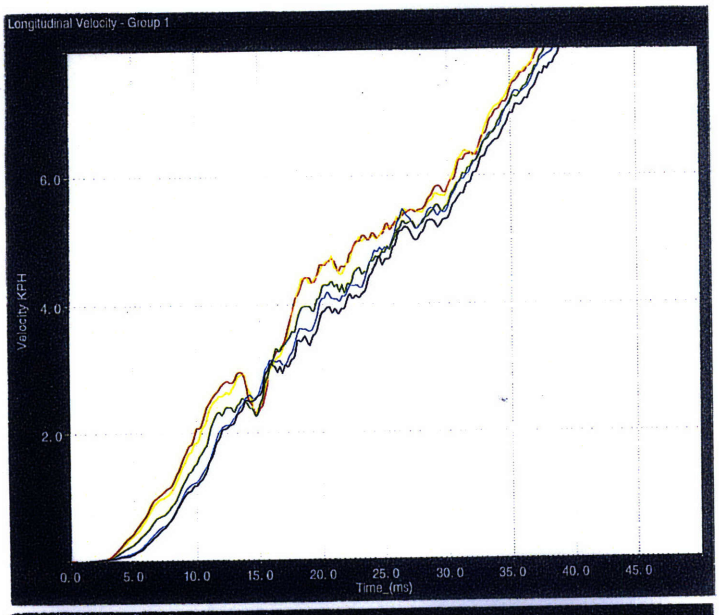

Red - Position 1
Yellow - Position 2
Green - Position 3
Light Blue - Position 4
Dark Blue - Position 5

Figure 20.a: Longitudinal Velocity Group 1

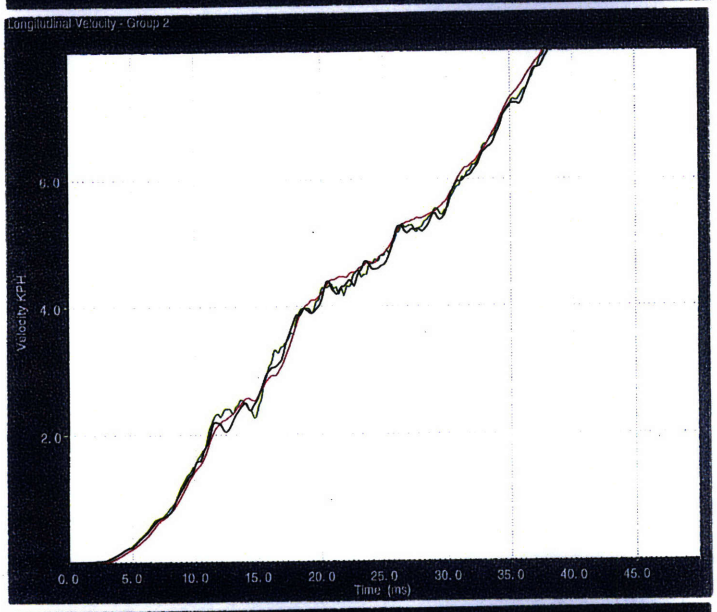

Green - Position 3
Pink - Position 6
DarkBrown - Position 9

Figure 20.b: Longitudinal Velocity Group 2

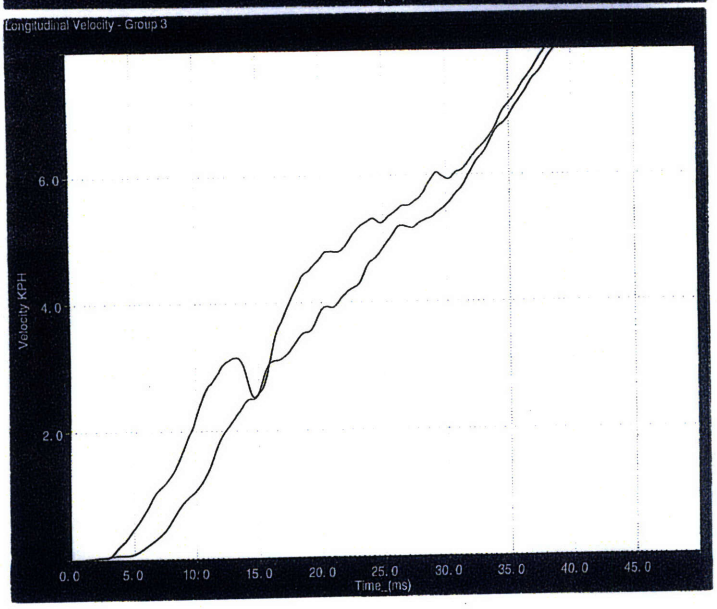

Moss - Position 10
Indigo - Position 11

Figure 20.c: Longitudinal Velocity Group 3

Group 1 is the composite of longitudinal velocity signal along the #2-Bar of the vehicle. Within the time frame of the dip, the longitudinal velocities at different locations vary. Similar to the lateral velocity, the magnitude of longitudinal velocity from the left side of the vehicle is higher than that from the right side. While the lateral velocity shows vehicle's lateral motion and direction, the longitudinal velocity shows the *deceleration* of the vehicle. In other words, the direction of the longitudinal velocity vector is toward the rear of the vehicle even though the vehicle is moving forward.

The plot of Group 2 locations shows the longitudinal signal extracted from the three accelerometers which are placed near the center of the vehicle along the center line. The three signals overlap significantly, and it is difficult to separate them apart. For practical reasons, the magnitude of these three signals can be considered to be similar, if not identical.

Lastly, Group 3 contains the longitudinal velocity from the left and right rear rockers. Contrary to the lateral velocity, the left rocker shows a significant larger longitudinal deceleration as compared to the right rocker in the initial 30 milliseconds.

Although very little information is available by observing separately the longitudinal and the lateral velocity signals at different locations, the motion of the vehicle becomes more apparent when the two velocity vectors are resolved into one. Following is a plot of all the locations of the accelerometers used to extract data. In addition, the longitudinal, lateral, and the resolved vectors are plotted at their respective positions. The instantaneous longitudinal and lateral velocity vectors are taken 12 milliseconds into the collision, the time when the dip is at the peak.

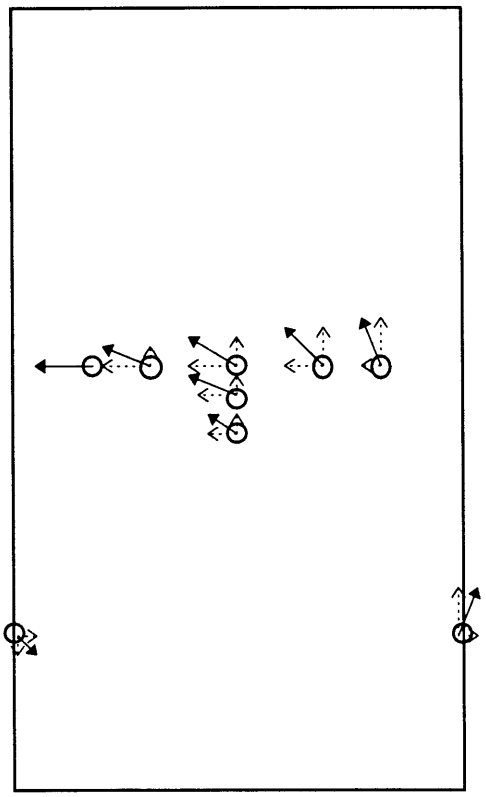

Figure 21: Resolved Vectors at the Peak of the "Dip"

The following simple analysis is based on several assumptions. First of all, the velocity vectors are formed by resolving the longitudinal and the lateral velocities at a single moment in time. Consequently, all the conclusions are derived from the instantaneous velocity vectors. In order for this assumption to hold true, the second assumption requires that the velocity vectors are linear in the region of concern. In other words, linearity of the signals guarantees that the while the magnitude of the velocity vectors at different locations may vary across time, the relative changes among the vectors are consistent. From the graphs, it appears that the magnitudes of the velocity signals are linear in the region prior to the peak of the dip.

Once the longitudinal and the lateral velocity signals are resolved into one vector, the direction and the magnitude of these vectors tell a very different story. Indeed, the vehicle does not move uniformly in the initial stage of collision, and more interestingly, the direction of these vectors suggest the vehicle is

rotating counterclockwise. Specifically, the velocity vector in the left front corner is pointing toward the right front direction while the velocity vector of the right rear corner is pointing to the left rear. This shows that completely opposite forces are acting on different locations of the vehicle. To take the analysis one step forward, if the vehicle is rotating, the moment arms of the velocity vectors at different locations must intersect at the center of the rotation. However, the moment arms do not intersect at a single point, but instead, the intersections tend to fall within the region behind the front passenger seat. The lack of a clear center of rotation may be explained by the fact that in addition to the rotational force, the vehicle, as a whole, is still moving forward even though it has begun to decelerate. Since the two motions exist simultaneously, it is difficult to determine the exact influence of the rotational force on the final velocity vector. In conclusion, the motion of the vehicle in an angle collision is influenced by the forward momentum of the vehicle and a rotational force induced by the barrier. Consequently, because of this rotational force, the longitudinal and lateral velocities at separate locations are different.

What is causing this rotation? First of all, the following is a simple topological view of a vehicle crashing into a barrier at an angle.

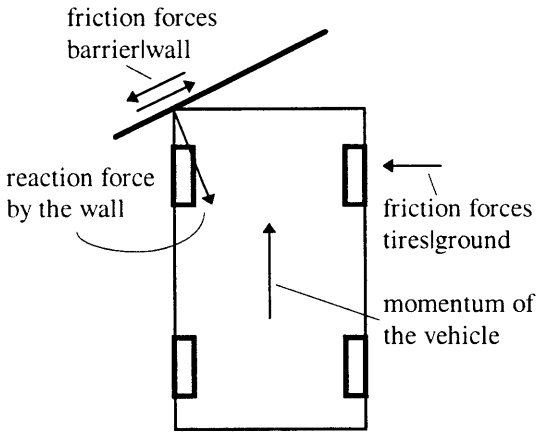

Figure 22: Forces in an Angle Collision

Upon the impact by the vehicle, the barrier exerts a reacting force back onto the vehicle. From the graph, the direction of the reaction force does not pass through the center of mass, assuming that the center of mass is approximated near the physical center of the vehicle. However, because of the friction force between the tire and the ground, the movement of the vehicle is restricted. Consequently, with the wheels firmly gripping the ground, the chassis of the vehicle rotates in the counterclockwise direction. As the vehicle continues to crumble and move forward, the lateral momentum begins to build up. The lateral momentum continues to accumulate until the friction force between the tire and the ground breaks. At that time, the vehicle begins to move laterally to the right.

In conclusion, the results from the analysis of the dip in the lateral velocity shows that this may be a behavior inherent in all the angle collisions.

6.3.1.2.2.2. *Algorithmic enhancements using the "dip"*

The characterization of the dip is now defined. These characterizations are the basis of the algorithm used to identify the high speed angle collisions. There are three ways to depict the high speed angle collisions using the dip characterization. First, while the velocity is calculated in the same way, the presence of the dip determines the threshold level of the velocity signal. In other words, the lateral velocity threshold is consist of two tiers. Second, the velocity is calculated by integrating the acceleration starting from the maximum/minimum peak of the dip. Lastly, using an entire different approach to calculate velocity, the lateral velocity is calculated by integrating the rectified acceleration signal. By forcing the acceleration to be converted to one direction, the velocity becomes the accumulation of the acceleration in only *that* direction. The procedure can be thought of as adding the magnitude of the dip onto the rest of the signal, and therefore, the magnitude of the modified signal is significantly larger than the conventional velocity values.

Method one depends heavily on the repeatability of the dip. In order for this method to work effectively, the size and the timing of the dip must be within certain specification. Because the consistency of the dip is relatively low, method one is not a robust approach. Method two increases the magnitude of the velocity by arbitrarily resetting the velocity at the peak of the dip. By setting the velocity

at zero at the peak of the dip, the velocity begins to gather positive or negative magnitude immediately. Although the measure does not accurate reflect the velocity of the vehicle, it decreases the dependence on the characterization of the dip. However, this method is not effective if the magnitude of the dip is small. Lastly, the third method is the most practical because it incorporates the size and the timing of the dip fully. This measure is actually placed under the rectified energy category, and it will be discussed in more detail later.

6.3.1.2.3. *Consistency of the velocity*

The analysis of the dip invokes another criteria. Because the lateral velocities of the angle collisions tend to one direction while the lateral velocities of other types of collisions oscillate along the x-axis, how often the signal crosses the x-axis can determine if the crash is an angle collision. Specifically, given the initial sign of the velocity is unknown and the fact that the signal must cross the x-axis when it is rebounding from the dip, the lateral velocity signal of an angle collision should not cross the x-axis more than twice.

6.3.1.2.4. *Rectified energy*

6.3.1.2.4.1. *Lateral rectified energy*

The lateral rectified energy is represented by integrating either the rectified acceleration (integrated rectified acceleration) or the rectified velocity signal (integrated rectified velocity). Because most collisions which require the deployment of the airbag do not have significant lateral motion, the net lateral displacement is small or zero. This generalization is applicable in the cases of frontal and pole collisions. However, even though the net result is small, the severity of the collision is reflected by the degree of activities in the lateral signals. In other words, although the net effect of the lateral signals may be small, the frequency and the magnitude of the original signal is influenced by the severity of the collision. Therefore, instead of the signals being canceled due to oscillation, a better approach is to first rectify the signal by taking the absolute values. Once the acceleration is rectified, the integrated values

become the accumulated sum of the activities in the acceleration signal. Even though the original acceleration signal has been altered, the unit of the integrated rectified acceleration is still length/time. Therefore, this is another way to represent the lateral velocity of the collision.

The method described above is the integrated rectified acceleration representation of the rectified energy. However, in the case of the high speed angle collision discussed in the *acceleration* section, the rectified energy calculated by the above method is small because the raw magnitude of the original acceleration is small. However, the signals consistently tends to only one direction. Therefore, another approach to capture this consistency is to represent the rectified energy by the integrated rectified velocity. By letting the acceleration signal be canceled due to oscillation, the lateral velocity of the angle collision is distinct because the signal clearly tends to one direction. Consequently, when the velocity is rectified and integrated, it retains a much higher magnitude compared to the signals of other types of collisions.

This approach well captures the effects of the dip in the lateral velocity signal of a high-speed angle collision. Instead of being canceled when the velocity is integrated, the area under the dip is added to the magnitude of the rectified energy. The integrated rectified velocity representation of the rectified energy has units in length. Therefore, this measure is an alternative way of expressing the lateral displacement. Specifically, it represents the total distance travelled by the vehicle in the lateral direction.

6.3.1.2.4.2. *Combined rectified energy*

Once all rectified energy components in different directions are calculated, they can be added to form a new measure. Combined rectified energy accumulates the instantaneous measurements of the rectified energy in all directions. Specifically, for simplicity and consistency, the combined rectified energy is calculated using only the integrated rectified acceleration in longitudinal, lateral, and vertical directions. The integrated rectified velocity is used primarily to depict the angle collisions, and it does not play a role in the calculation of the combined rectified energy.

Instead of summing all rectified energy components equally, an arbitrary weight can be assigned to each component before the summation. Specifically, assigning a heavier weight on the lateral and the vertical components allows these components to carry a more significant factor in the combined rectified energy measure. To evaluate the initial effectiveness, the following proportion of the components are used to calculate the combined rectified energy:

combined_energy_**111** = **1** * longitudinal component + **1** * lateral component + **1** * vertical component

combined_energy_**112** = **1** * longitudinal component + **1** * lateral component + **2** * vertical component

combined_energy_**121** = **1** * longitudinal component + **2** * lateral component + **1** * vertical component

combined_energy_**122** = **1** * longitudinal component + **2** * lateral component + **2** * vertical component

However, the effectiveness of this approach is disappointing low. The following 4 graphs represents the 4 different methods of calculating the combined rectified energy. Each graph contains 6 separate types of collisions including high and low severity frontal, angle, and pole collisions. Enclosed between the two same color lines is a region where the combined rectified energy of all the collisions of a particular type falls. For example, the region enclosed by the purple lines in the combined rectified energy 111 chart represents all the high speed frontal collisions when longitudinal, lateral, and vertical components are summed in equal proportion. Although the magnitudes of the four sets of energy measures are different, the patterns of the signals are consistent in all of them.

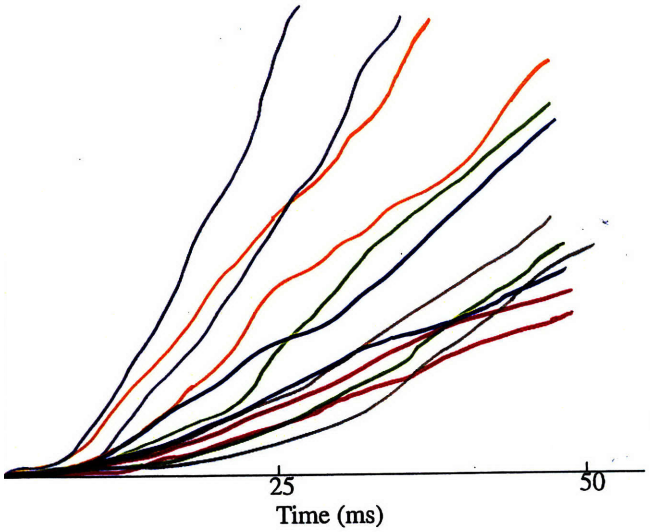

Figure 23a: Energy 111

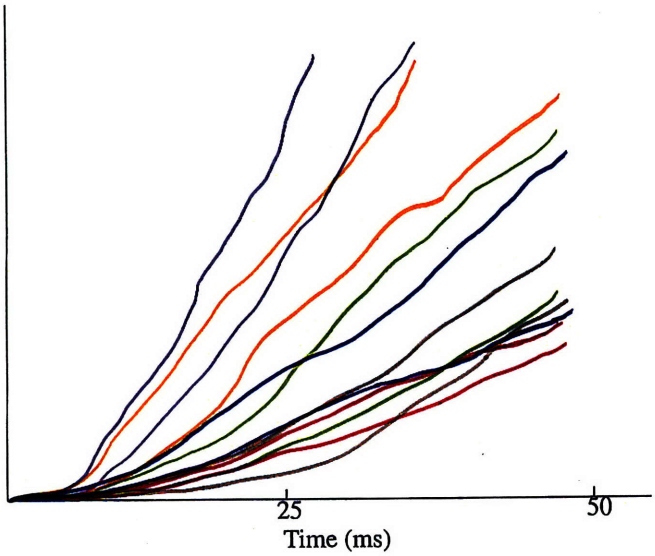

Figure 23b: Energy 112

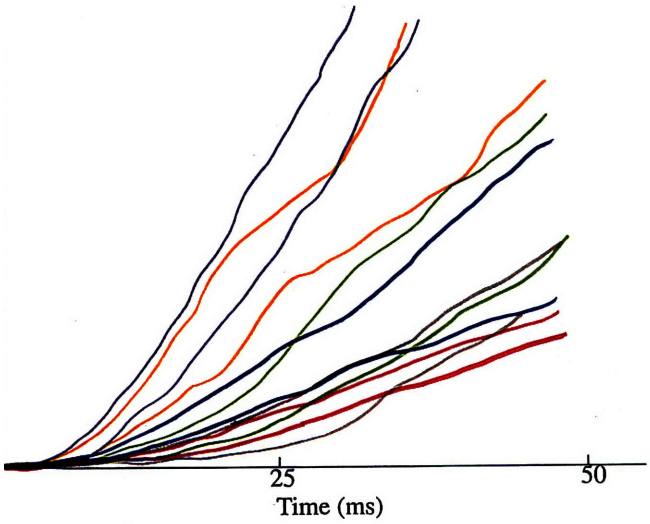

Figure 23c: Energy 121

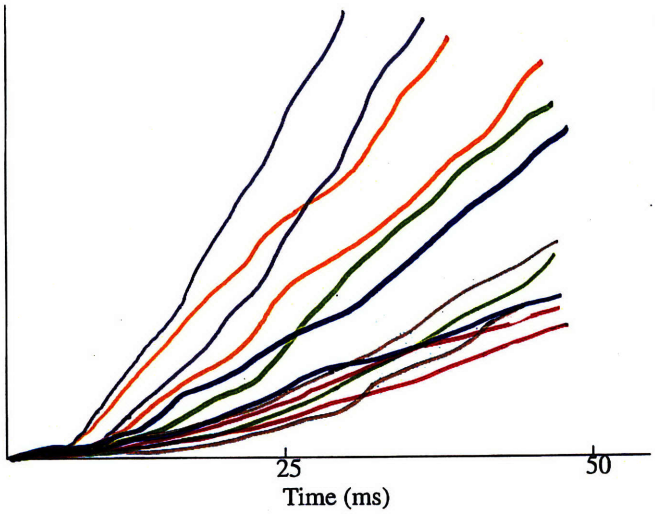

Figure 23d: Energy 122

purple	- high speed frontal collisions
brown	- low speed frontal collisions
orange	- high speed angle collisions
green	- low speed angle collisions
blue	- high speed pole collisions
red	- low speed pole collisions

Figure 23: Four Methods of Combining Rectified Energy Components

6.3.1.2.4.2.1. *Arbitrary decay*

Because the combined rectified energy is a higher order waveform (the sum of the individual rectified energy component where the integration raises the order of the waveform), artificial decay is introduced to facilitate the threshold definition. This becomes clear through the following illustration.

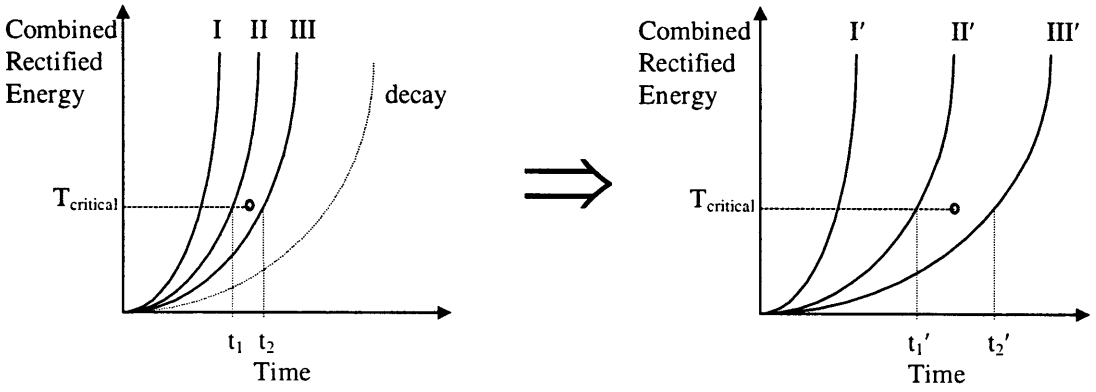

Figure 24: Signal Decay

In the left figure above, waveforms I, II, and III represent three separate combined rectified energy waveforms. Furthermore, let the deploy threshold be between crash signal II and III such that crash signal II is a deploy event and crash signal III is a non-deploy event. Let $T_{critical}$ be the threshold of the combined rectified energy. As the left figure illustrates, the threshold has magnitude $T_{critical}$ and is valid between t_1 and t_2. Consequently, the threshold is crossed when the combined rectified energy of a crash exceeds the threshold $T_{critical}$ within t_1 and t_2.

The dotted line in the left figure represents the decay signal which is subtracted from the original signal. Subsequently, the "decayed" representation of these waveforms are plotted on the right figure labels as I′, II′, and III′. To be consistent with the above case, the threshold is held at $T_{critical}$. One thing that becomes immediately clear is that the range which $T_{critical}$ is valid has expanded to t_1' and t_2'. Because the margin in time $(t_1' - t_2') >> (t_1 - t_2)$, the threshold $T_{critical}$ has a larger margin of error. However, the trade-off is that the region which threshold $T_{critical}$ is valid has been delayed from $[t_1, t_2]$ to

$[t_1', t_2]$. This approach has its disadvantages since early detection may be a critical issue. However, depending on the increase in the margin of error and the relationship between this margin and the timeliness of the decision, decaying the signal may be a useful strategy.

The following is an example to show the improvement in robustness by using the signal decay. The top graph is the original undecayed combined rectified energy signals of the angle collisions at various speeds. The magnitudes of the signals are very similar, and the threshold must be able to distinguish the 20-mph deploy event (yellow) from the 15-mph non-deploy event (green). The bottom graph contains the decayed version of the same signals where each has been decayed by a 2^{nd} degree function. The separation between the deploy and the non-deploy signals widens, and the threshold shown in the graph is more robust.

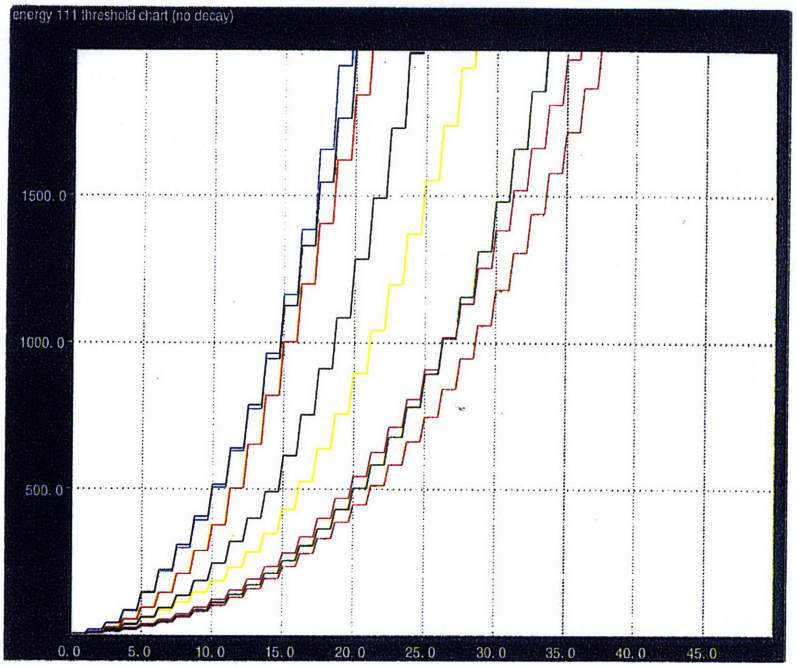

Figure 25a:
Original Combined
Rectified Energy

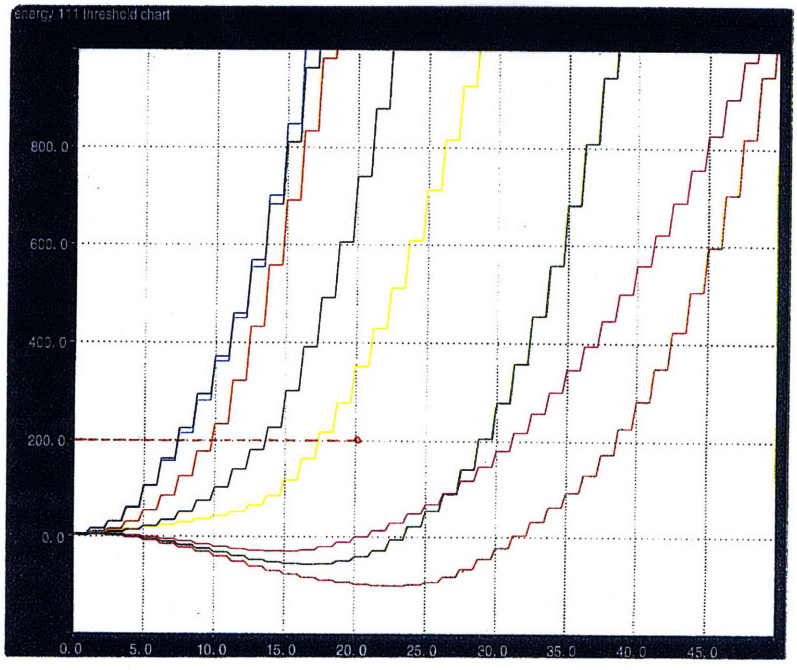

Figure 25b:
Decayed Combined
Rectified Energy

Figure 25: Combined Rectified Energy 111, Before and After the Decay

In the above case, however, the threshold is bounded by t_2, a time when the threshold $T_{critical}$ is no longer valid. However, a more advanced decay strategy can eliminate the dependency on timing.

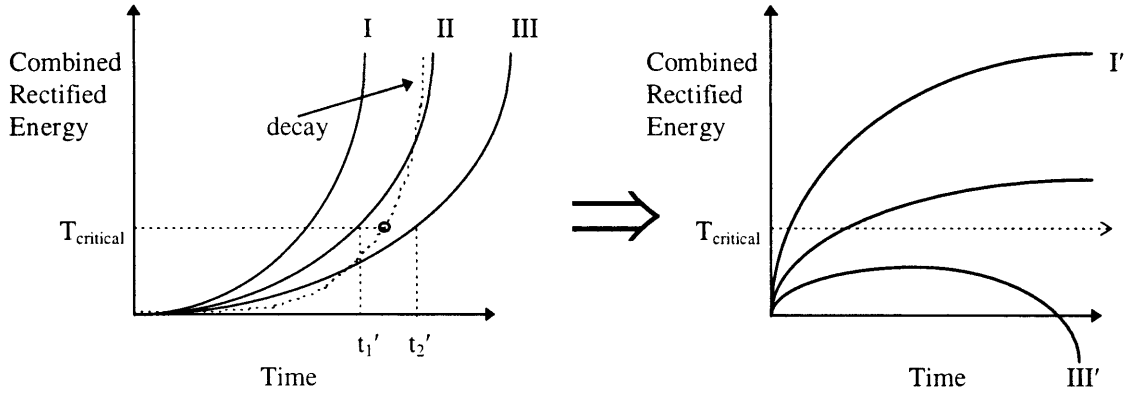

Figure 26: Advanced Signal Decay

In the above figure, the task is again to separate crash signal II from crash signal III. The decay function, unlike the previous case, has higher degree than the original signal. Consequently, the resulting decayed signals no longer behave like positively-sloped higher degree polynomial functions. Instead, the waveform reaches a local maximum after a period of time, depending on the degree of severity of the original signal and the magnitude of the decay, and begins to decline. The advantage of this approach, as the graph indicates, is that the local maxima are clearly separated from each other. In addition, assuming that the original signals can be represented as *n*th degree polynomial functions and the decay function is of (n+1)th order or higher, the local maxima shown above are the absolute maxima. In other words, the magnitude threshold $T_{critical}$ no longer has a time limit. This limits the complexity of the threshold requirements and is easier to implement.

However, the drawback of the high-order exponential decay is in the amount of computational power needed for the implementation. The numerical computation required is proportional to n. In the later section, the calculation of combined rectified energy is discussed in more details.

6.3.1.2.4.2.2. *Combined rectified energy calculation*

Before defining the combined rectified energy, the following is a brief summary all the components of the rectified energy.

IACC_LONG = Integrated rectified ACCeleration_LONGitudinal = $\int$ | longitudinal acceleration |

IACC_LAT = Integrated rectified ACCeleration_LATeral = $\int$ | lateral acceleration |

IACC_VER = Integrated rectified ACCeleration_VERtical = $\int$ | vertical acceleration |

IVEL_LONG = Integrated rectified VELocity_LONGitudinal = $\int$ | longitudinal velocity |

IVEL_LAT = Integrated rectified VELocity_LATeral = $\int$ | lateral velocity |

IVEL_VER = Integrated rectified VELocity_VERtical = $\int$ | vertical velocity |

Instantaneous Combined Rectified Energy =

ENRG[t] = IACC_LONG[t] + IACC_LAT[t] + IACC_VER[t]

= $\int$ | longitudinal acceleration[t] | +

$\int$ | lateral acceleration[t] | +

$\int$ | vertical acceleration[t] |

Accumulated Decayed Combined Rectified Energy =

ENRG_DCY[t] = ENRG_DCY[t-1] + ENRG[t] - t

For simplicity, the decay function is derived from the time index. As the algorithm proceeds, the internal clock maintains the time index of the present sample point. In other words, the decay introduced into the combined rectified energy measure is the value of the running time.

$$ENRG\_DCY[t] = \sum_{n=o}^{n=t} ENRG[n] - n$$

$$ENRG\_DCY[t] = \sum_{n=0}^{n=t} ENRG[n] - \sum_{n=o}^{n=t} n$$

$$ENRG\_DCY[t] = \sum_{n=0}^{n=t} ENRG[n] - \frac{t(t+1)}{2}$$

$$ENRG\_DCY[t] = \sum_{n=0}^{n=t} ENRG[n] - \frac{t^2+t}{2}$$

Mathematically, the decayed combined rectified energy measure is summation of the instantaneous rectified energy less the time counter. Through the derivation above, the decayed combined rectified energy measure can be represented as the integrated rectified energy decayed by a 2nd degree function, namely $(t^2+t)/2$.

The following pseudo-code is a representation of how the decayed combined rectified energy is implemented in the algorithm.

```
For (time = 0, time < total_length_of_time, t++)
{
  accumulated_decayed_combined_rectified_energy =
    accumulated_decayed_combined_rectified_energy + raw_combined_rectified_energy - time
}
```

The decay function, which is 2nd degree, is not calculated separately and subtracted from the measure. The above implementation is short and simple, and at the same time, it saves computational steps.

6.3.1.3. *Vertical Requirements*

Unlike the lateral signals, the vertical acceleration in general is much weaker and uneventful. In addition, while the vehicle is capable of having permanent longitudinal and lateral movements, any movement in the vertical direction is only temporary. The net displacement in the vertical direction must be zero.

6.3.1.3.1. *Vertical velocity*

Since the vertical acceleration signal is noisy, the velocity signal is easier to analyze. The vertical velocity plots can be found in appendix A. Appendix A contains the longitudinal, lateral, and vertical velocity plots of typical frontal, angle, and pole collisions. Specifically, the vertical velocity signals of frontal, angle, and pole collisions can be found in plots 3, 6, and 9, respectively .

The magnitude of the vertical velocity of frontal collisions is large compared to other types of collisions. In addition, it also appears to have higher degrees of oscillation. In general, the vertical velocities of the frontal collisions are negative, suggesting that vehicles are moving upwards. As the severity of the collision increases, the larger this upward velocity becomes. For milder, non-deploy frontal events, the vertical velocity is near zero, and in one case, the velocity is positive. Furthermore, for most cases, the vertical velocity remains mostly negative for a period of approximately 40-50 milliseconds after the bumper contact.

However, these observations are no longer valid in the cases of angle collisions. The high speed angle collision has a pattern of its own. In the first 15 milliseconds, the vertical velocity decreases linearly. Then, the velocity beings to rebound and increase for the next 20-25 milliseconds after which it begins to decline again. It is difficult to generate a reasonable explanation for this phenomenon, and it is likely that the behavior is restricted to the specific platform of the vehicle.

Lastly, the vertical velocity of the pole collisions has the weakest magnitude. From the graphs, it appears that the signals have a general pattern similar to that of the severe angle collisions. Furthermore, although the margin of separation between the deploy and the non-deploy pole collisions is not as large as in the cases of frontal or angle collisions, it appears that the magnitude of the vertical velocities of the high speed pole collisions is separable from the low speed angle and low speed frontal collisions. It is not important if the algorithm can properly classify the type of collision involved. The algorithm is designed to distinguish the deploy events from the non-deploy events. Therefore, the vertical velocity may allow the algorithm to differentiate a deploy from a non-deploy event (deploying a high speed pole collisions

while rejecting the low speed frontal and angle collisions) without determining the type of collision involved.

In order to detect these patterns, a single threshold becomes insufficient. To catch multiple peaks in the signal or depict a characterization which is time-dependent, multiple thresholds are needed. For example, to catch the oscillating vertical velocity of the angle collisions would require dual thresholds. The first threshold, which is valid for a short period of time, intends to catch the first dip of the velocity signal. The second threshold, which is valid only after the first threshold has expired, attempts to catch the later rise of the velocity. However, the pattern recognition is satisfied of both thresholds have been crossed. The specifications of the thresholds are discussed in the later section.

6.3.1.3.2. *Vertical rectified energy*

The vertical rectified energy is represented by the integrating the vertical rectified acceleration signal or the velocity signal. However, because the net displacement in the vertical direction is zero, the vertical velocity signal does not tend toward positive or negative. Therefore, it is not necessary to calculate the rectified energy by integrating the rectified vertical velocity.

The following is a composite of the vertical integrated rectified energy of different types of collisions. The collisions are divided into six categories: high speed frontal, high speed angle, high speed pole, low speed frontal, low speed angle, and low speed pole collisions. In each category, a few representative crashes are chosen. The region enclosed by two same color lines represents where all the collisions of the same type falls. This graph illustrates the separation in the regions where different types of collisions fall and facilitates the threshold definition.

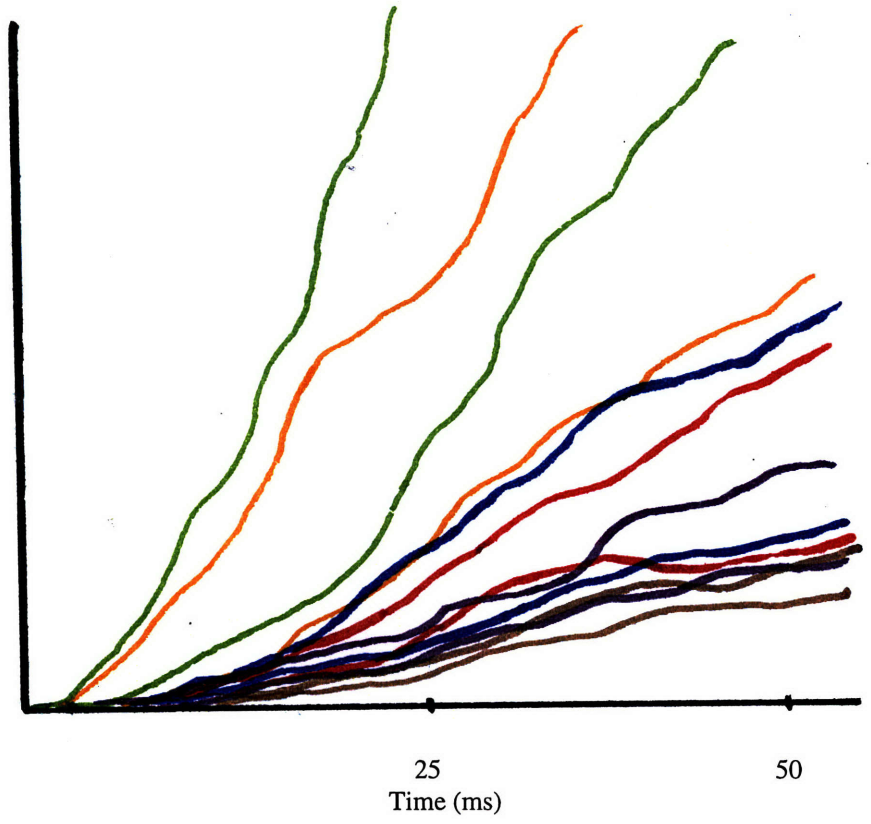

Figure 27: Composite of the Vertical Integrated Rectified Acceleration

Overall speaking, the region of the rectified energy of the high pole collisions is *higher* in magnitude compared to the regions of low speed frontal, angle, and low speed pole collisions. However, as the plot shows, the region of the rectified energy of high speed pole collisions is not clearly separated from the regions of other collisions. Frequent sharing and intersecting of the border of these regions suggest that it is difficult to establish the thresholds such that the most severe non-deploy event is not mistaken as a deploy event and the least severe deploy event can be detected.

6.3.2. Structure of the Algorithm

The purpose of the above discuss and analysis is to establish the characterizations of the different crash scenarios using the additional lateral and vertical signals. Given that each crash scenario has a distinct set of characteristics, criteria thresholds are used to distinguish these characterizations and identify the type and the severity of the collision.

Because the full frontal collisions are well established and easy to identify, the primary goal of the algorithm is to identify angle and pole collisions. Therefore, the algorithm is divided into two sections. The first section of the algorithm scans for the characterizations of an angle collision and determine the severity if a collision is detected. The second section looks specifically for the characterizations of a pole collision. The two sections are independent from each other, and they are executed concurrently within the algorithm. A deployment decision from either section, which suggests that either a severe angle or pole collision has been detected, triggers the deployment of the airbag.

6.3.2.1. *Angle Collision Detection*

The function of the angle collision detection algorithm is to scan and detect the severe angle collisions. It is likely that this section of the algorithm is not able to detect the severe frontal or pole collisions, but these other types of collisions are the main targets of other sections of the algorithm. Nevertheless, all sections must be able to recognize the non-deploy events which include the low speed frontal, angle, and pole collisions as well as the rough road events.

There are total of 12 criteria used to detect the severe angle collisions, and these criteria are selected based on their ability to separate the severe angle collisions from the others. The criteria are listed in the table below. Depending on the needs of the characterization process, these criteria are implemented using both crossing and latching thresholds.

Crossing Criteria

VEL = longitudinal velocity
OSC = longitudinal oscillation
ACCW = filtered longitudinal acceleration
SLP = slope of the longitudinal acceleration
IACCL = integrated lateral acceleration
IACCV = integrated vertical acceleration
IVELL = integrated lateral velocity
ENRG_DCY = decayed combined rectified energy
CONS = consistency of the velocity

Latching Criteria

L_SLPLATCH = slope of the lateral velocity
DIPLATCH = presence of the dip
VELVLATCH = vertical velocity

Once the criteria are selected and the threshold conditions are established, the threshold levels must be calibrated. Eight representative crash signals are used to calibrate the thresholds. There are three high speed and three low speed angle collisions, and one high speed and one low speed frontal collisions selected as the calibration crashes. The calibration process involves setting and adjusting the criteria thresholds using the seven crash signals as the deployment guideline. Once the thresholds are established such that these eight events are correctly identified and the deployment decisions are timely, more extensive simulation and evaluation of these thresholds are carried out using all the available crash data. If undesirable results are encountered during this extensive testing phase, the thresholds are reexamined and improved. Furthermore, the results of the extensive testing are presented in the results section as well as in Appendix C. The analysis of the results is carried out later in the evaluation section.

The exact threshold levels used in the algorithm are available in appendix B. Appendix B contains a set of plots where each plot represents a criteria threshold used in the algorithm. The plots contain the seven crashes described earlier, and on each plot, the threshold(s) of the criteria is(are) plotted. The plots demonstrates how the thresholds are determined, and in some cases, it also shows the special considerations needed to calibrate the thresholds.

In order to ensure the validity of the deployment decision, *all* threshold requirements must be met in order to trigger the airbag. Other methods of arriving at the deployment decision include requiring

only a number of threshold conditions are met or calculate the overall severity measure by assigning arbitrary weight to the threshold conditions. Both of these methods try to introduce more flexibility into the algorithm, but at the same time, they increase the margin of error. By requiring that all the threshold conditions are met, the algorithm can consistently reject all the non-deploy events.

Since the deployment logic requires that all the threshold conditions are crossed *simultaneously*, latches are used to detect the one time events. An example of the one time event is the dip in the lateral velocity. Once the dip is detected, a latch is set indicating that a dip has been detected. The latch will stay true until the algorithm has been reset. Consequently, although the dip measure may not indicate the presence of a dip at a later time when all the other threshold conditions are met, the dip latch will indicate that a dip has been detected.

6.3.2.2. *Pole Collision Detection*

The pole collision detection section is aimed at detecting high severity pole collisions while being able to remain immune to the non-deploy events. The structure of the pole collision detection algorithm is very similar to that of the angle collision detection. While the deployment logic (deployment is true if *all* the criteria are satisfied simultaneously) remains the same, the criteria used are slight different from those used for the angle detection. The ten criteria used are those which provide the greatest ability to detect pole collisions, and since the lateral signals of a pole collision are weak, the emphasis of the algorithm is placed on the vertical signals.

Following is a list of some of the crossing and the latching criteria.

Crossing Criteria	Latching Criteria
VEL = longitudinal velocity	VELVLATCH = vertical velocity
OSC = longitudinal oscillation	DSPVLATCH = vertical displacement
ACCW = filtered longitudinal acceleration	
SLP = slope of the longitudinal acceleration	
IACCL = integrated lateral acceleration	
IACCV = integrated vertical acceleration	
ENRG_DCY = decayed combined rectified energy	
DSPV = vertical displacement	

Similarly, nine crash events are selected to calibrate the threshold levels. The events selected are three high speed and one low speed pole events, one high speed and two low speed angle collisions, and two low speed frontal collisions. Appendix B also contains the criteria/threshold plots of all the criteria used in the pole collision detection algorithm. The performance results are discussed in results section, and the analysis is presented in the evaluation section.

Chapter 7

7. RESULTS

7.1. Initial Results

The multi-axes crash detection algorithm is divided into the angle collision detection and the pole collision detection sections, and each section is tested separately. The thresholds of each section are detailed in Appendix B, and the testing of the algorithm consists of two phases: the initial validity assessment phase and the extensive testing phase.

The validity assessment selects a few crashes to understand the behavior of the algorithm and to establish the baseline timeliness performance. The initial assessment is carried out using eight angle

collisions. The angle of these eight collisions are constant at 30°, but the velocity varies from 9 mph to 30 mph. Following is a chart detailing the performance of the new algorithm compared to the required triggering time and the performance of the single-axis algorithm.

Crash Sequence type - speed - seq. #	Desired Deploy Time (ms)	Single-Axis Algorithm (ms)	Multi-Axes Algorithm (ms)
30° Angle - 30 mph - 01	36	26	17
30° Angle - 30 mph - 02	36	22	17
30° Angle - 30 mph - 03	36	28	23
30° Angle - 30 mph - 04	36	18	22
30° Angle - 20 mph - 01	44	33	33
30° Angle - 15 mph - 01	no trigger	no trigger	no trigger
30° Angle - 12 mph - 01	no trigger	no trigger	no trigger
30° Angle - 9 mph - 01	no trigger	no trigger	no trigger

Table 1: Initial Results - Angle Collision Detection

In all these collisions, the multi-axes algorithm met the required triggering time in all deploy events, and furthermore, the time required to reach the deployment decision is shorter compared to the performance of the single-axis algorithm. The second phase of the evaluation subjects the algorithm to all available crash data within the vehicle platform, and in addition to timeliness, the robustness of the algorithm is also evaluated.

The evaluation of the pole collision detection section is similar to above. However, nine pole collisions are used, and the velocity ranges from 10 mph to 30 mph.

Crash Sequence type - speed - seq. #	Desired Deploy time (ms)	Single-Axis Algorithm (ms)	Multi-Axes Algorithm (ms)
pole - 30 mph - 01	43	43	35
pole - 30 mph - 02	43	41	64
pole - 25 mph - 01	56	36	38
pole - 21 mph - 01	75	75	71
pole - 18 mph - 01	75	no trigger	no trigger
pole - 18 mph - 02	75	88	92
pole - 15 mph - 01	no trigger	no trigger	no trigger
pole - 14 mph - 01	no trigger	no trigger	no trigger
pole - 10 mph - 01	no trigger	no trigger	no trigger

Table 2: Initial Results - Pole Collision Detection

In general, the results of the pole collision detection are comparable to the performance of the current algorithm. However, in some cases, the performance of the multi-axes algorithm is worse than the single-axis algorithm, suggesting that using the lateral and vertical components as the primary criteria for crash detection is not better than using only the longitudinal component.

Even after the thresholds have been calibrated to provide the best results, the performance of the pole collision detection remains undesirable. Not only did the algorithm fail to detect a deploy event, in other deploy events, the algorithm failed to reach the deployment decision on time. Further testing conducted revealed similar non-beneficial performances. Therefore, this section of the algorithm was not subjected to extensive testing, and the reason for poor performance is discussed in the evaluation section.

7.2. Complete Crash Detection Statistics

After it has demonstrated validity in the initial testing, the angle collision detection algorithm is then tested against the angle deploy events as well as *all* the non-deploy events. Because this section of the algorithm is aimed at sensing only the severe angle collisions and rejecting all the non-deploy events, it does not need to detect severe frontal or severe pole collisions.

Once the algorithm is tested against all severe angle collisions and all non-deploy events, the robustness is evaluated by varying the magnitudes of these crash signals. These signals are varied by a constant coefficient ranging from 0.1 to 1.5 in the increments of 0.1. The complete record of the extensive testing is available in appendix C.

In order to understand the enhancement, the performance of the single-axis (longitudinal) algorithm is used as a control algorithm. Specifically, a version of the single-axis crash sensing algorithm is used for comparison. The algorithm is subjected to all the evaluation performed on the angle collision detection section, and the complete results are presented side by side to the multi-axes algorithm in appendix C. The analysis of the performance is discussed in the evaluation section.

7.2.1. Timeliness of the Deployment

7.2.1.1. *Angle collisions - single-axis algorithm vs. multi-axes algorithm*

Overall, the angle collision detection algorithm performs well in detecting the severe angle collisions. It has detected all the severe angle collision approximately 10-15 milliseconds faster than the required time. In addition, compared to the single-directional algorithm, new algorithm is faster by 5-8 milliseconds. Lastly, the multi-axes algorithm does not deploy in the case of the 15 mph angle collision in which the original algorithm improperly deploys.

It has been discussed in previous section that early deployment can dampen the effectiveness of the airbags. Therefore, it is undesirable that the algorithm deploys the airbag approximately 10-15 seconds faster than the required time. However, this extra time can serve as a margin for error. Specifically, there are two ways to capitalize this margin. First, because the crash signals are crossing the thresholds early, the threshold levels can be raised to delay the deployment. By raising the deployment thresholds, the algorithm can be further immunized from non-deploy events. Second, the deployment event can be delayed by an arbitrary amount of time. Within this period, another set of thresholds can be used to check the validity of the deployment decision thus increasing the robustness of the algorithm.

7.2.1.2. *pole collisions - single-axis algorithm vs. multi-axes algorithm*

The pole collision detection of the new algorithm performed poorly compared to the single-directional algorithm. It had failed to detect one severe pole collision, and in many other cases, the time required to come to the deployment decision is worse than the present algorithm.

There are several reasons for the poor performance. First, even in a severe pole collision, the lateral signal is almost zero in the initial 40-50 milliseconds of the collision. Therefore, the thresholds imposed on the lateral signals were low which resulted in a lack of robustness. Second, although the vertical signals were speculated to be useful in depicting the pole collisions, the margin for errors was very small. Specifically, the vertical velocity of the severe pole collisions can be separated from the low speed frontal, angle, and pole collisions. However, the degree of separation is small which causes the algorithm to be sensitive to noise and inherent variations in the signals. The vertical energy also had very small margin for errors.

7.2.2. Robustness of the Algorithm | angle collisions - single-axis algorithm vs. multi-axes algorithm

The robustness of the algorithm was tested by altering the original signal using a constant coefficient ranging from 0.1 to 1.5 in the increments of 0.1. For the new algorithm, the data showed a very consistent behavior. As the magnitude of the crash signal is increased, the amount of time needed for deployment decreases and vise versa. However, in the cases when the magnitude of the crash signal is decreased, there is a point where the algorithm should fail to deploy the airbag. For the 30 mph, 30° angle collisions, the algorithm failed to deploy when the magnitude was decreased to approximately 50% of the original. This may be comparable to a 15-mph angle collision which is the deployment threshold velocity of the angle collisions[22]. However, in all the non-deploy events, the algorithm did not trigger even when the signals had been increased by 50%.

The robustness of the single-directional algorithm showed the same consistent behavior when the magnitude of the signal was decreased. However, as the magnitudes of the non-deploy events were increased, some began to trigger. Specifically, the 10 mph angle collision begins to trigger when the magnitude is raised by 30% and the 15 mph angle collision triggers when the magnitude is raised by 20%.

With the respective percentage increase in the signals, the increase in the severity causes the collisions to become deploy events.

The weakness of the new algorithm lies in the robustness when the magnitude of the non-deploy events are increased. However, this may be caused by the characterizations of the crash signals. The selected method to test robustness relies heavily on the linearity of the crash signals. However, many thresholds used were time dependent, because certain characterizations of the angle collision is directly related to the amount of time elapsed since the start of the collision. It may be true that linearity persists in a smaller time frame, but the exact time the linearity fails to hold true remains unknown. Therefore, without appropriately scaling the time of the signal, it is difficult to assess precisely the validity of the robustness measure of altering only the magnitude.

7.3. Rough Road Discrimination

In addition to separating the low speed, non-deploy frontal, angle, and pole collisions, the algorithm must also be able to identify the rough road events. The angle detection section of the algorithm was subjected to a series of rough road events. The initial results are shown in the following table.

Rough Road Description	Scale	Single-axis Algorithm (ms)	Multi-axes Algorithm (ms)
3 lb. hammer, #2 bar	2.0	NT	NT
3 lb. hammer, front of SDM	2.0	NT	63
3 lb. hammer, center tunnel	2.0	NT	70
3 lb. hammer, center stabilizer	2.0	NT	NT
3 lb. hammer, #2 bar near SDM	2.0	NT	NT
3 lb. hammer, tunnel @#2 bar	2.0	NT	70
8 lb. hammer, center stabilizer	2.0	NT	NT
12 inch vertical drop	2.0	NT	108
12 inch vertical drop	1.5	NT	108
12 inch vertical drop	1.0	NT	109
hop, panic stop - 30 mph - 01	2.0	NT	218
hop, panic stop - 30 mph - 02	2.0	NT	206
hop, panic stop - 30 mph - 03	1.9	NT	208
tramp, panic stop - 30 mph - 01	2.0	NT	NT
tramp, panic stop - 30 mph - 02	2.0	NT	NT
square block, panic stop - 30 mph	2.0	NT	23
washboard rd. med. brake - 40 mph	2.0	NT	18
left side max. pot hole - 25 mph	2.0	NT	NT
right side max. pot hole - 25 mph	2.0	NT	NT
chatterbumps, panic stop - 60 mph	2.0	NT	41
massoit bump - 45 mph	2.0	NT	NT
curb impact, 5 inches - 5 mph	2.0	NT	NT
curb drop off, 5 inches - 20 mph	2.0	NT	NT
Belgian blocks - 35 mph	2.0	NT	124

Table 3: Initial Results - Rough Road Discrimination using Angle Collision Detection

The results indicate that the method of using the lateral and the vertical components in the angle detection is not immune to the rough road events. During the design phase, the separation of the rough road events was to be achieved through the use of the energy measures. The assumption was that during a rough road event, the total energy dissipated in all three directions is low compared to an actual collision. However, the definition of energy used did not produce the distinction.

In order to achieve better rough road discrimination, the longitudinal thresholds were adjusted. The results are shown in the next table.

Rough Road Description	Scale	Single-axis Algorithm (ms)	Multi-axes Algorithm (ms)
3 lb. hammer, #2 bar	2.0	NT	NT
3 lb. hammer, front of SDM	2.0	NT	NT
3 lb. hammer, center tunnel	2.0	NT	NT
3 lb. hammer, center stabilizer	2.0	NT	NT
3 lb. hammer, #2 bar near SDM	2.0	NT	NT
3 lb. hammer, tunnel @#2 bar	2.0	NT	NT
8 lb. hammer, center stabilizer	2.0	NT	NT
12 inch vertical drop	2.0	NT	NT
12 inch vertical drop	1.5	NT	NT
12 inch vertical drop	1.0	NT	NT
hop, panic stop - 30 mph - 01	2.0	NT	NT
hop, panic stop - 30 mph - 02	2.0	NT	NT
hop, panic stop - 30 mph - 03	1.9	NT	NT
tramp, panic stop - 30 mph - 01	2.0	NT	NT
tramp, panic stop - 30 mph - 02	2.0	NT	NT
square block, panic stop - 30 mph	2.0	NT	**76**
washboard rd. med. brake - 40 mph	2.0	NT	NT
left side max. pot hole - 25 mph	2.0	NT	NT
right side max. pot hole - 25 mph	2.0	NT	NT
chatterbumps, panic stop - 60 mph	2.0	NT	**73**
massoit bump - 45 mph	2.0	NT	NT
curb impact, 5 inches - 5 mph	2.0	NT	NT
curb drop off, 5 inches - 20 mph	2.0	NT	NT
Belgian blocks - 35 mph	2.0	NT	NT

Table 4: Rough Road Events Discrimination Using the Angle Collision Detection

The improvement is clear. After the longitudinal thresholds had been raised by only 10% to 20%, almost all rough road events had been prevented from deploying the airbag. Although there remained a few events which still triggered deployment, it was clear that further adjustments to the thresholds can easily isolate these cases. In addition, these few deploying events are not difficult to distinguish by the single-axis algorithm. Therefore, with more emphasis placed on the longitudinal signals, the rough road events can be separated.

Chapter 8

8. CONCLUSION

The objective of the thesis is to explore and study the possible benefits of using multiple accelerometers in different directions for crash sensing. While some of the existing publications and papers suggest the usefulness of the lateral and the vertical components of the crash signal, the results of the research are often inconclusive. Therefore, some of the approaches from the literature and many original ideas are studied in depth to understand the effectiveness of the lateral and the vertical crash signals.

One approach in using multiple accelerometers for crash detection is to exploit the relationship between these signals. Given the correlation is clear and consistent, the separate components can be

manipulated to maximize the ability to differentiate the severity of the collisions. However, from the available crash data, there is no clear correlation between the signals of different directions, and even in some cases where the correlation exists, it is too weak for any practical purpose.

Another approach is to place the accelerometers along arbitrary axis. By resolving the signals based on geometric laws, the magnitude and the direction of the force of impact can be derived. Using this information, the deployment thresholds can adjusted to accommodate the angle of the collision. In addition, each of the accelerometers placed at an offset angle from the longitudinal direction can be broken down into both the longitudinal and the lateral components. Because of redundancy, the algorithm can function even if one of the accelerometers fails. However, the method used to resolve the signals from the offset accelerometers can be applied to the longitudinal and the lateral signals, thus no new information is available by offsetting the directions of the accelerometers.

The effectiveness of the independent threshold approach depends heavily on the characterizations of the lateral and the vertical signals. If well-defined and consistent characterizations of the different types of collisions can be established using the signals from all directions, both time and magnitude thresholds can be employed to depict these characterizations.

The crashes can be divided roughly into four different categories: full frontal collisions, angle collisions, pole collisions, and rough road events. Each category of events are examined carefully to look for distinctive patterns and measures of severity. The criteria used for examination include acceleration, velocity, displacement, slope, oscillation, and energy. Using these criteria as the skeleton of the algorithm, two subsections were constructed specifically to detect angle and pole collisions.

Overall, high speed angle collisions were detected repeatedly while the pole collisions were more difficult to distinguish. Furthermore, the robustness of the angle collision detection algorithm ensures the benefits and the usefulness of the lateral and the vertical signals.

However, the drawback of using the lateral and the vertical signals for crash detection is in the inability to distinguish the rough road events. Because of the similarities in magnitude and behavior, the lateral and the vertical components of the rough road events can be easily interpreted as those from a

deploy event. The best method to counter this problem is to use the longitudinal signals to differentiate the rough road events.

However, there is one weakness in the conclusions. Because the evaluation did not include other platforms of vehicles, there are doubts as to whether the characterizations are specific to the vehicle. Many characterizations including the slope and the oscillation of the signals, the energy dissipation, and the patterns in the primary criteria can be easily affected by the size, weight, and structure of the vehicle. Since the algorithm was not applied to other platforms, the applicability may be in question.

In conclusion, using multiple accelerometers placed at different directions can better detect and differentiate the types and the severity of the collisions. However, the limiting factors include the inherent inconsistencies in the relationships between the signals, the added complexity and the difficulties, and, finally, the platform-dependency. While the multiple-directional crash sensing algorithm may be effective, the variables and the limitations must be well controlled.

Appendix A

Appendix A contains 9 graphs representing longitudinal, lateral, and vertical velocity signals of typical frontal, angle, and pole collisions. Within each crash category, collisions of various severity are represented. This section is intended to familiarize the readers with the typical crash signals.

Frontal Collisions - Longitudinal Velocity

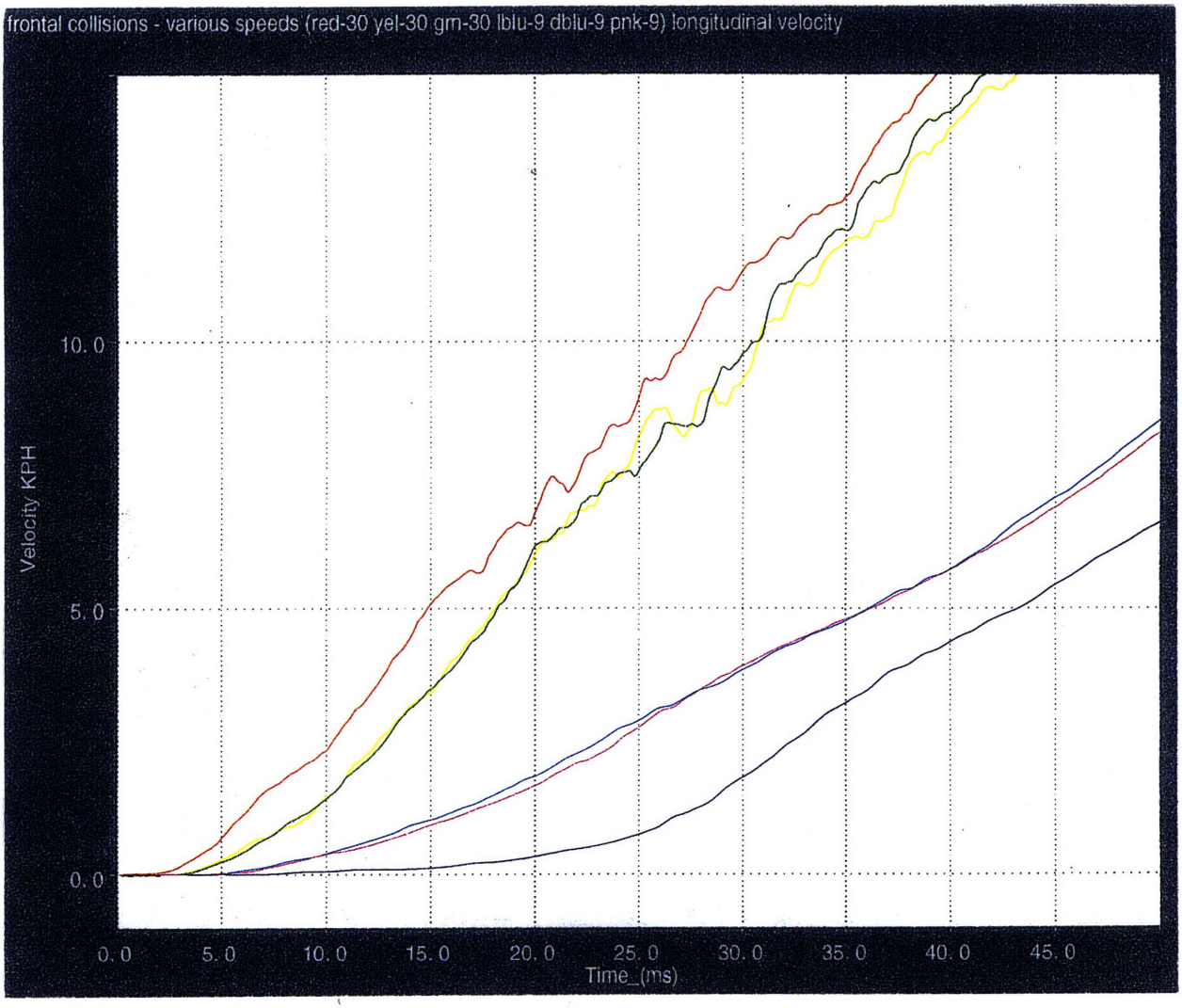

Longitudinal Velocity Signals of Various Frontal Collisions

red	= 30-mph frontal collision *
yellow	= 30-mph frontal collision *
green	= 30-mph frontal collision *
light blue	= 9-mph frontal collision
dark blue	= 9-mph frontal collision
pink	= 9-mph frontal collision

The collisions indicated by the asterisks are deploy events.

Frontal Collisions - Lateral Velocity

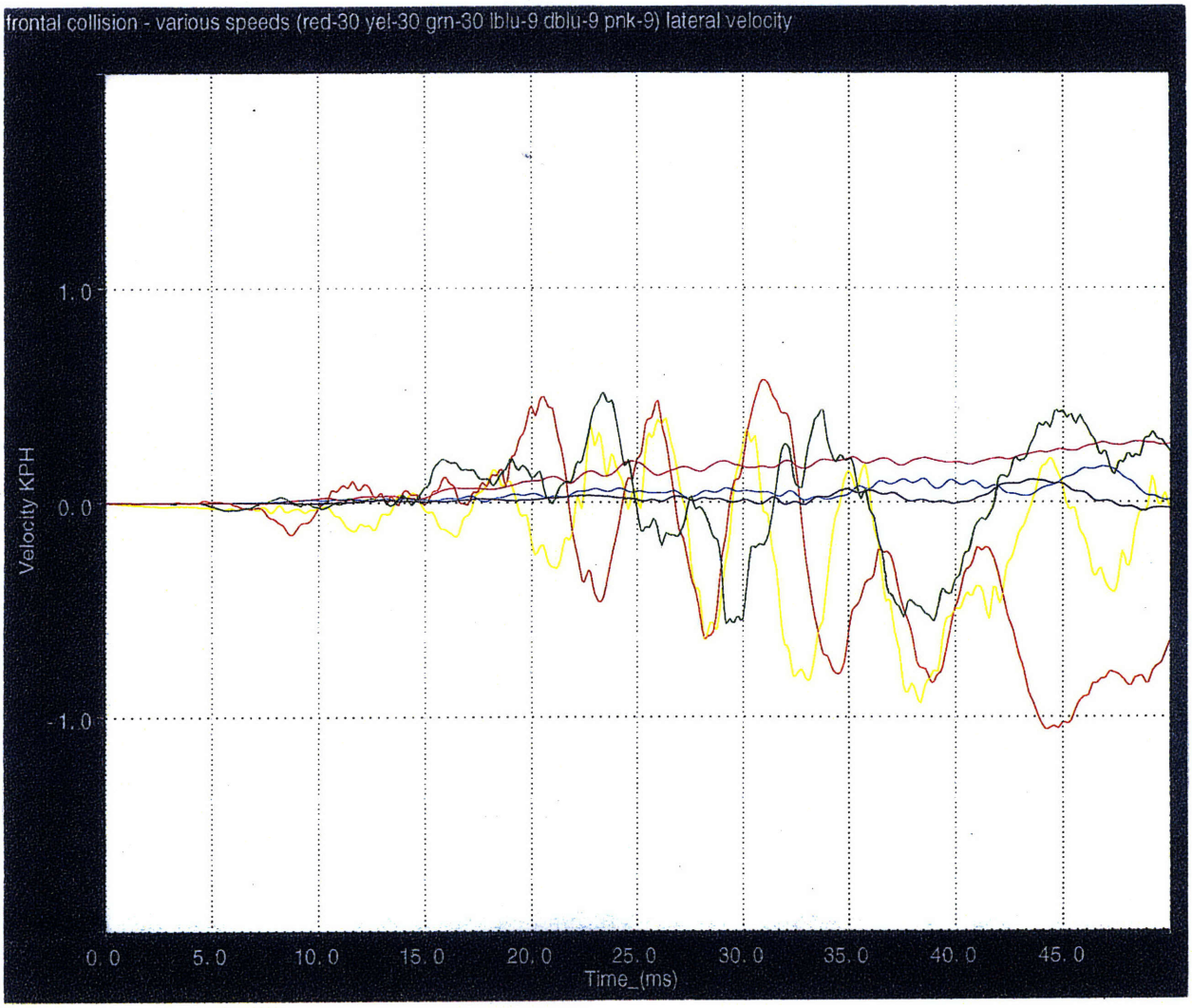

Lateral Velocity Signals of Various Frontal Collisions

red	= 30-mph frontal collision *
yellow	= 30-mph frontal collision *
green	= 30-mph frontal collision *
light blue	= 9-mph frontal collision
dark blue	= 9-mph frontal collision
pink	= 9-mph frontal collision

The collisions indicated by the asterisks are deploy events.

Frontal Collisions - Vertical Velocity

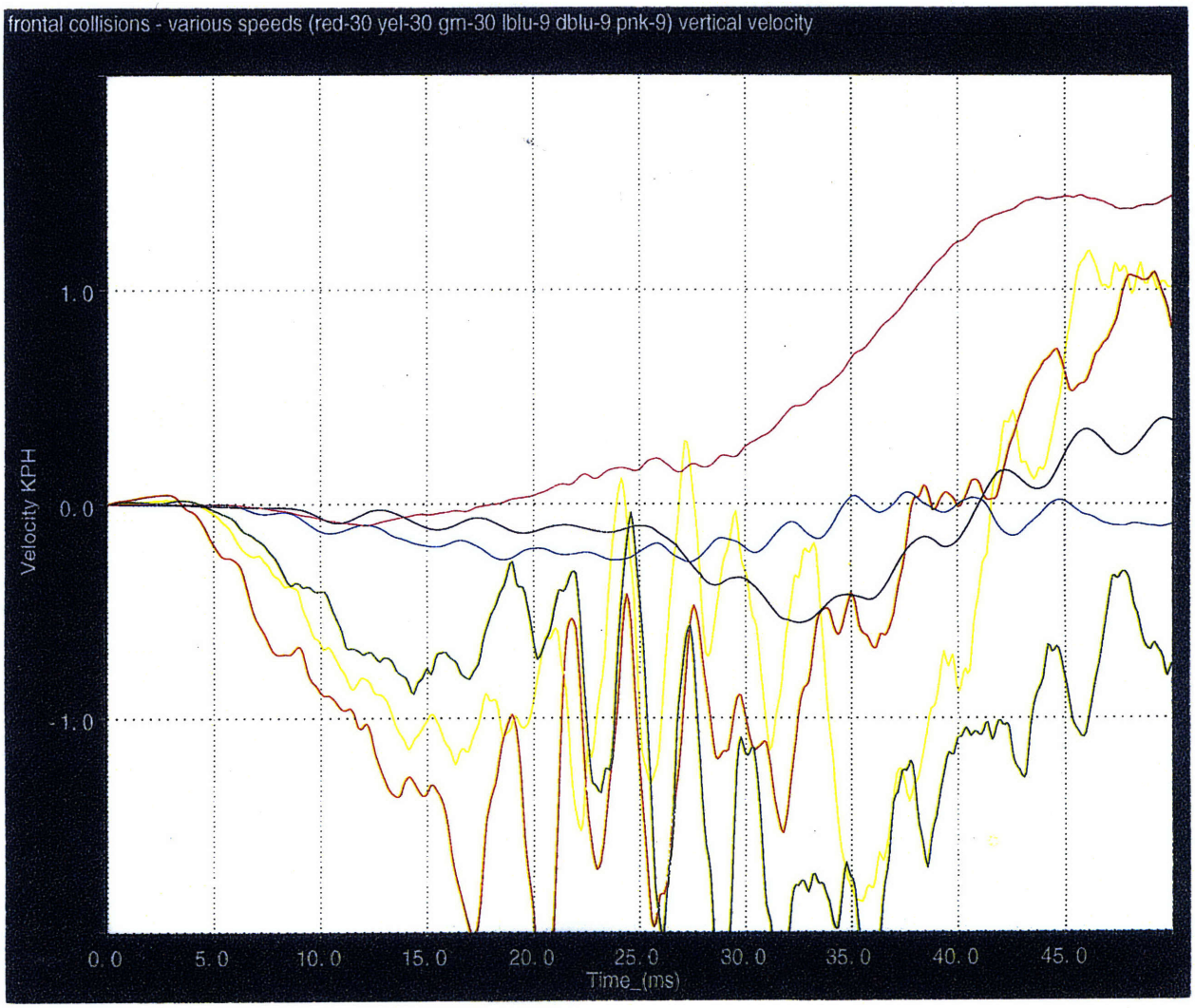

Vertical Velocity Signals of Various Frontal Collisions

red	= 30-mph frontal collision *
yellow	= 30-mph frontal collision *
green	= 30-mph frontal collision *
light blue	= 9-mph frontal collision
dark blue	= 9-mph frontal collision
pink	= 9-mph frontal collision

The collisions indicated by the asterisks are deploy events.

Angle Collisions - Longitudinal Velocity

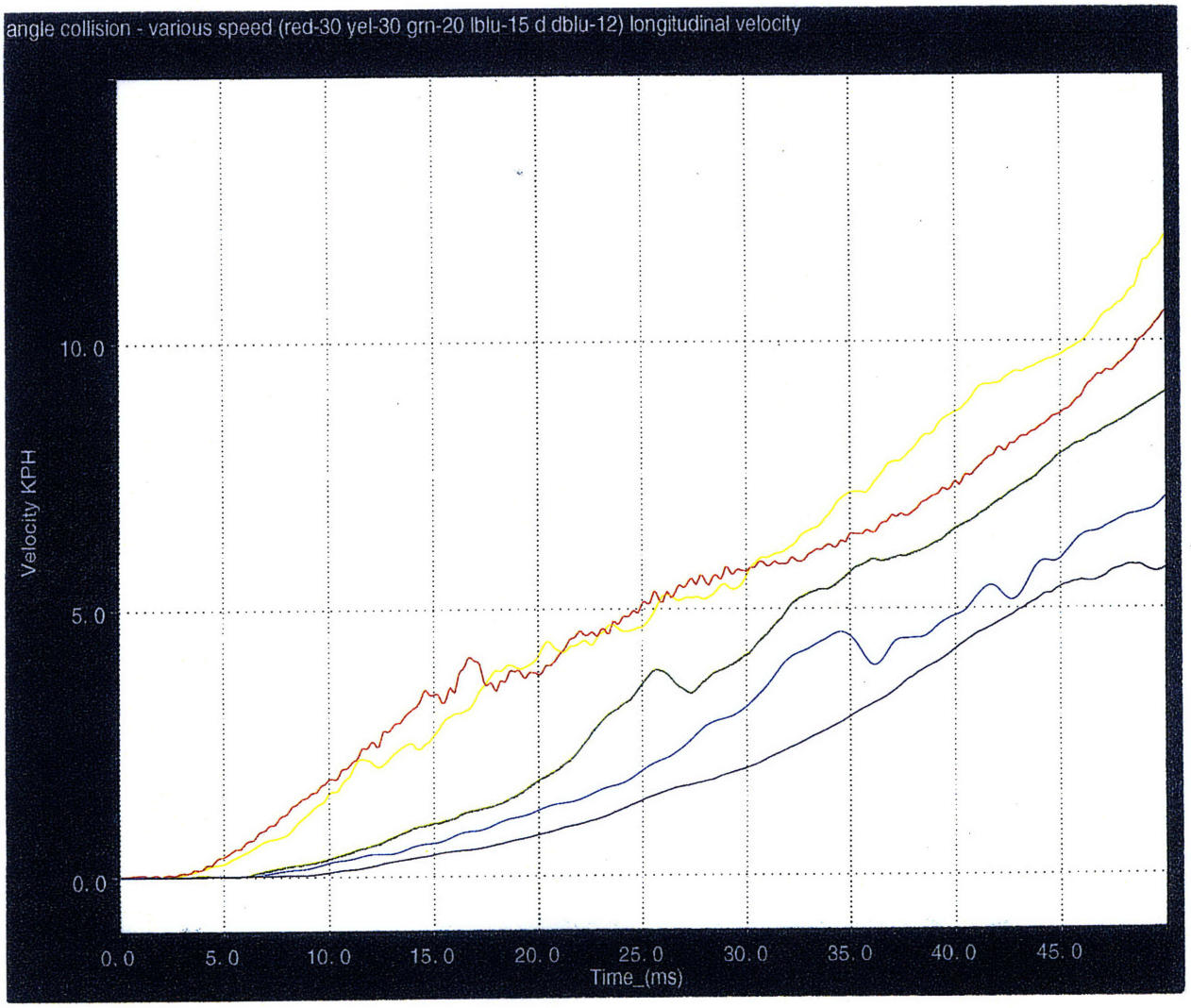

Longitudinal Velocity Signals of Various Angle Collisions

red	= 30-mph, 30° angle collision *
yellow	= 30-mph, 30° angle collision *
green	= 20-mph, 30° angle collision *
light blue	= 15-mph, 30° angle collision
dark blue	= 12-mph, 30° angle collision

The collisions indicated by the asterisks are deploy events.

Angle Collisions - Lateral Velocity

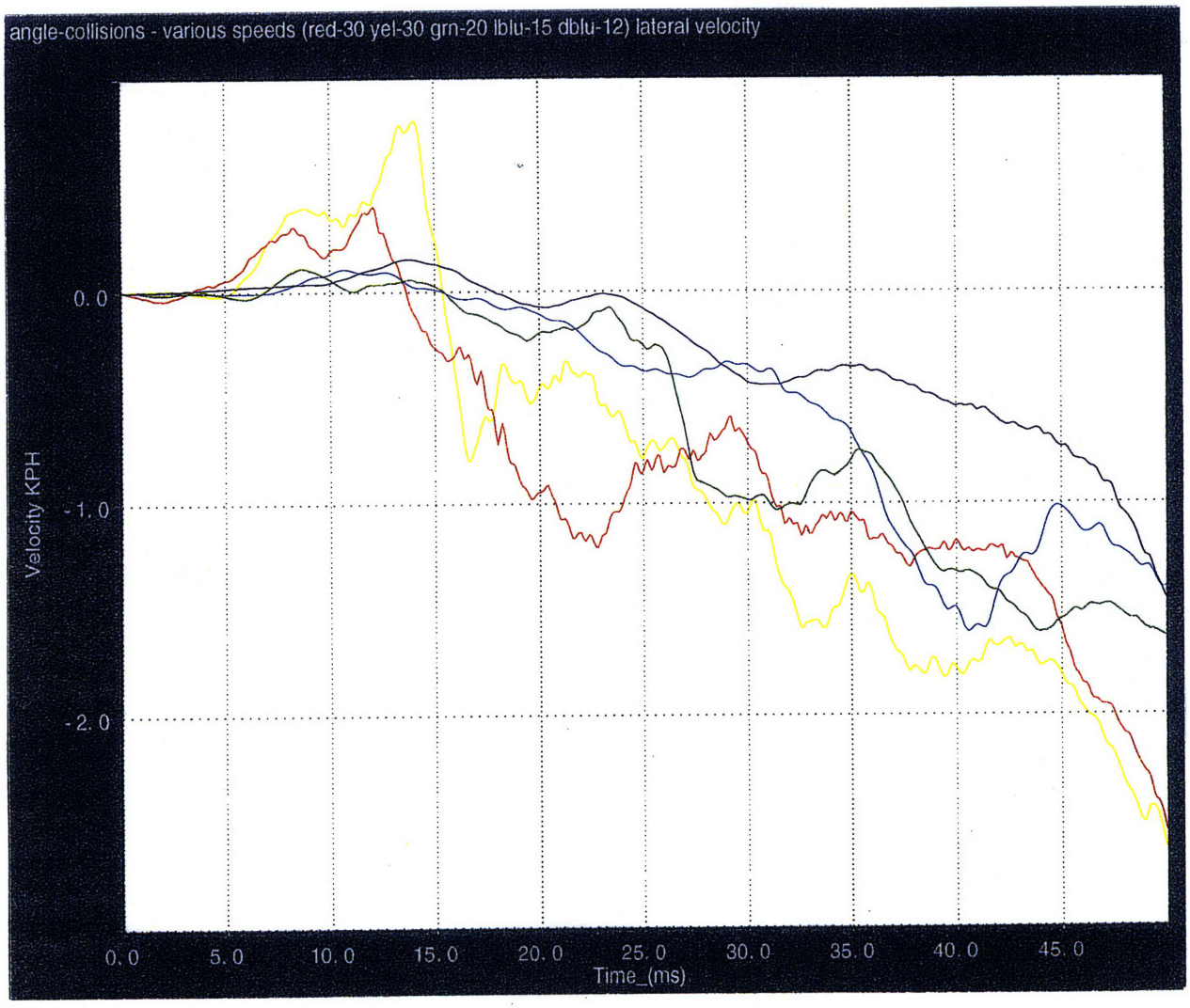

Lateral Velocity Signals of Various Angle Collisions

red = 30-mph, 30° angle collision *
yellow = 30-mph, 30° angle collision *
green = 20-mph, 30° angle collision *
light blue = 15-mph, 30° angle collision
dark blue = 12-mph, 30° angle collision

The collisions indicated by the asterisks are deploy events.

Angle Collisions - Vertical Velocity

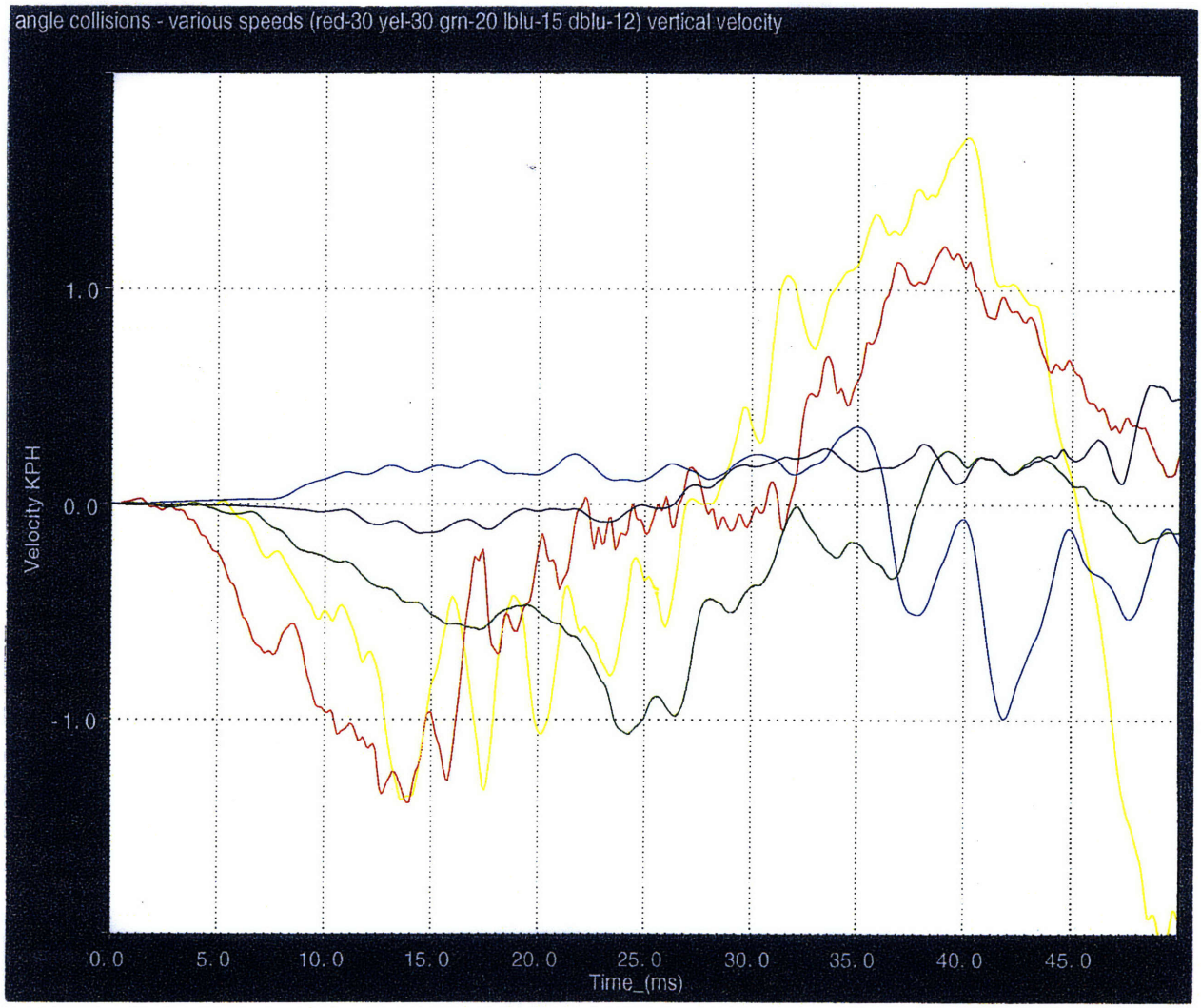

Vertical Velocity Signals of Various Angle Collisions

red	= 30-mph, 30° angle collision *
yellow	= 30-mph, 30° angle collision *
green	= 20-mph, 30° angle collision *
light blue	= 15-mph, 30° angle collision
dark blue	= 12-mph, 30° angle collision

The collisions indicated by the asterisks are deploy events.

Pole Collisions - Longitudinal Velocity

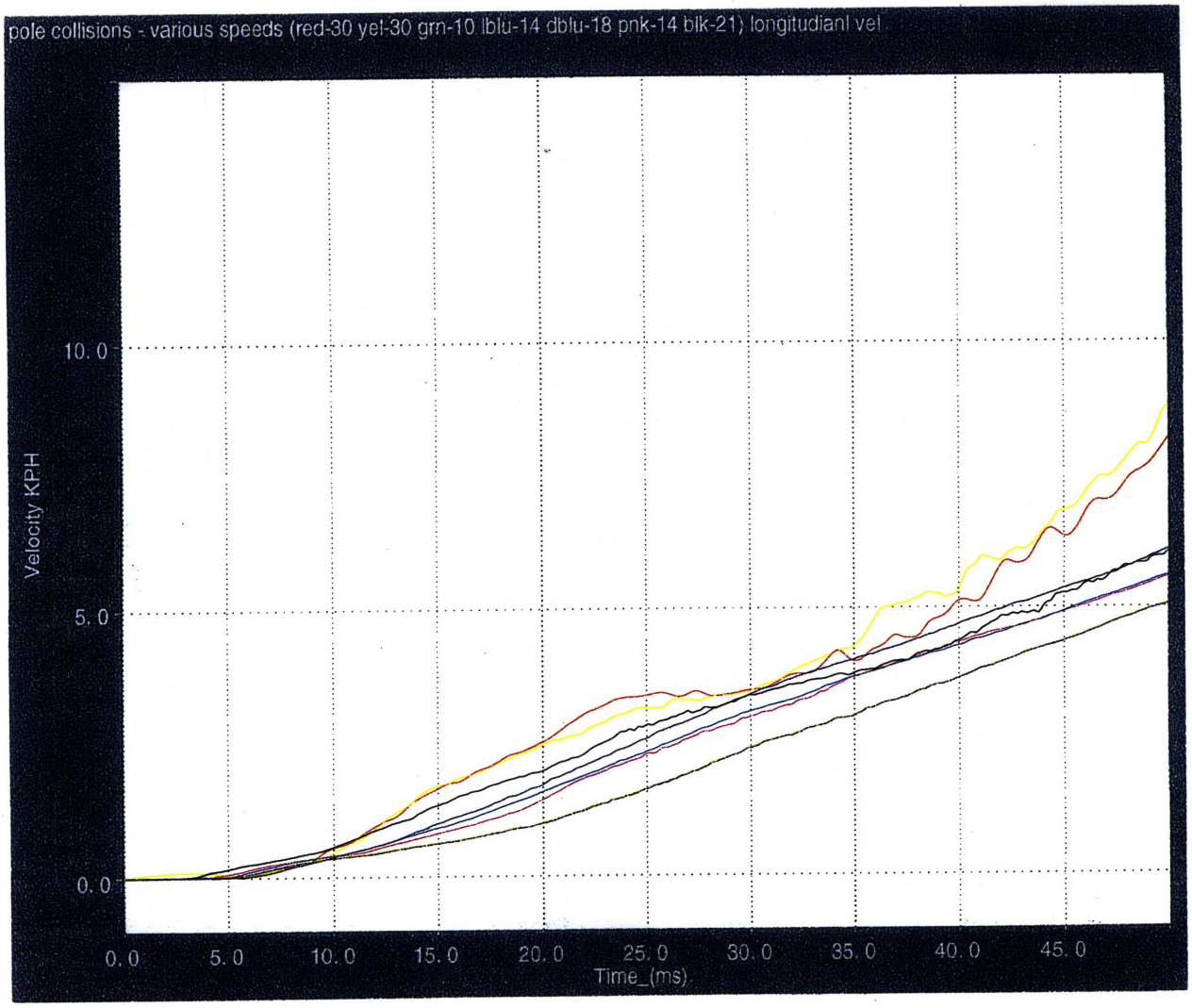

Longitudinal Velocity Signals of Various Pole Collisions

red	= 30-mph pole collisions *
yellow	= 31-mph pole collisions *
black	= 21-mph pole collisions *
dark blue	= 18-mph pole collisions *
light blue	= 14-mph pole collisions
pink	= 14-mph pole collisions
green	= 10-mph pole collisions

The collisions indicated by the asterisks are deploy events.

Pole Collisions - Lateral Velocity

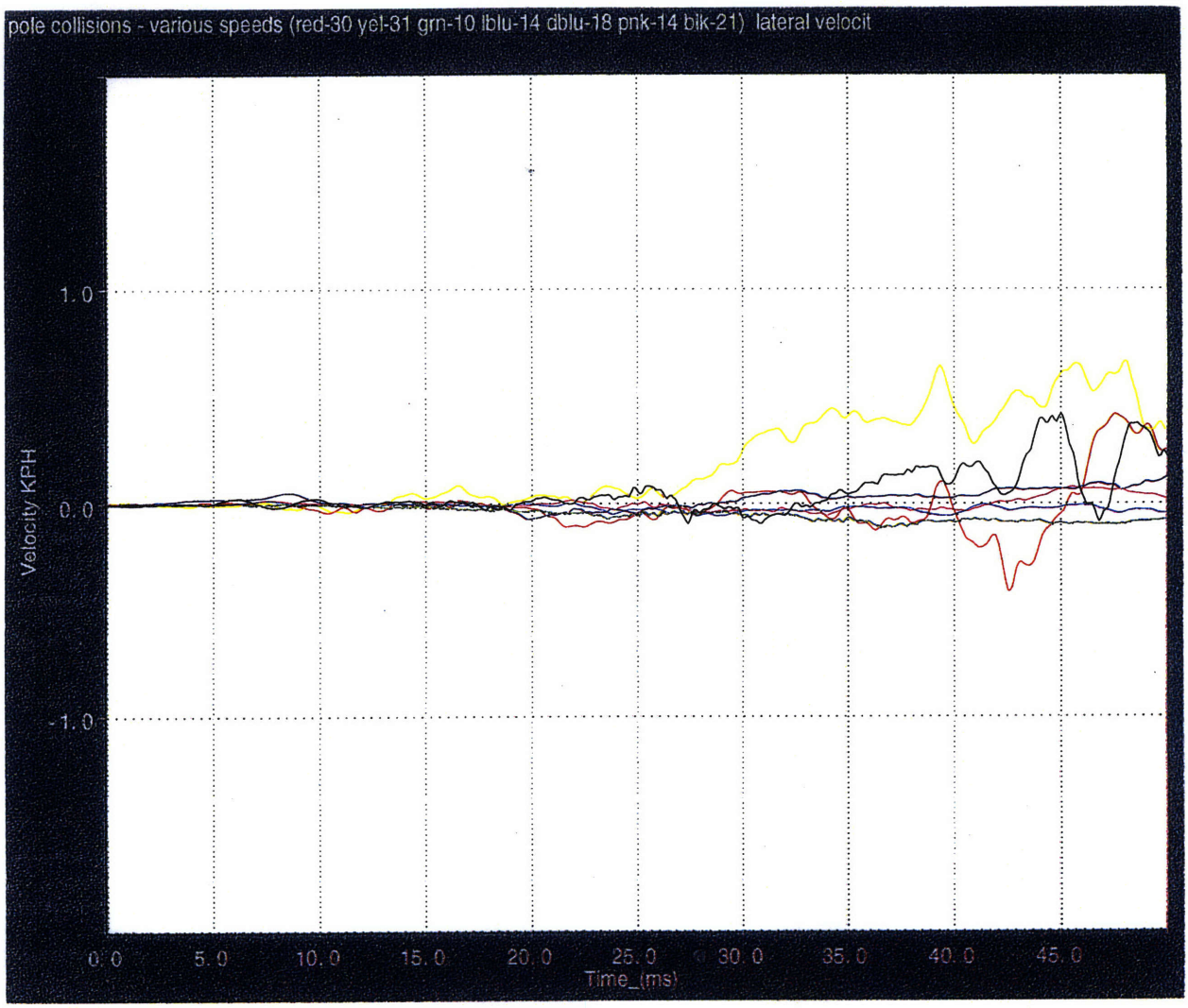

Lateral Velocity Signals of Various Pole Collisions

red	= 30-mph pole collisions *
yellow	= 31-mph pole collisions *
black	= 21-mph pole collisions *
dark blue	= 18-mph pole collisions *
light blue	= 14-mph pole collisions
pink	= 14-mph pole collisions
green	= 10-mph pole collisions

The collisions indicated by the asterisks are deploy events.

Pole Collisions - Vertical Velocity

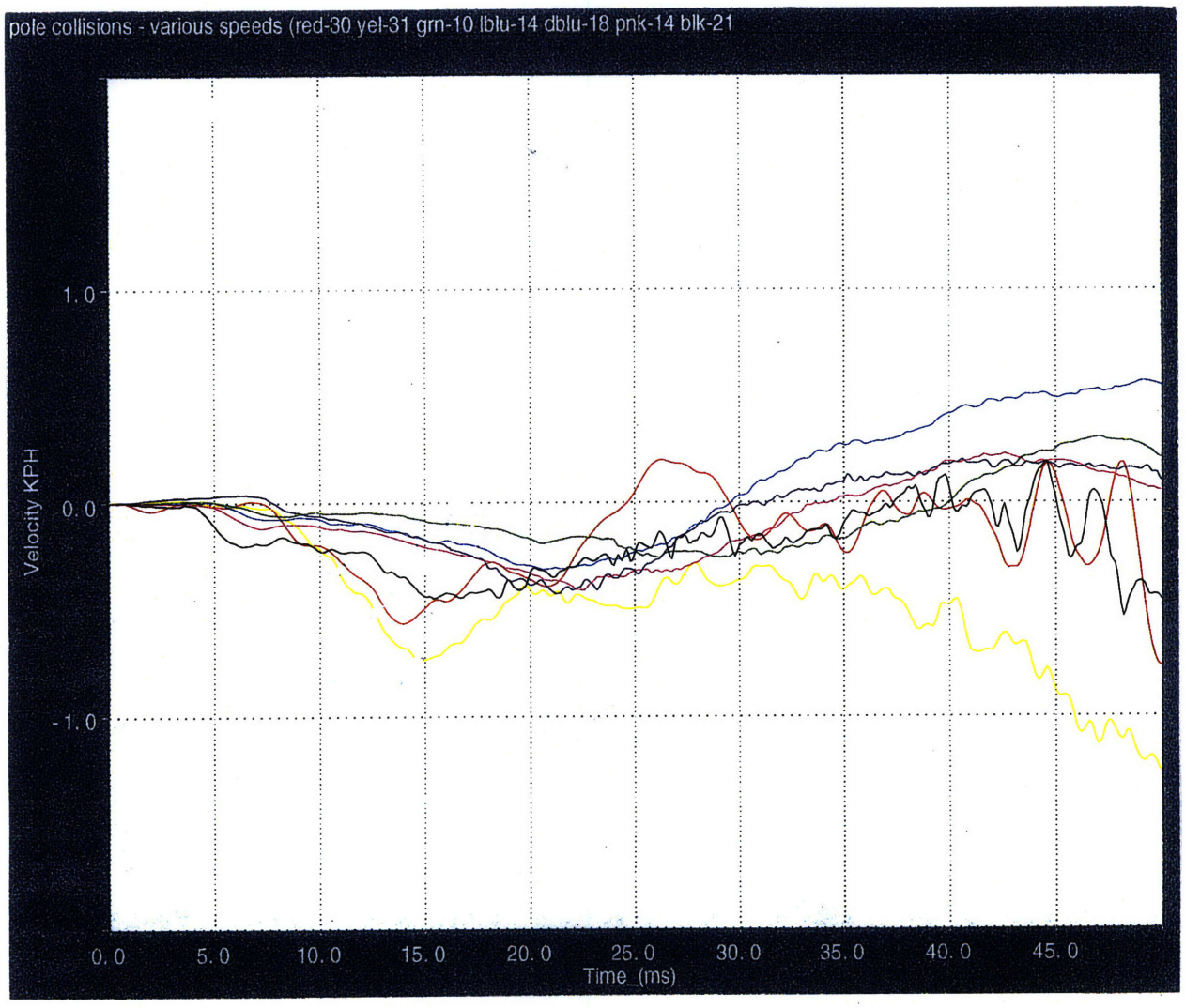

Vertical Velocity Signals of Various Pole Collisions

red	= 30-mph pole collisions *
yellow	= 31-mph pole collisions *
black	= 21-mph pole collisions *
dark blue	= 18-mph pole collisions *
light blue	= 14-mph pole collisions
pink	= 14-mph pole collisions
green	= 10-mph pole collisions

The collisions indicated by the asterisks are deploy events.

Appendix B

Angle Collision Detection Thresholds

Following are 11 graphs demonstrating how the thresholds were determined. Each graph contains 8 crashes, and each crash is represented by a distinct color. The correlation is as the following:

red	- 30° angle, 30 mph *
dark blue	- 30° angle, 30 mph *
light blue	- 30° angle, 30 mph *
black	- 30° angle, 30 mph *
yellow	- 30° angle, 20 mph *
green	- 30° angle, 15 mph
brick	- 30° angle, 12 mph
pink	- frontal, 9 mph

Both 30-mph and 20-mph angle collisions require deployment and they are indicated by asterisks. The rest are non-deploy events.

Latching: VELVLATCH - Vertical Velocity Latch Threshold

The vertical velocity latch is used to detect the magnitude of the vertical velocity. It is latched, which means that the criteria remains true once the threshold is crossed even if the signal then falls below the threshold, because of the shape of the curves. The threshold is set at -10 counts. In addition, the threshold expires 20 milliseconds after the algorithm enables.

red	- 30° angle, 30 mph *
dark blue	- 30° angle, 30 mph *
light blue	- 30° angle, 30 mph *
black	- 30° angle, 30 mph *
yellow	- 30° angle, 20 mph *
green	- 30° angle, 15 mph
brick	- 30° angle, 12 mph
pink	- frontal, 9 mph

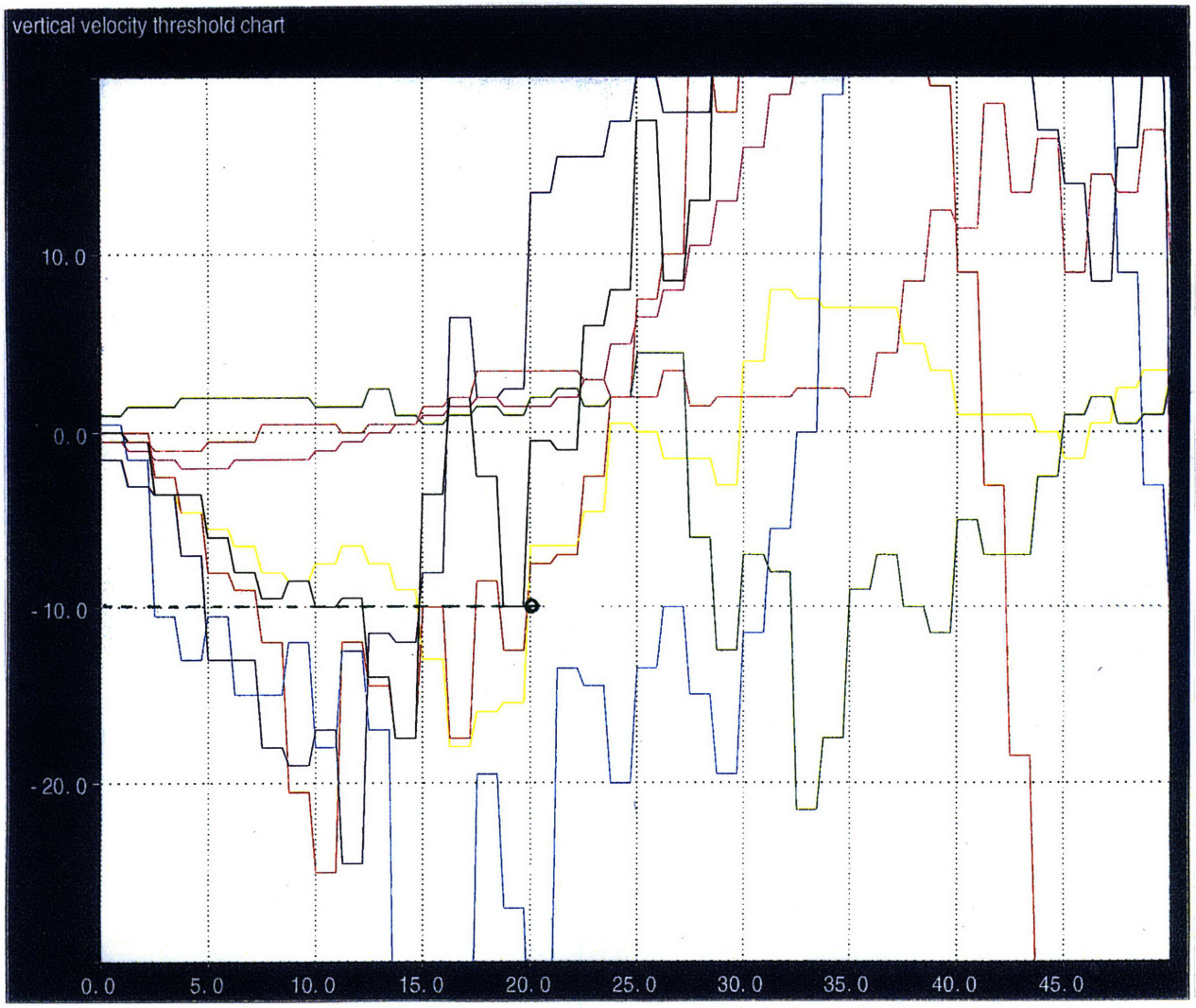

Latching: DIPLATCH - Dip Latch

The dip latch is used to detect the presence of the dip. The threshold is placed on the dip measure which is the integration of the rectified velocity. The threshold is set at 6 counts, and the since the dip measure stops collection data after 10 milliseconds, the value remains fixed. Therefore, the threshold expires after 10 milliseconds.

red	- 30° angle, 30 mph *
dark blue	- 30° angle, 30 mph *
light blue	- 30° angle, 30 mph *
black	- 30° angle, 30 mph *
yellow	- 30° angle, 20 mph *
green	- 30° angle, 15 mph
brick	- 30° angle, 12 mph
pink	- frontal, 9 mph

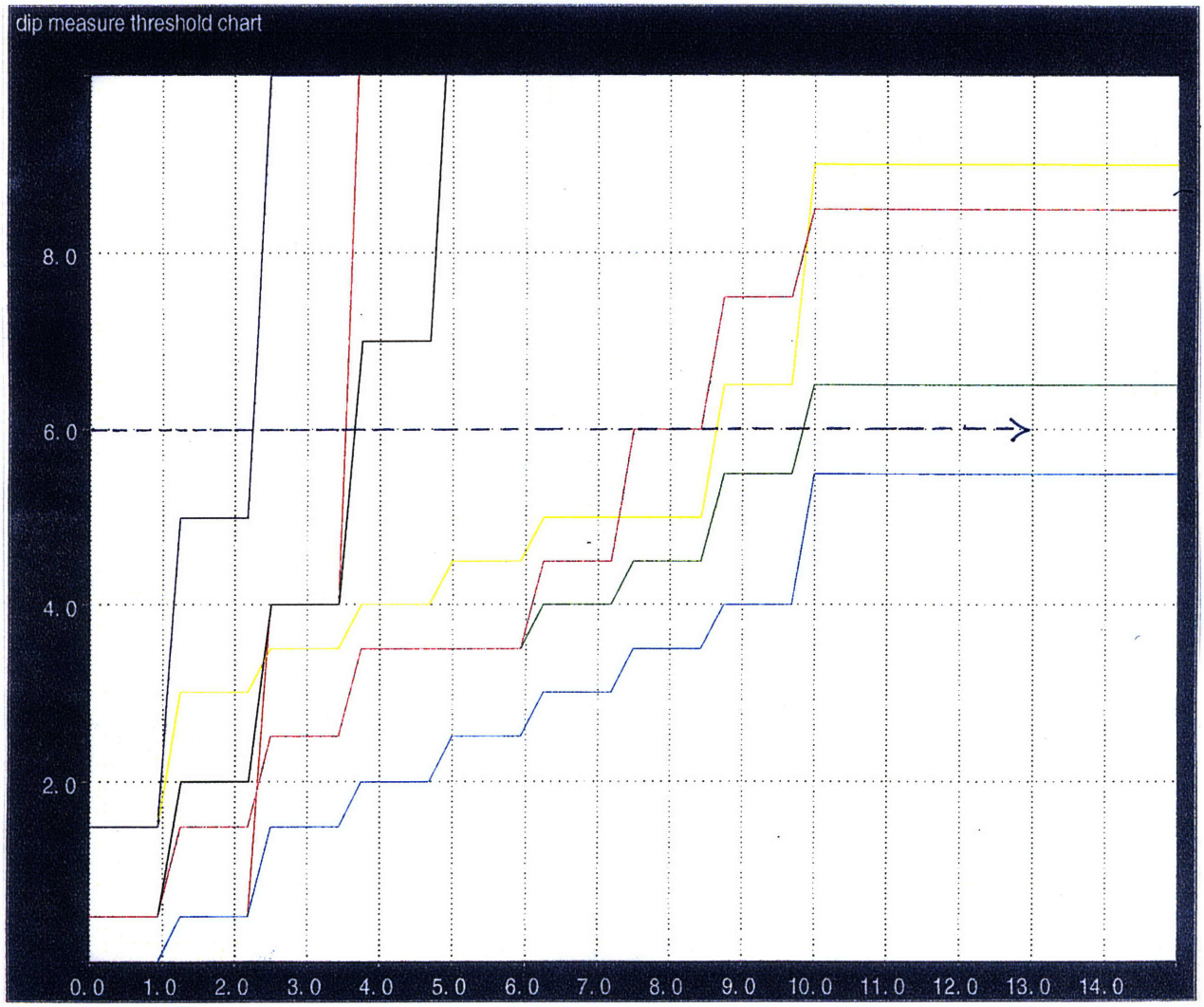

Latching: L_SLPLACH - Slope of the Lateral Velocity Latch

This latch monitors the slope of the lateral velocity. It is an absolute threshold which means that the threshold is crossed either because the signal is greater than the upper threshold or lower than the lower threshold. In this case, the upper threshold is 5 counts and the lower threshold is -5 counts. In addition, the thresholds expire 25 milliseconds after the algorithm has enabled.

red	- 30° angle, 30 mph *
dark blue	- 30° angle, 30 mph *
light blue	- 30° angle, 30 mph *
black	- 30° angle, 30 mph *
yellow	- 30° angle, 20 mph *
green	- 30° angle, 15 mph
brick	- 30° angle, 12 mph
pink	- frontal, 9 mph

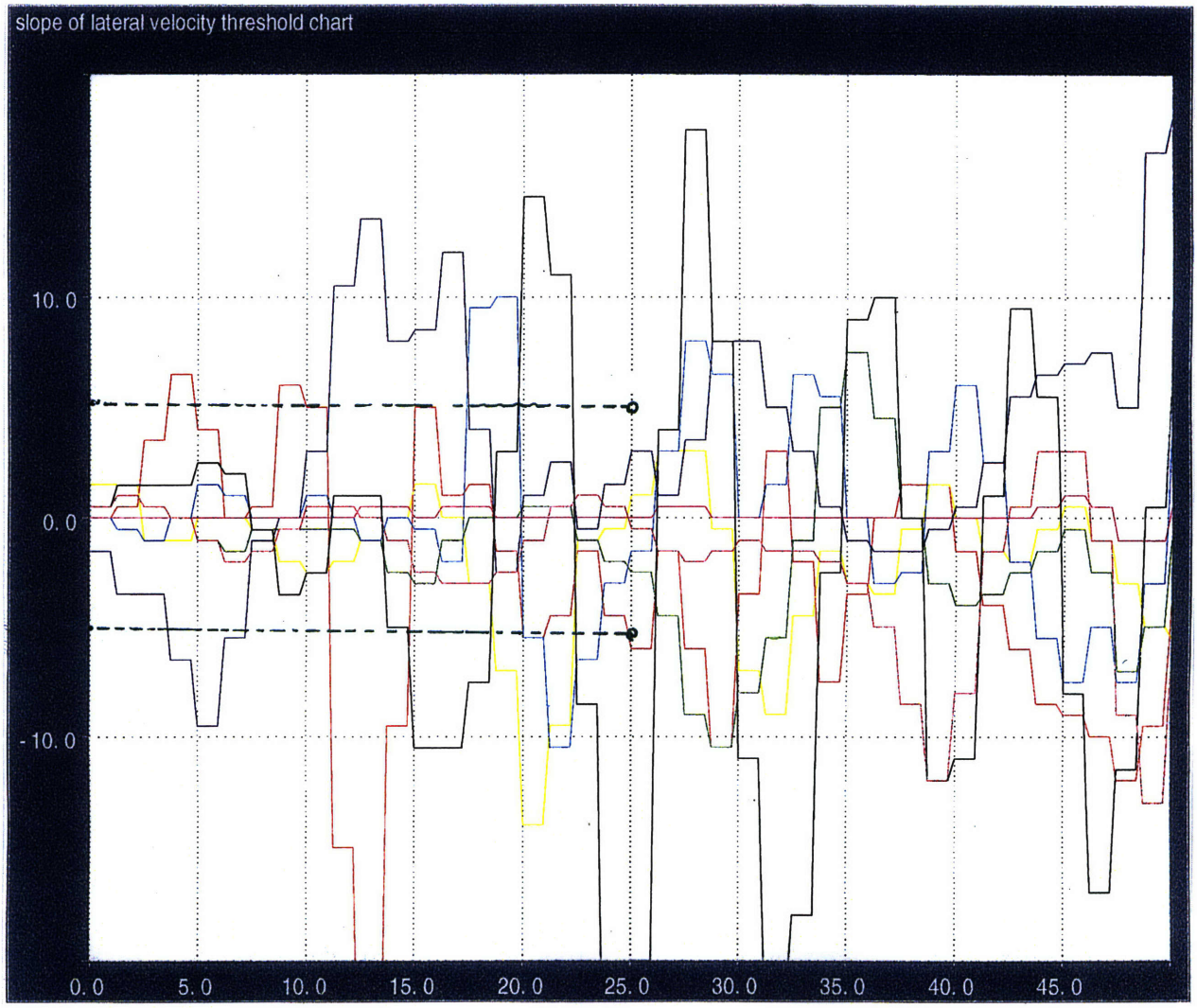

Crossing: ENRG_DCY - Decayed Combined Rectified Energy Indicator

The decayed energy indicator is a crossing criteria which monitors the magnitude of the combined energy. The threshold is set at 200 counts, and it expires 20 milliseconds after the algorithm has enabled.

red	- 30° angle, 30 mph *
dark blue	- 30° angle, 30 mph *
light blue	- 30° angle, 30 mph *
black	- 30° angle, 30 mph *
yellow	- 30° angle, 20 mph *
green	- 30° angle, 15 mph
brick	- 30° angle, 12 mph
pink	- frontal, 9 mph

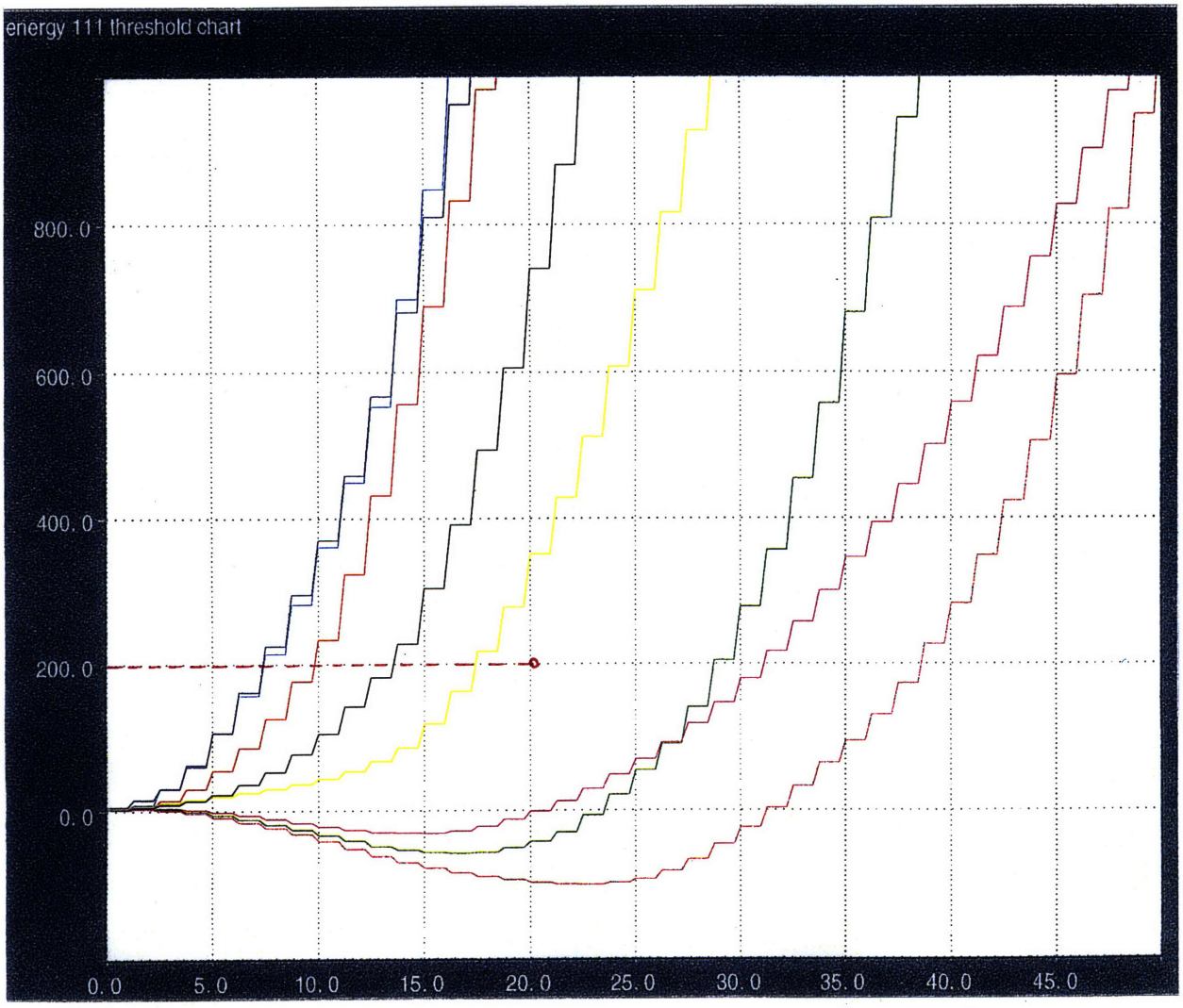

Crossing: IVELL - Lateral Integrated Rectified Lateral Velocity (Rectified Energy)

The integrated lateral velocity monitors the magnitude of the energy measure in the lateral direction. The measure is taken by integrating the rectified lateral velocity signal. The threshold is set at 40 counts, and it expires 25 milliseconds after the algorithm has enabled.

red	- 30° angle, 30 mph *
dark blue	- 30° angle, 30 mph *
light blue	- 30° angle, 30 mph *
black	- 30° angle, 30 mph *
yellow	- 30° angle, 20 mph *
green	- 30° angle, 15 mph
brick	- 30° angle, 12 mph
pink	- frontal, 9 mph

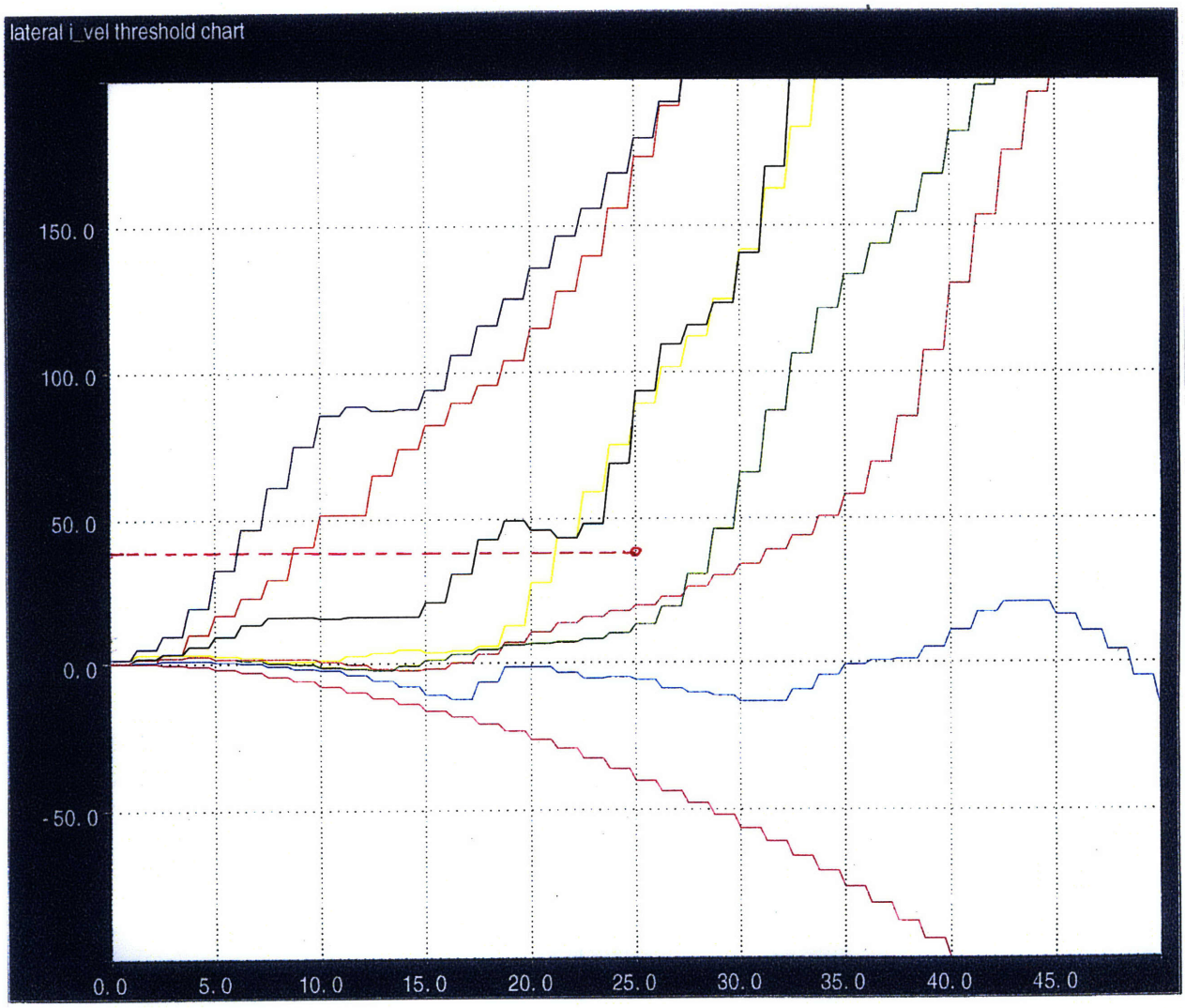

Crossing: IACCL - Lateral Integrated Rectified Acceleration (Rectified Energy)

The integrated lateral acceleration monitors the magnitude of the energy measure in the lateral direction. The measure is taken by integrating the rectified lateral acceleration signal. The threshold is set at 10 G, and the threshold expires 25 milliseconds after the algorithm has enabled.

red	- 30° angle, 30 mph *
dark blue	- 30° angle, 30 mph *
light blue	- 30° angle, 30 mph *
black	- 30° angle, 30 mph *
yellow	- 30° angle, 20 mph *
green	- 30° angle, 15 mph
brick	- 30° angle, 12 mph
pink	- frontal, 9 mph

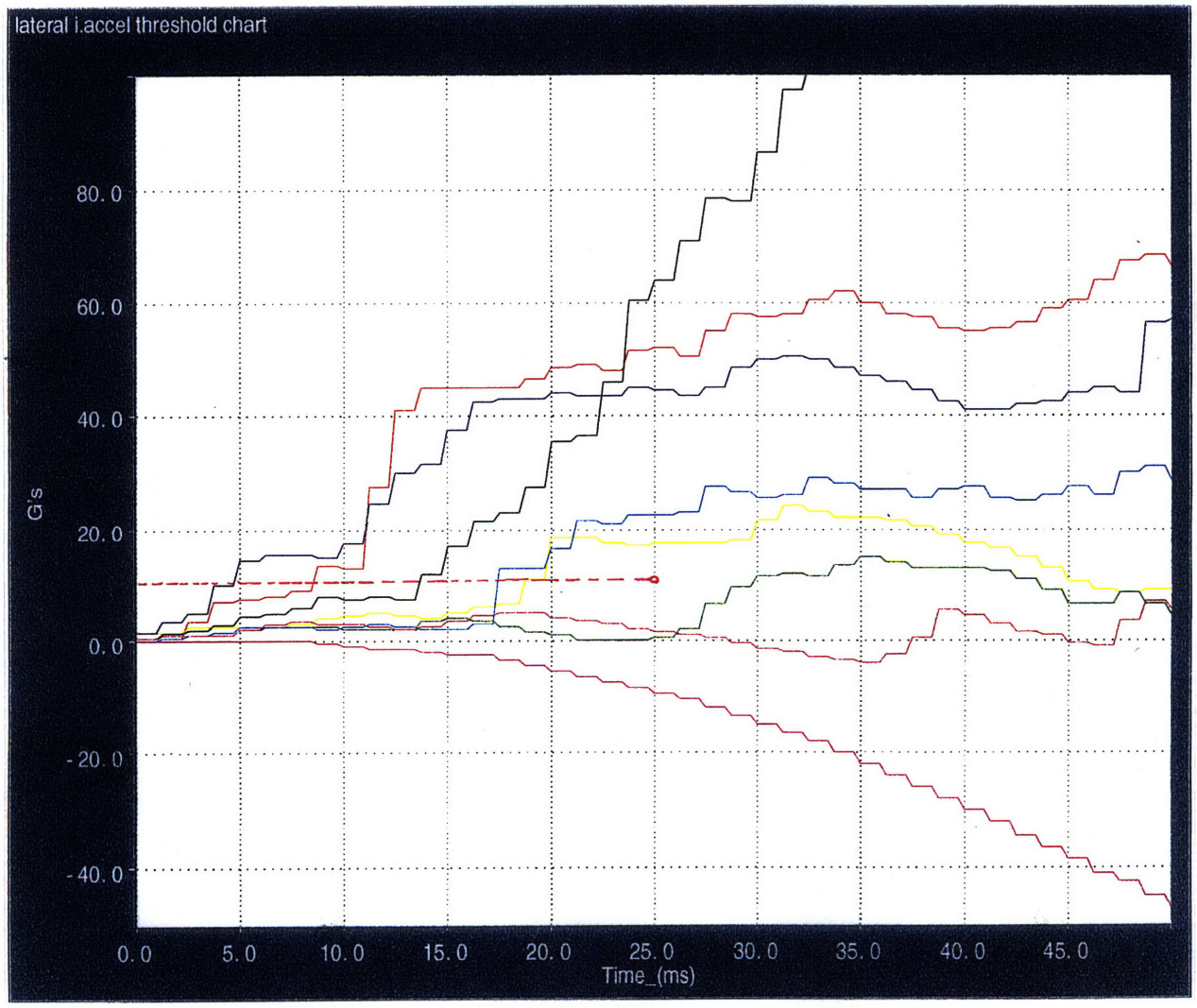

Crossing: IACCV - Vertical Integrated Rectified Acceleration (Rectified Energy)

The integrated vertical acceleration monitors the magnitude of the energy measure in the vertical direction. The measure is taken by integrating the rectified vertical acceleration signal. The threshold is set at 19 counts, and the threshold expires 20 milliseconds after the algorithm has enabled.

red	- 30° angle, 30 mph *
dark blue	- 30° angle, 30 mph *
light blue	- 30° angle, 30 mph *
black	- 30° angle, 30 mph *
yellow	- 30° angle, 20 mph *
green	- 30° angle, 15 mph
brick	- 30° angle, 12 mph
pink	- frontal, 9 mph

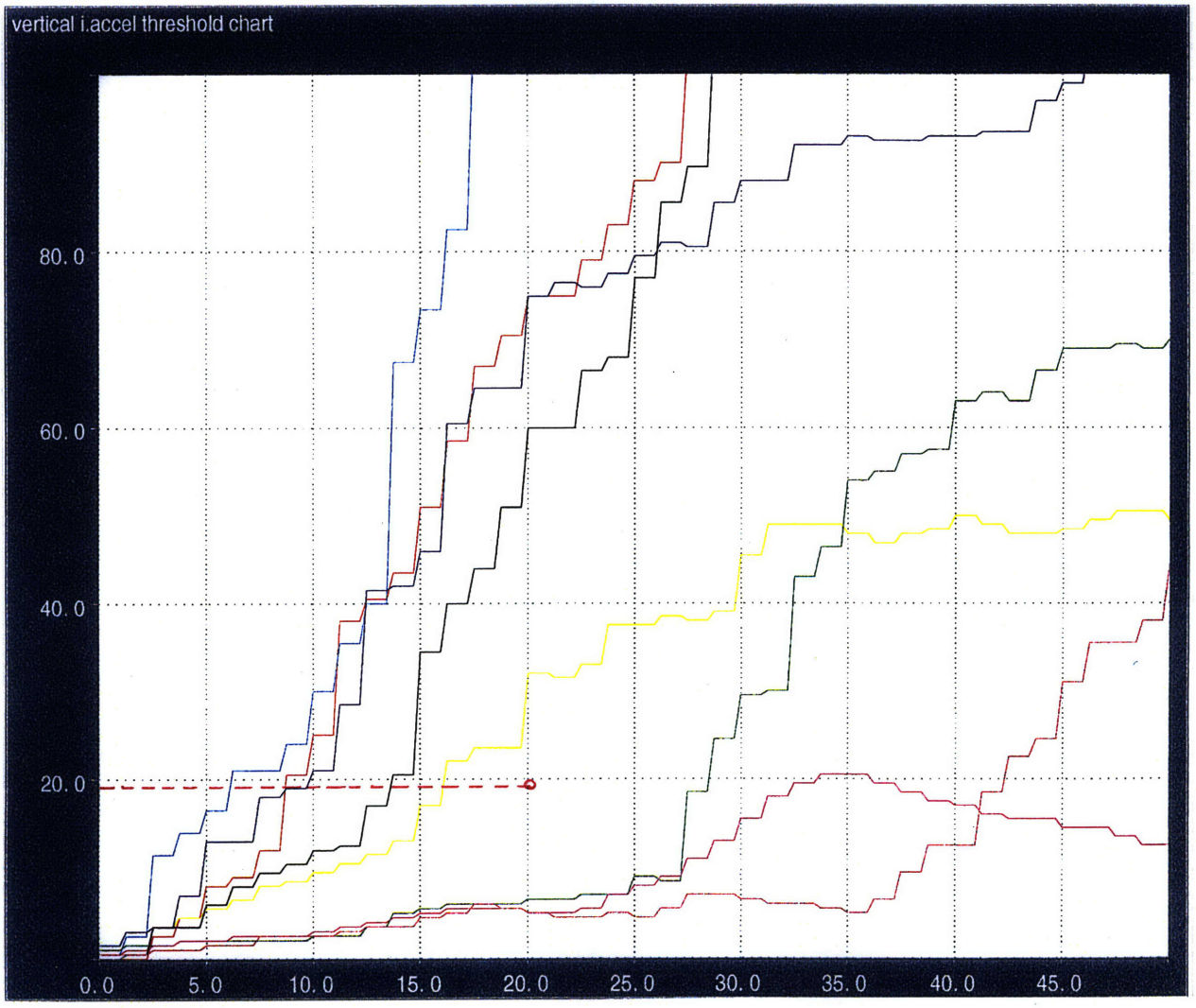

Crossing: SLP - Longitudinal Slope

The longitudinal slope threshold is designed to monitor the activities in the longitudinal slope. It is a two tier threshold such that after a certain amount of time after the algorithm has enabled, the threshold is moved to a different level. Tier 1 is set at -10 counts, and tier 2 is set at - 5 counts. The threshold expires 25 milliseconds after the algorithm has enabled.

red	- 30° angle, 30 mph *
dark blue	- 30° angle, 30 mph *
light blue	- 30° angle, 30 mph *
black	- 30° angle, 30 mph *
yellow	- 30° angle, 20 mph *
green	- 30° angle, 15 mph
brick	- 30° angle, 12 mph
pink	- frontal, 9 mph

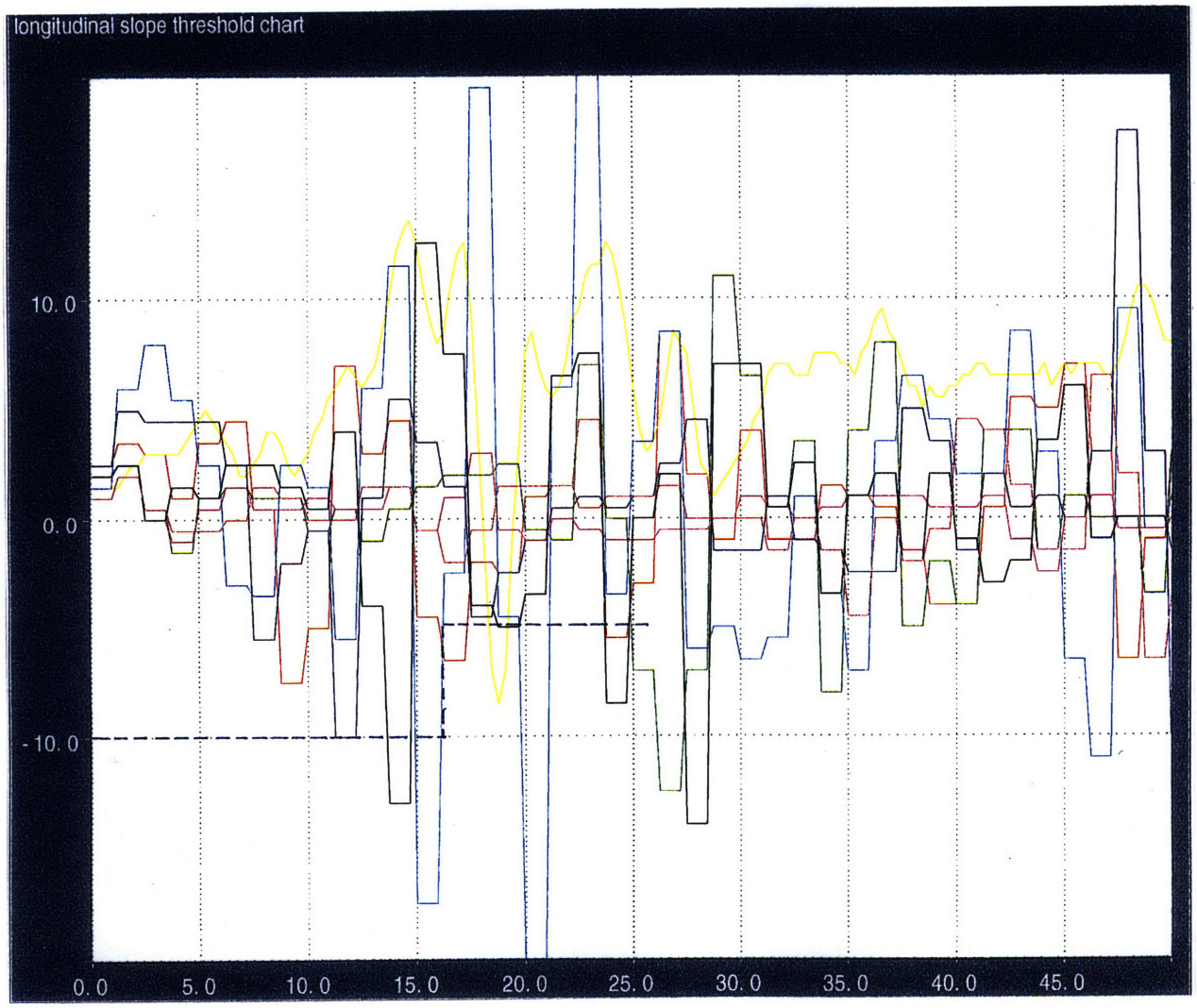

Crossing: ACCW - Longitudinal Acceleration

The longitudinal acceleration threshold is used to monitor the magnitude of the filtered acceleration signal. The threshold is placed at 5 counts, and it expires 26 milliseconds after the algorithm has enabled.

red	- 30° angle, 30 mph *
dark blue	- 30° angle, 30 mph *
light blue	- 30° angle, 30 mph *
black	- 30° angle, 30 mph *
yellow	- 30° angle, 20 mph *
green	- 30° angle, 15 mph
brick	- 30° angle, 12 mph
pink	- frontal, 9 mph

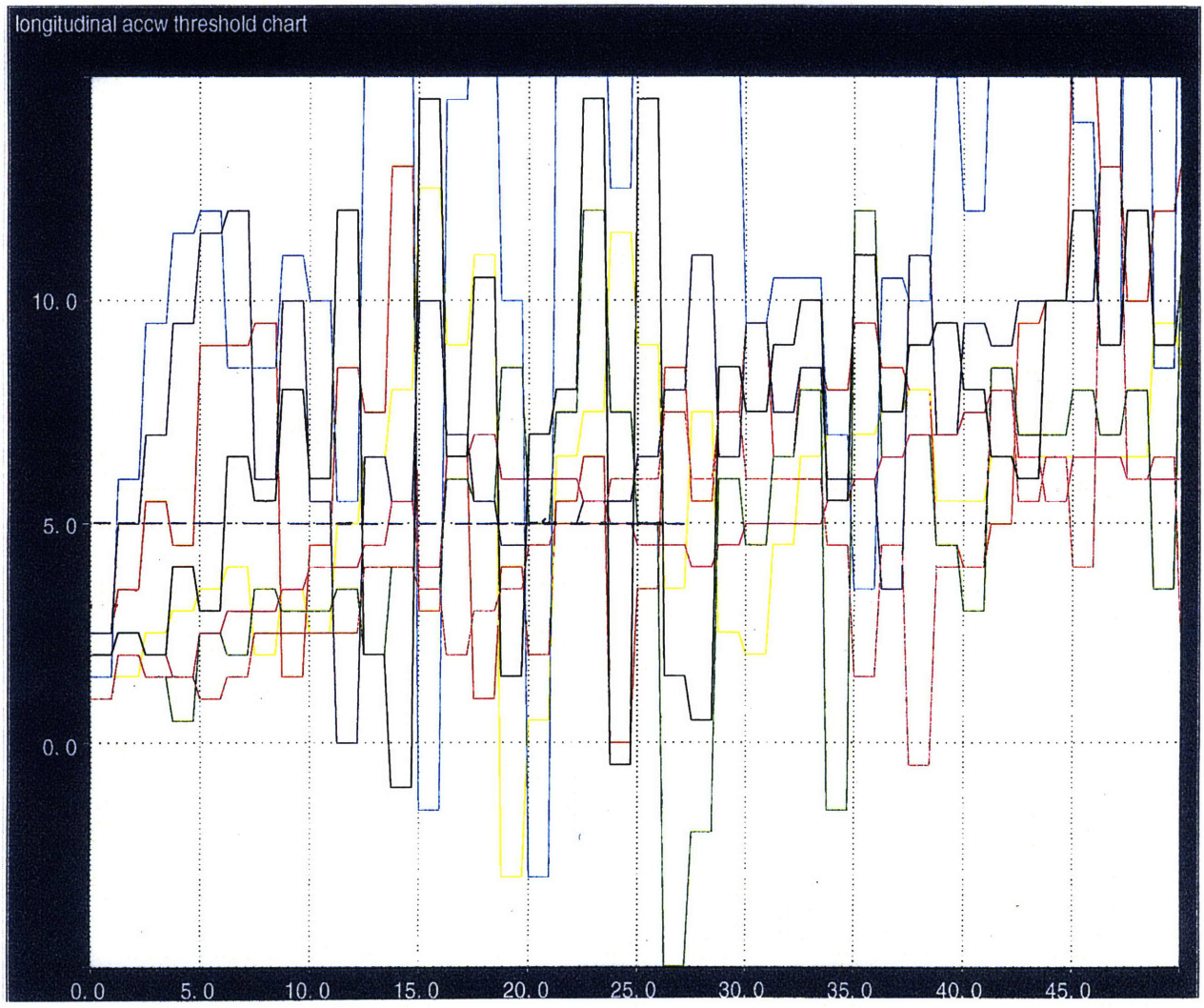

Crossing: OSC - Longitudinal Oscillation Measure

The longitudinal oscillation measure monitors the level of oscillation in the acceleration signal. The threshold consists of 2 tiers. The first tier is set at 12 counts and after 16 millisecond, the threshold is raised to the second tier at 25 counts. The threshold expires 28 milliseconds after the algorithm has enabled.

red	- 30° angle, 30 mph *
dark blue	- 30° angle, 30 mph *
light blue	- 30° angle, 30 mph *
black	- 30° angle, 30 mph *
yellow	- 30° angle, 20 mph *
green	- 30° angle, 15 mph
brick	- 30° angle, 12 mph
pink	- frontal, 9 mph

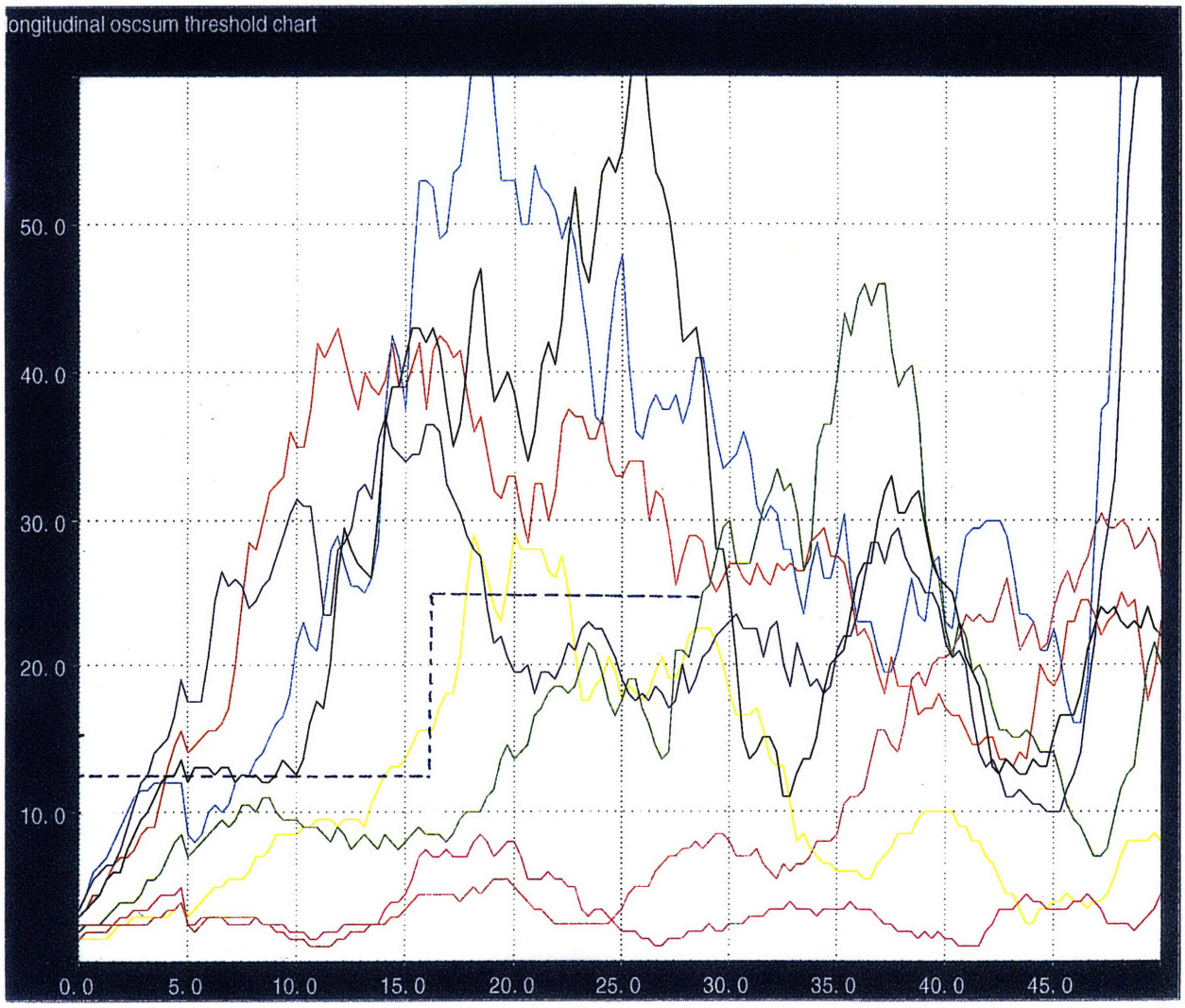

Crossing: VEL - Longitudinal Velocity

The longitudinal velocity threshold consists of 2 tiers. The first tier is set at 1 mph, and after 16 milliseconds, the threshold is raised to the second tier at 2.5 mph. The threshold expires 25 milliseconds after the algorithm has enabled.

red	- 30° angle, 30 mph *
dark blue	- 30° angle, 30 mph *
light blue	- 30° angle, 30 mph *
black	- 30° angle, 30 mph *
yellow	- 30° angle, 20 mph *
green	- 30° angle, 15 mph
brick	- 30° angle, 12 mph
pink	- frontal, 9 mph

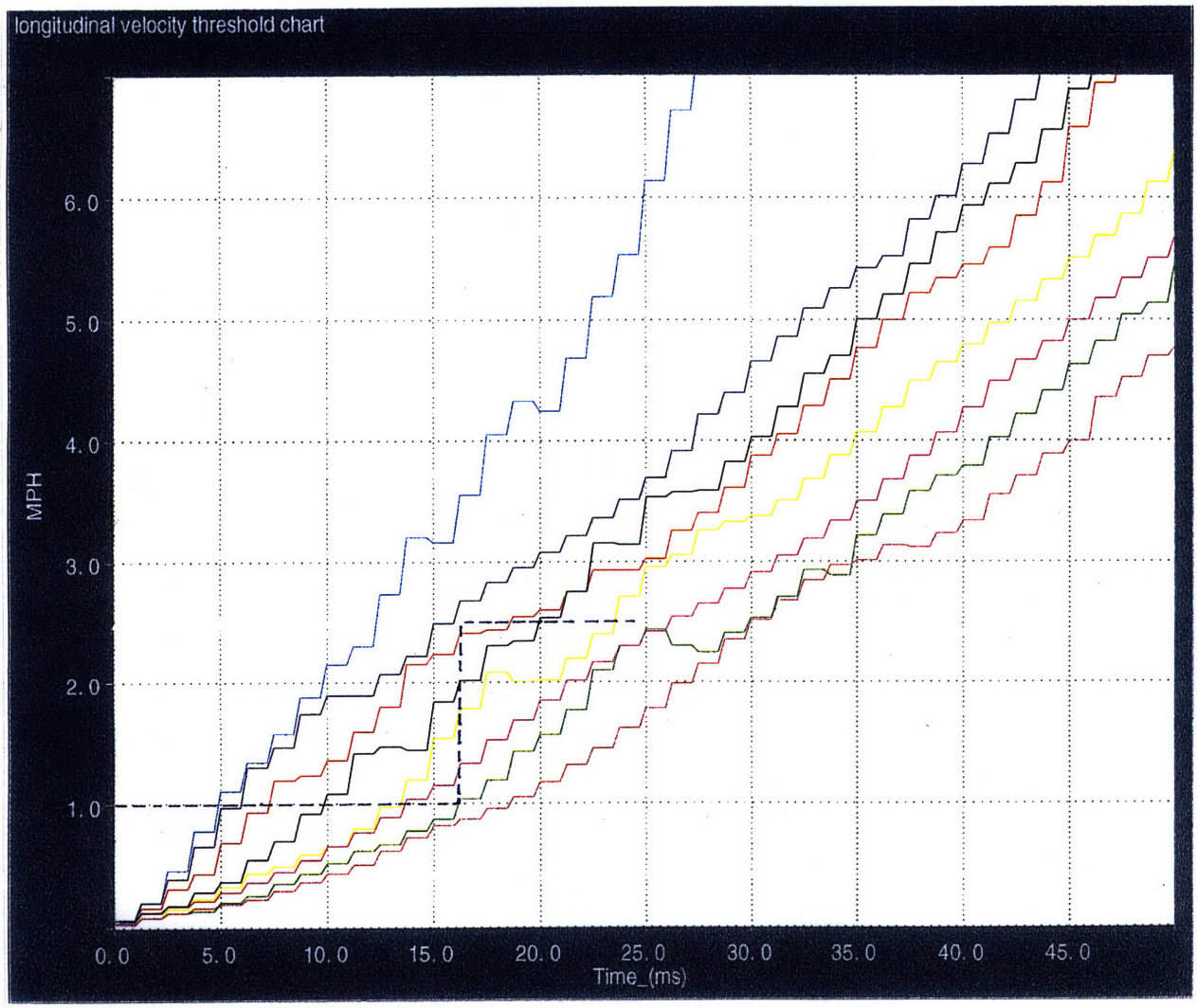

Pole Collision Detection Thresholds

Following are 8 graphs demonstrating how the thresholds were determined. Each graph contains 9 crashes, and each crash is represented by a distinct color. The correlation is as the following:

green	- pole, 30 mph *
dark brown	- pole, 21 mph *
pink	- pole, 18 mph *
red	- 30° angle, 20 mph *
brick	- pole, 14 mph
yellow	- 30° angle, 15 mph
black	- 30° angle, 12 mph
light blue	- frontal, 9 mph
dark blue	- frontal, 9 mph

The collisions indicated by asterisks are deploy events. In addition to the severe pole collisions, the high speed angle collision was also included to compare the contrast the behavior.

Latching: DSPVLATCH - Vertical Displacement Latch
Crossing: DSPV - Vertical Displacement

The following graph is used to illustrate 2 thresholds, the vertical displacement latching (green) and crossing thresholds (red). The latching threshold is set at -0.035 inches and expires 40 milliseconds after the algorithm has enabled. The crossing threshold consists of 2 tiers. The first tier is set at -0.03 inches, and after 40 milliseconds after the start of the collision, the threshold is lowered to -0.115 inches. The crossing threshold expires at 70 milliseconds.

green	- pole, 30 mph *
dark brown	- pole, 21 mph *
pink	- pole, 18 mph *
red	- 30° angle, 20 mph *
brick	- pole, 14 mph
yellow	- 30° angle, 15 mph
black	- 30° angle, 12 mph
light blue	- frontal, 9 mph
dark blue	- frontal, 9 mph

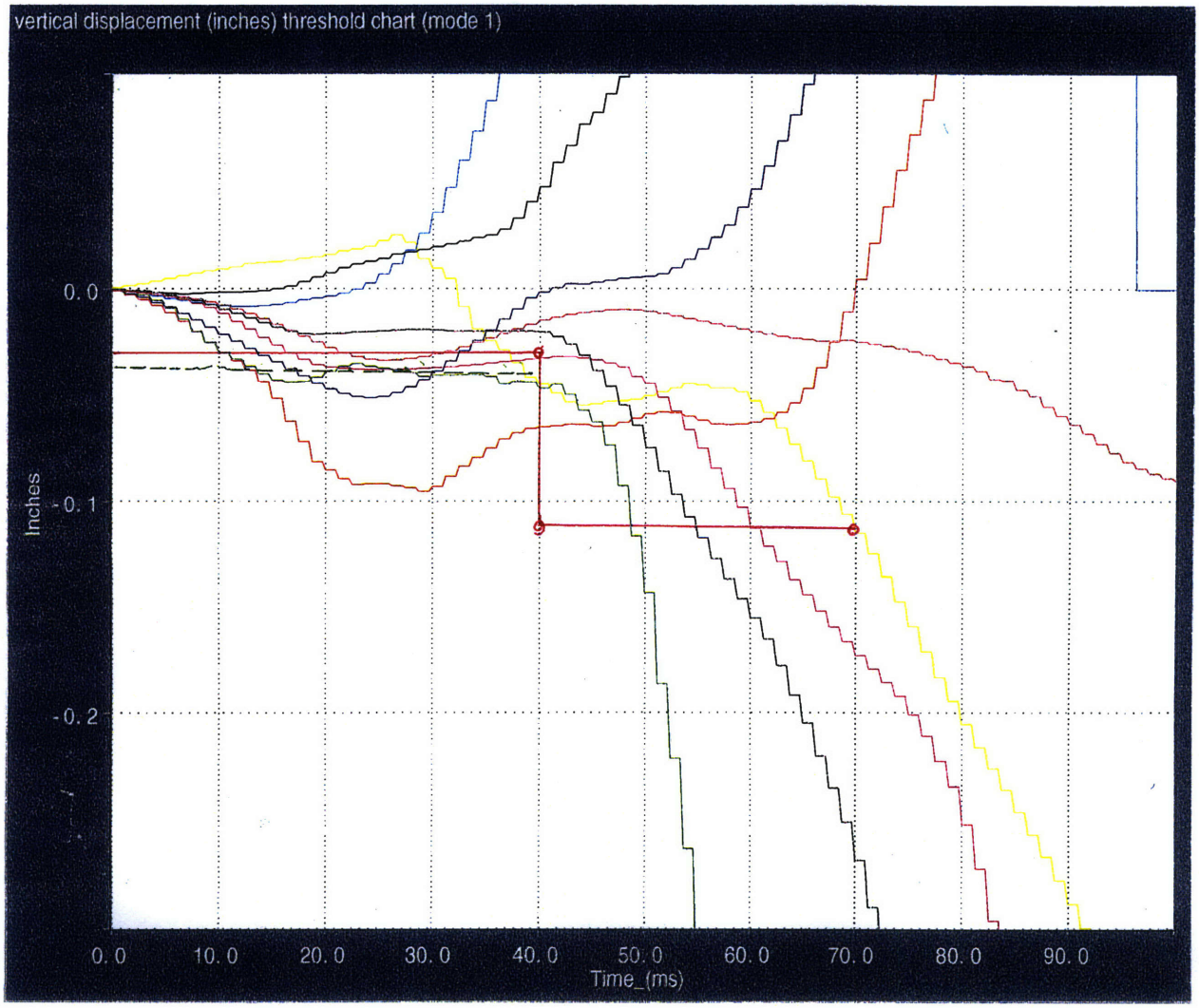

Latching: VELVLATCH - Vertical Velocity Latch

The vertical velocity latch is used to identify the shape of a common high severity pole collision. The first tier is set at -0.2 mph for the initial 25 milliseconds. The threshold is disabled until 40 milliseconds when the second tier is in place. The threshold is set at -0.4 mph, and the criteria is true only if the signal crosses the tier 2 threshold and the tier 1 threshold has also been crossed. The threshold is disabled completely at 70 milliseconds.

green	- pole, 30 mph *
dark brown	- pole, 21 mph *
pink	- pole, 18 mph *
red	- 30° angle, 20 mph *
brick	- pole, 14 mph
yellow	- 30° angle, 15 mph
black	- 30° angle, 12 mph
light blue	- frontal, 9 mph
dark blue	- frontal, 9 mph

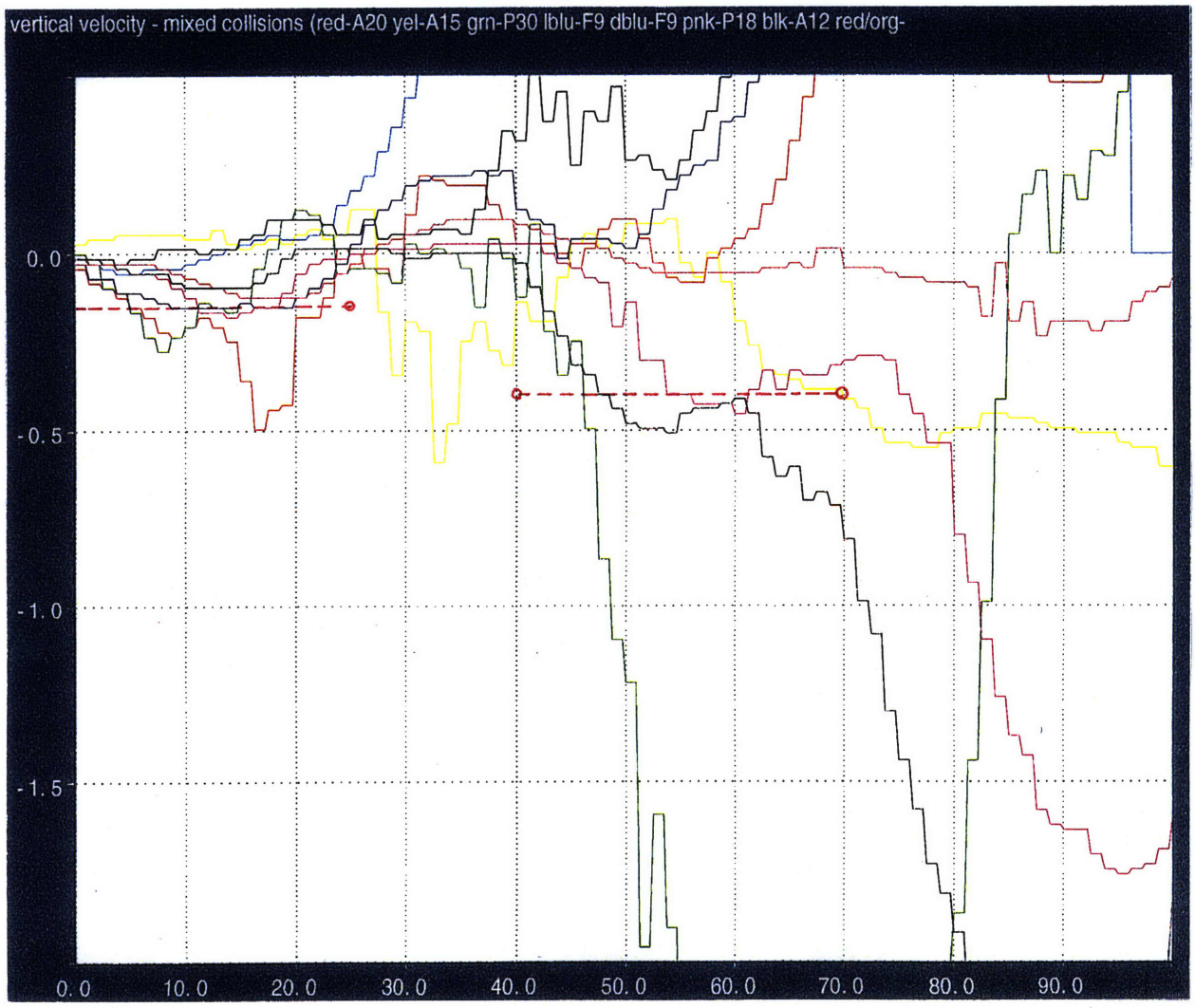

Crossing: IACCL - Integrated Lateral Acceleration

The integrated lateral acceleration monitors the levels of the energy in the lateral direction. The first tier is placed at 3 counts, and after 40 milliseconds, the threshold is raised to 11 counts. The threshold expires at 65 milliseconds.

green	- pole, 30 mph *
dark brown	- pole, 21 mph *
pink	- pole, 18 mph *
red	- 30° angle, 20 mph *
brick	- pole, 14 mph
yellow	- 30° angle, 15 mph
black	- 30° angle, 12 mph
light blue	- frontal, 9 mph
dark blue	- frontal, 9 mph

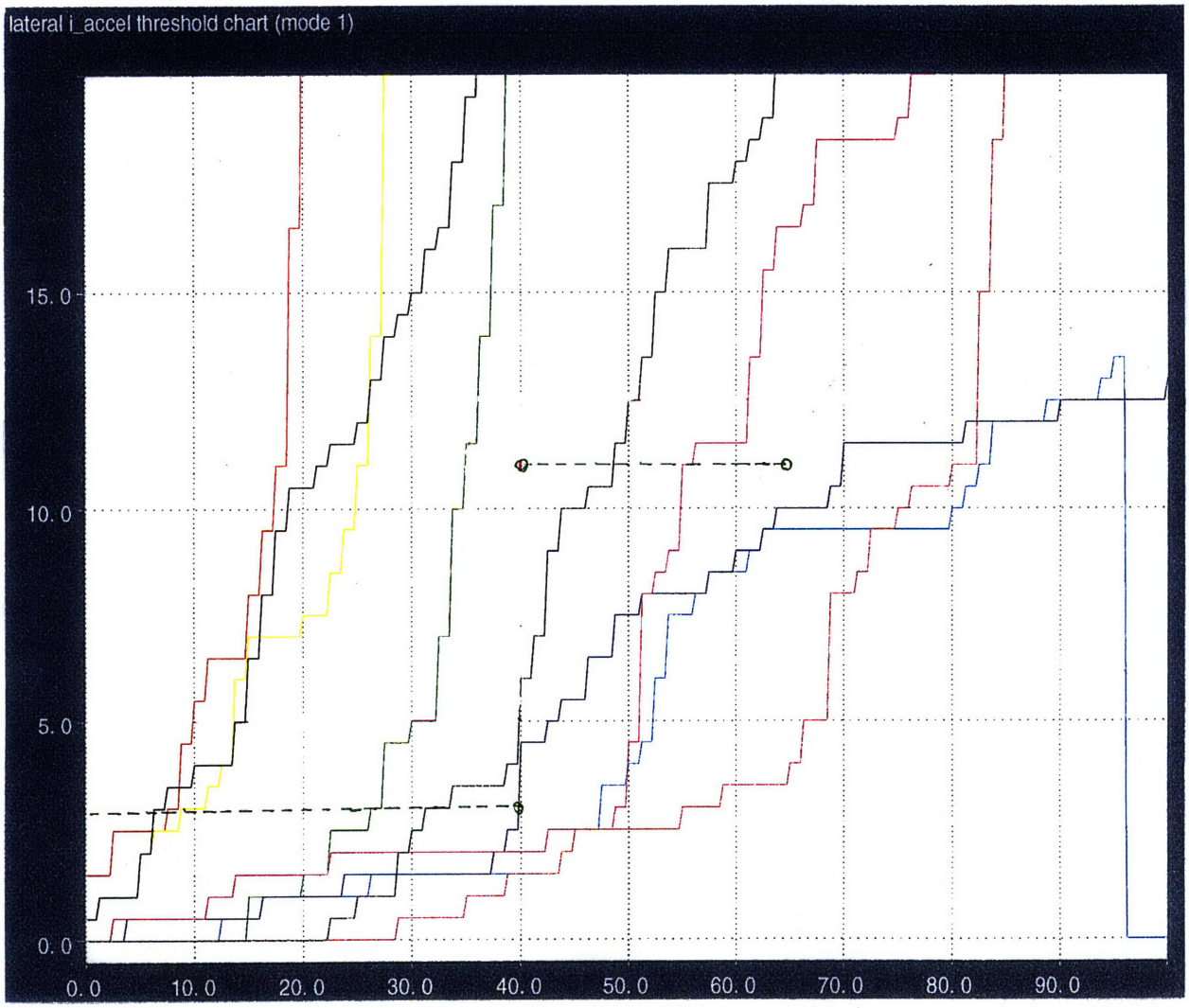

Crossing: IACCV - Integrated Vertical Acceleration

The integrated vertical acceleration monitors the levels of energy in the vertical direction. The first tier is placed at 30 counts, and after 40 milliseconds from the time of enable, the threshold is lowered to 25 counts. The threshold expires at 70 milliseconds.

green	- pole, 30 mph *
dark brown	- pole, 21 mph *
pink	- pole, 18 mph *
red	- 30° angle, 20 mph *
brick	- pole, 14 mph
yellow	- 30° angle, 15 mph
black	- 30° angle, 12 mph
light blue	- frontal, 9 mph
dark blue	- frontal, 9 mph

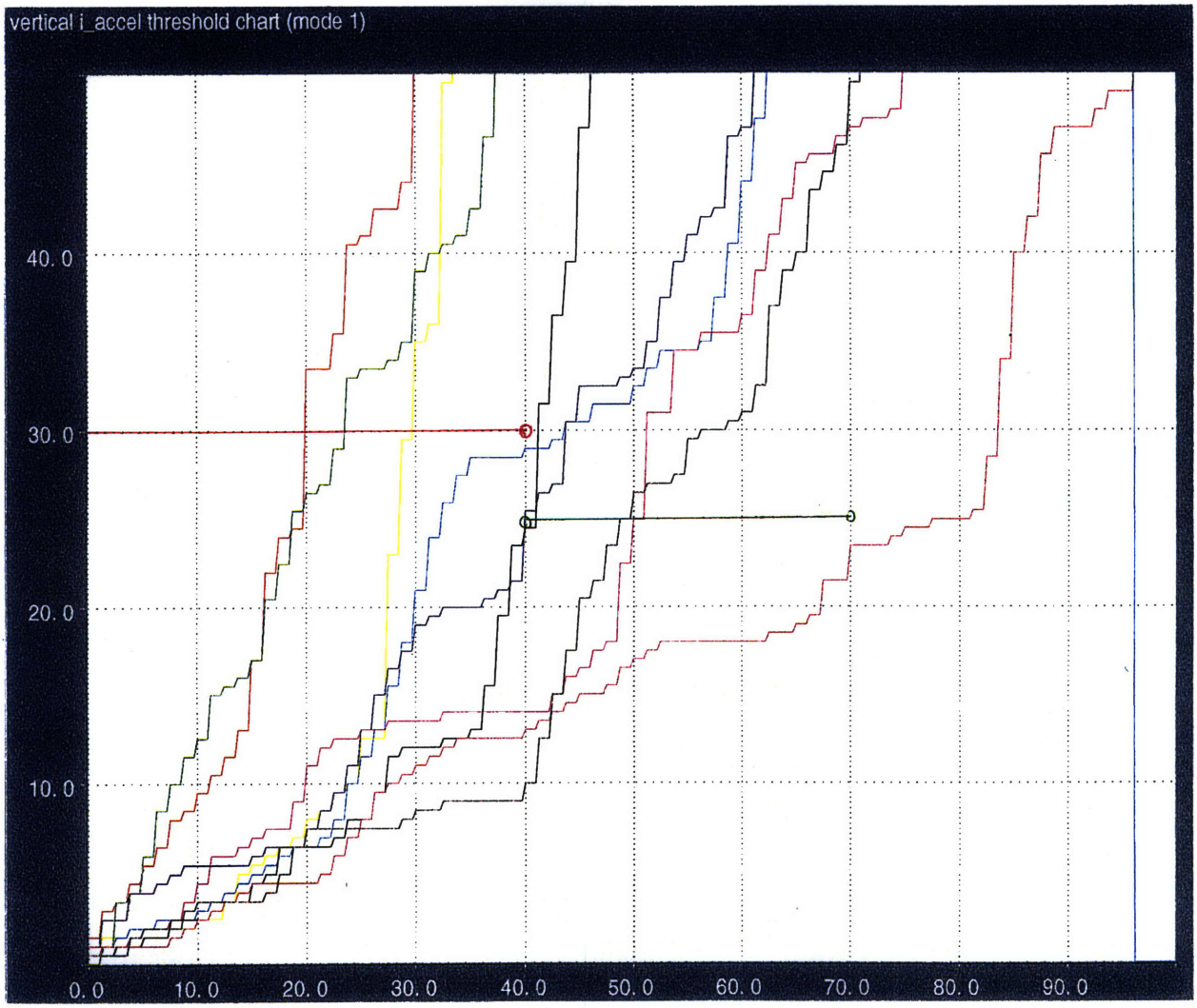

Crossing: ENRG_DCY - Decayed Combined Energy

The decayed combined energy measures the total energy dissipation in all three direction. The threshold is set at 300 counts, and it expires at 30 milliseconds after the algorithm has enabled.

green	- pole, 30 mph *
dark brown	- pole, 21 mph *
pink	- pole, 18 mph *
red	- 30° angle, 20 mph *
brick	- pole, 14 mph
yellow	- 30° angle, 15 mph
black	- 30° angle, 12 mph
light blue	- frontal, 9 mph
dark blue	- frontal, 9 mph

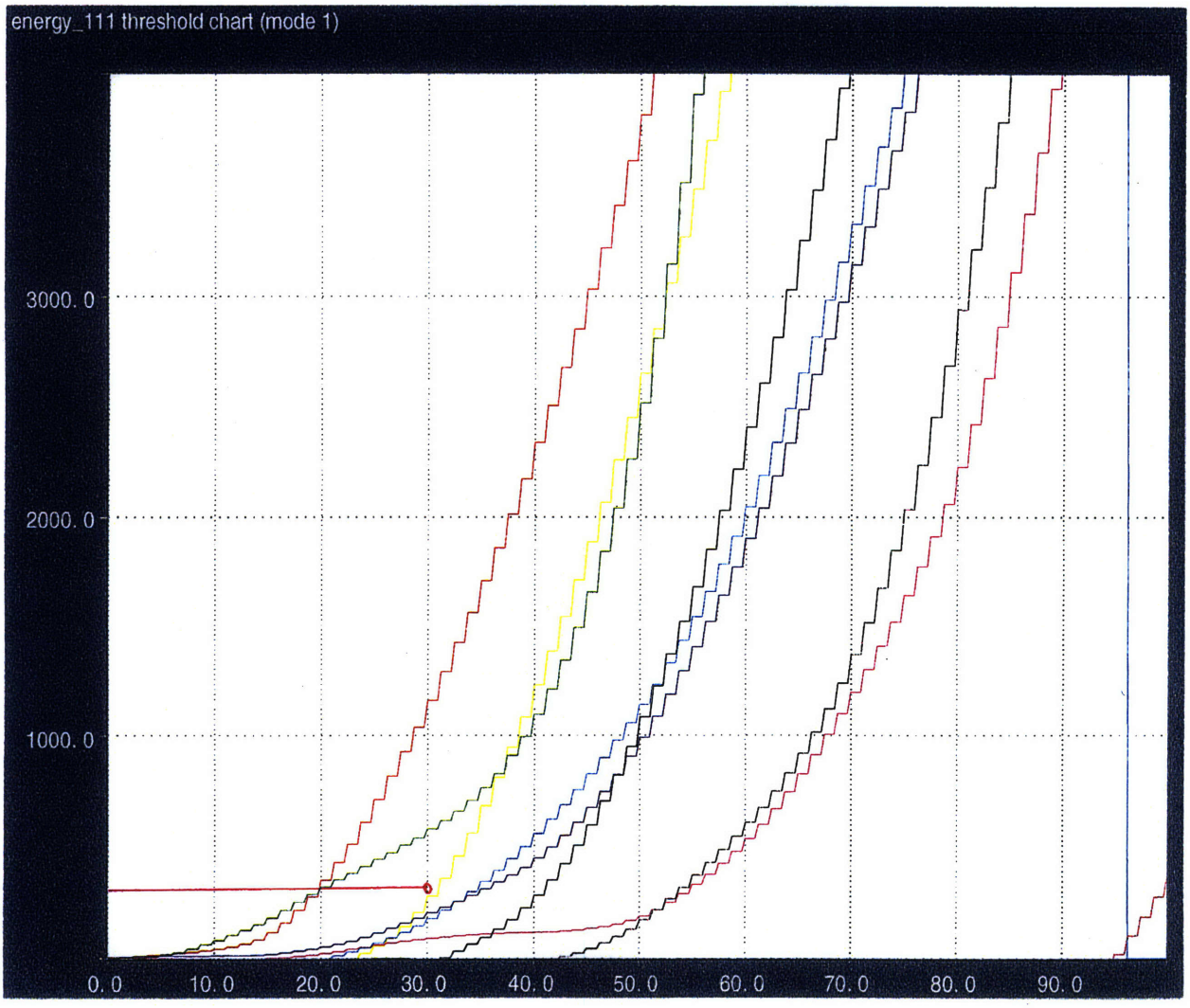

Crossing: SLP - Longitudinal Slope

The longitudinal slope monitors the activities in the longitudinal acceleration signal. The threshold is placed at 3 counts, and the threshold does not have a expiration time.

green	- pole, 30 mph *
dark brown	- pole, 21 mph *
pink	- pole, 18 mph *
red	- 30° angle, 20 mph *
brick	- pole, 14 mph
yellow	- 30° angle, 15 mph
black	- 30° angle, 12 mph
light blue	- frontal, 9 mph
dark blue	- frontal, 9 mph

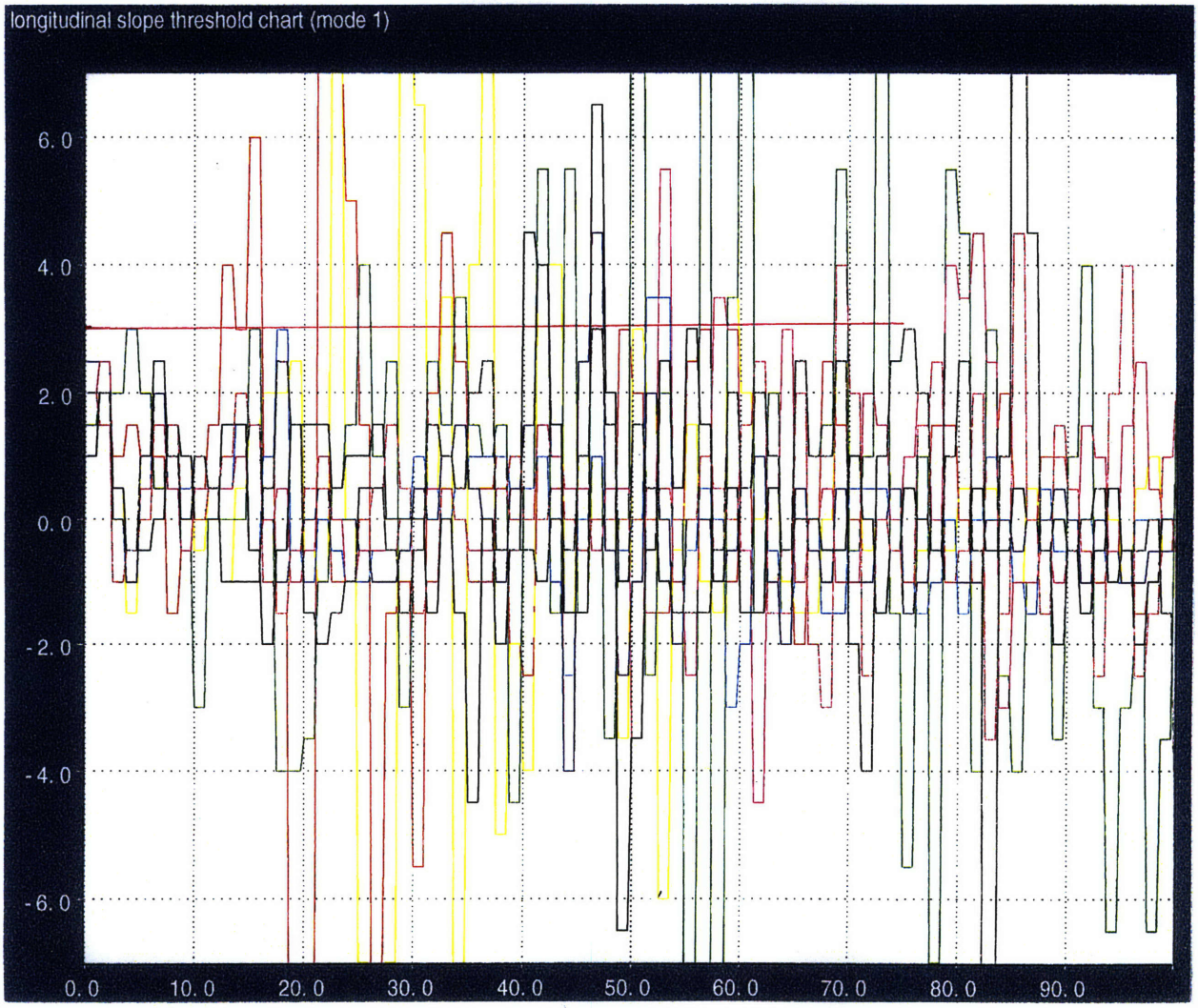

Crossing: ACCW - Longitudinal Acceleration

The longitudinal acceleration is used to keep track of the magnitude of the acceleration in the longitudinal direction. The threshold is placed at 4.5 counts, and once again, there is no time limit.

green	- pole, 30 mph *
dark brown	- pole, 21 mph *
pink	- pole, 18 mph *
red	- 30° angle, 20 mph *
brick	- pole, 14 mph
yellow	- 30° angle, 15 mph
black	- 30° angle, 12 mph
light blue	- frontal, 9 mph
dark blue	- frontal, 9 mph

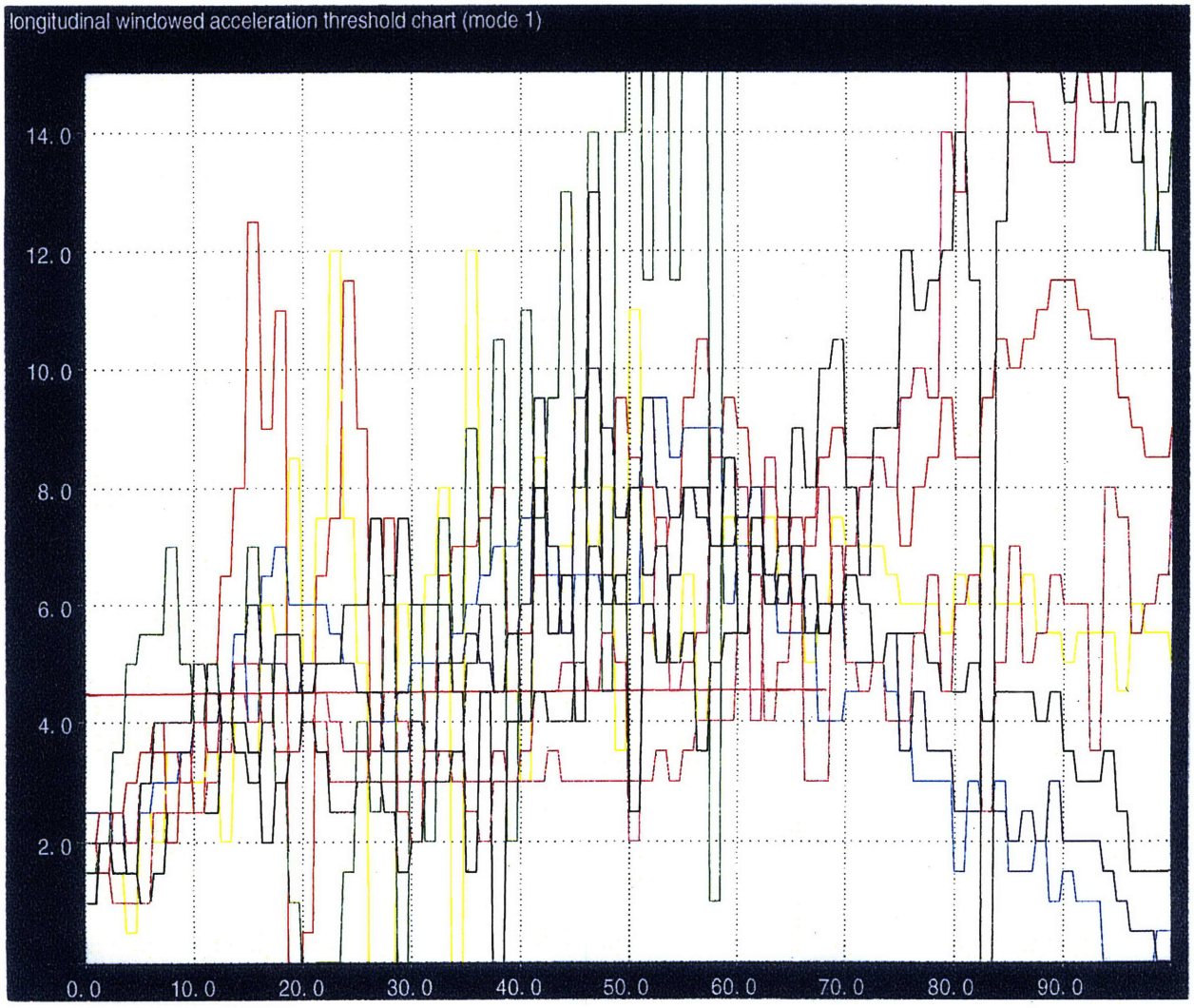

Crossing: VEL - Longitudinal Velocity

The longitudinal velocity threshold is set at 1.5 counts, and it does not have a time limit.

green	- pole, 30 mph *
dark brown	- pole, 21 mph *
pink	- pole, 18 mph *
red	- 30° angle, 20 mph *
brick	- pole, 14 mph
yellow	- 30° angle, 15 mph
black	- 30° angle, 12 mph
light blue	- frontal, 9 mph
dark blue	- frontal, 9 mph

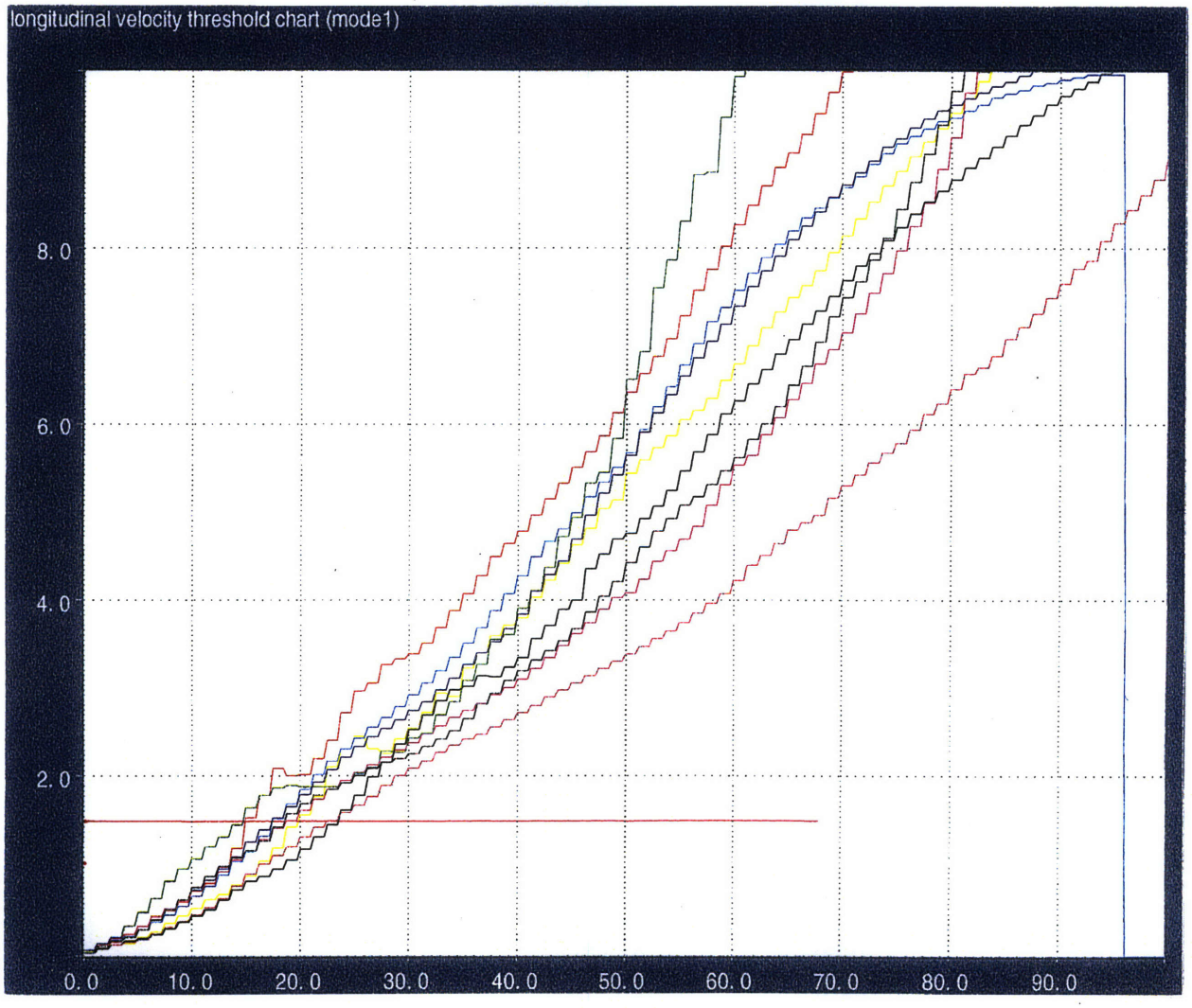

Crossing: OSC - Longitudinal Oscillation

The longitudinal oscillation measures the degree of oscillation in the acceleration signal. The threshold consists of two tiers. The first tier is set at 7.5 counts, and at 40 milliseconds after the start of the collision, the threshold is raised to 10 counts. The threshold expires at 70 milliseconds.

green	- pole, 30 mph *
dark brown	- pole, 21 mph *
pink	- pole, 18 mph *
red	- 30° angle, 20 mph *
brick	- pole, 14 mph
yellow	- 30° angle, 15 mph
black	- 30° angle, 12 mph
light blue	- frontal, 9 mph
dark blue	- frontal, 9 mph

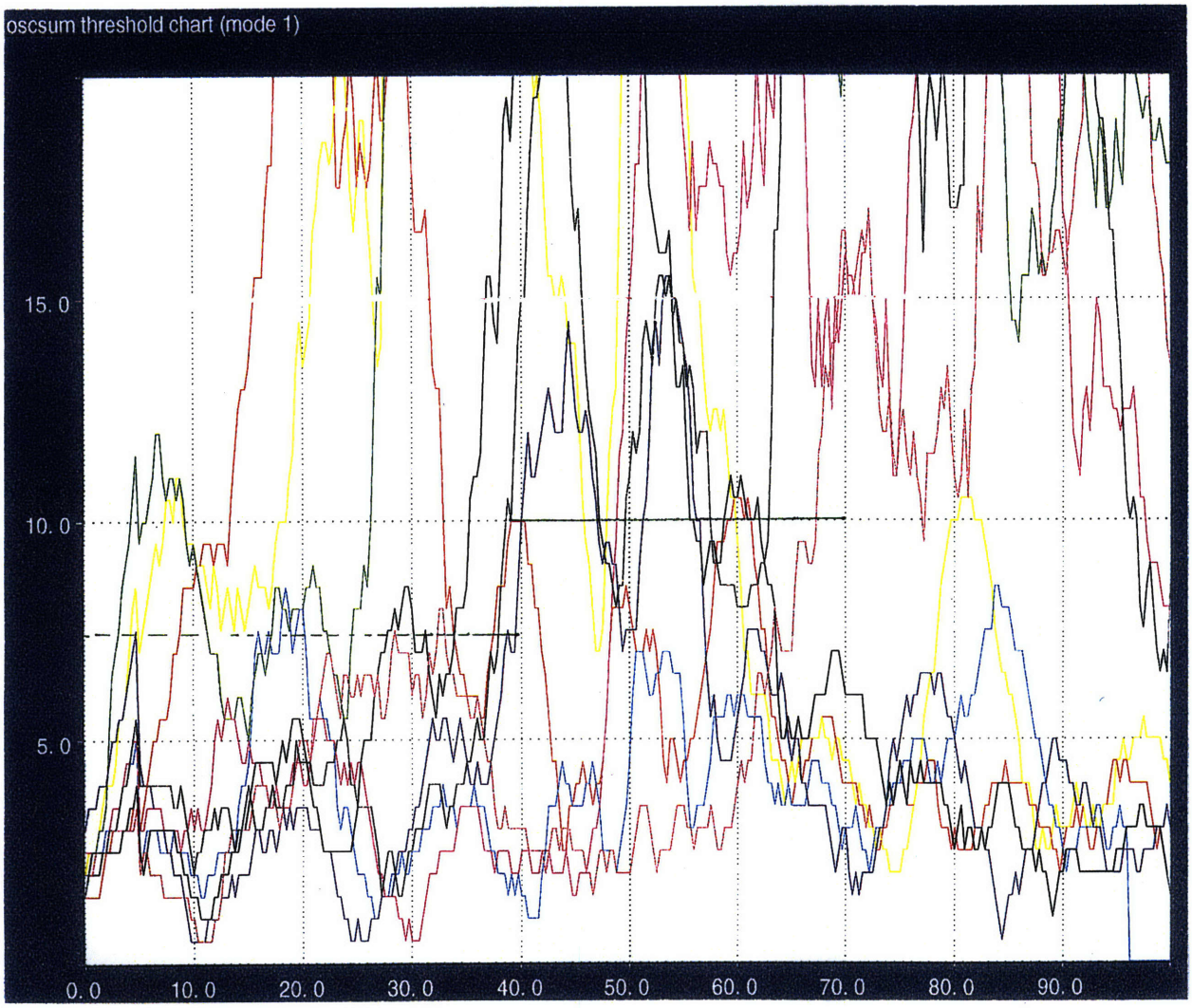

Appendix C

Performance: Timeliness

- single-axis algorithm vs. multi-axes algorithm (angle collision detection)
- (NT = No Trigger)
- asterisks indicate the events which are used for the calibration of the thresholds.

Crash Description type - speed - seq. #	Desired Deploy Time (ms)	single-axis algorithm (ms)	multi-axes algorithm (ms)
*30° angle - 30 mph - 01	36	24	17
30° angle - 30 mph - 02	36	31	27
*30° angle - 30 mph - 03	36	32	23
30° angle - 30 mph - 04	36	31	18
30° angle - 30 mph - 05	36	28	18
30° angle - 30 mph - 06	36	28	20
*30° angle - 30 mph - 07	36	28	22
30° angle - 30 mph - 08	36	29	23
*30° angle - 30 mph - 09	36	28	17
*30° angle - 20 mph - 01	44	NT	33
*30° angle - 15 mph - 01	NT	NT	NT
*30° angle - 12 mph - 01	NT	NT	NT
*30° angle - 10 mph - 01	NT	NT	NT
pole - 14 mph - 01	NT	NT	NT
pole - 14 mph - 02	NT	NT	NT
pole - 10 mph - 01	NT	NT	NT
frontal - 15 mph - 01	50	32	NT
frontal - 9 mph - 01	NT	NT	NT
frontal - 9 mph - 01	NT	NT	NT
frontal - 9 mph - 01	NT	NT	NT
frontal - 9 mph - 01	NT	NT	NT
frontal - 9 mph - 01	NT	NT	NT

Performance: Robustness

- single-axis algorithm vs. multi-axes algorithm (angle collision detection)
- (NT = No Trigger)

Crash Description type - speed - seq. #	scale factor	Desired Deploy Time (ms)	single-axis algorithm (ms)	multi-axes algorithm (ms)
30° angle - 30 mph - 01	0.1	-	not available	NT
30° angle - 30 mph - 01	0.2	-	not available	NT
30° angle - 30 mph - 01	0.3	-	not available	NT
30° angle - 30 mph - 01	0.4	-	not available	NT
30° angle - 30 mph - 01	0.5	-	not available	24
30° angle - 30 mph - 01	0.6	-	not available	23
30° angle - 30 mph - 01	0.7	-	45	23
30° angle - 30 mph - 01	0.8	-	29	22
30° angle - 30 mph - 01	0.9	-	28	22
30° angle - 30 mph - 01	1.0	36	27	21
30° angle - 30 mph - 01	1.1	-	not available	21
30° angle - 30 mph - 01	1.2	-	not available	21
30° angle - 30 mph - 01	1.3	-	not available	21
30° angle - 30 mph - 01	1.4	-	not available	19
30° angle - 30 mph - 01	1.5	-	not available	18
30° angle - 30 mph - 02	0.1	-	not available	NT
30° angle - 30 mph - 02	0.2	-	not available	NT
30° angle - 30 mph - 02	0.3	-	not available	NT
30° angle - 30 mph - 02	0.4	-	not available	NT
30° angle - 30 mph - 02	0.5	-	not available	NT
30° angle - 30 mph - 02	0.6	-	not available	NT
30° angle - 30 mph - 02	0.7	-	40	31
30° angle - 30 mph - 02	0.8	-	36	31
30° angle - 30 mph - 02	0.9	-	32	24
30° angle - 30 mph - 02	1.0	36	29	23
30° angle - 30 mph - 02	1.1	-	not available	23
30° angle - 30 mph - 02	1.2	-	not available	23
30° angle - 30 mph - 02	1.3	-	not available	23
30° angle - 30 mph - 02	1.4	-	not available	20
30° angle - 30 mph - 02	1.5	-	not available	17

Crash Description type - speed - seq. #	scale factor	Desired Deploy Time (ms)	single-axis algorithm (ms)	multi-axes algorithm (ms)
30° angle - 30 mph - 03	0.1	-	not available	NT
30° angle - 30 mph - 03	0.2	-	not available	NT
30° angle - 30 mph - 03	0.3	-	not available	NT
30° angle - 30 mph - 03	0.4	-	not available	28
30° angle - 30 mph - 03	0.5	-	not available	20
30° angle - 30 mph - 03	0.6	-	not available	18
30° angle - 30 mph - 03	0.7	-	39	17
30° angle - 30 mph - 03	0.8	-	36	16
30° angle - 30 mph - 03	0.9	-	32	14
30° angle - 30 mph - 03	1.0	36	27	14
30° angle - 30 mph - 03	1.1	-	not available	14
30° angle - 30 mph - 03	1.2	-	not available	14
30° angle - 30 mph - 03	1.3	-	not available	14
30° angle - 30 mph - 03	1.4	-	not available	13
30° angle - 30 mph - 03	1.5	-	not available	13
30° angle - 30 mph - 04	0.1	-	not available	NT
30° angle - 30 mph - 04	0.2	-	not available	NT
30° angle - 30 mph - 04	0.3	-	not available	NT
30° angle - 30 mph - 04	0.4	-	not available	NT
30° angle - 30 mph - 04	0.5	-	not available	NT
30° angle - 30 mph - 04	0.6	-	not available	21
30° angle - 30 mph - 04	0.7	-	45	19
30° angle - 30 mph - 04	0.8	-	38	18
30° angle - 30 mph - 04	0.9	-	36	15
30° angle - 30 mph - 04	1.0	36	26	14
30° angle - 30 mph - 04	1.1	-	not available	14
30° angle - 30 mph - 04	1.2	-	not available	13
30° angle - 30 mph - 04	1.3	-	not available	12
30° angle - 30 mph - 04	1.4	-	not available	12
30° angle - 30 mph - 04	1.5	-	not available	12
30° angle - 30 mph - 05	0.1	-	not available	NT
30° angle - 30 mph - 05	0.2	-	not available	NT
30° angle - 30 mph - 05	0.3	-	not available	NT
30° angle - 30 mph - 05	0.4	-	not available	NT
30° angle - 30 mph - 05	0.5	-	not available	NT
30° angle - 30 mph - 05	0.6	-	not available	23
30° angle - 30 mph - 05	0.7	-	45	21
30° angle - 30 mph - 05	0.8	-	41	19
30° angle - 30 mph - 05	0.9	-	29	19
30° angle - 30 mph - 05	1.0	36	26	18
30° angle - 30 mph - 05	1.1	-	not available	18
30° angle - 30 mph - 05	1.2	-	not available	17
30° angle - 30 mph - 05	1.3	-	not available	16
30° angle - 30 mph - 05	1.4	-	not available	13
30° angle - 30 mph - 05	1.5	-	not available	13

Crash Description type - speed - seq. #	scale factor	Desired Deploy Time (ms)	single-axis algorithm (ms)	multi-axes algorithm (ms)
30° angle - 30 mph - 06	0.1	-	not available	NT
30° angle - 30 mph - 06	0.2	-	not available	NT
30° angle - 30 mph - 06	0.3	-	not available	NT
30° angle - 30 mph - 06	0.4	-	not available	NT
30° angle - 30 mph - 06	0.5	-	not available	NT
30° angle - 30 mph - 06	0.6	-	not available	23
30° angle - 30 mph - 06	0.7	-	42	22
30° angle - 30 mph - 06	0.8	-	36	19
30° angle - 30 mph - 06	0.9	-	31	19
30° angle - 30 mph - 06	1.0	36	24	18
30° angle - 30 mph - 06	1.1	-	not available	17
30° angle - 30 mph - 06	1.2	-	not available	17
30° angle - 30 mph - 06	1.3	-	not available	17
30° angle - 30 mph - 06	1.4	-	not available	13
30° angle - 30 mph - 06	1.5	-	not available	13
30° angle - 30 mph - 07	0.1	-	not available	NT
30° angle - 30 mph - 07	0.2	-	not available	NT
30° angle - 30 mph - 07	0.3	-	not available	NT
30° angle - 30 mph - 07	0.4	-	not available	55
30° angle - 30 mph - 07	0.5	-	not available	23
30° angle - 30 mph - 07	0.6	-	not available	19
30° angle - 30 mph - 07	0.7	-	34	19
30° angle - 30 mph - 07	0.8	-	31	18
30° angle - 30 mph - 07	0.9	-	24	18
30° angle - 30 mph - 07	1.0	36	23	14
30° angle - 30 mph - 07	1.1	-	not available	14
30° angle - 30 mph - 07	1.2	-	not available	14
30° angle - 30 mph - 07	1.3	-	not available	14
30° angle - 30 mph - 07	1.4	-	not available	12
30° angle - 30 mph - 07	1.5	-	not available	12
30° angle - 30 mph - 08	0.1	-	not available	NT
30° angle - 30 mph - 08	0.2	-	not available	NT
30° angle - 30 mph - 08	0.3	-	not available	NT
30° angle - 30 mph - 08	0.4	-	not available	NT
30° angle - 30 mph - 08	0.5	-	not available	NT
30° angle - 30 mph - 08	0.6	-	not available	NT
30° angle - 30 mph - 08	0.7	-	48	NT
30° angle - 30 mph - 08	0.8	-	36	27
30° angle - 30 mph - 08	0.9	-	33	25
30° angle - 30 mph - 08	1.0	36	27	25
30° angle - 30 mph - 08	1.1	-	not available	24
30° angle - 30 mph - 08	1.2	-	not available	24
30° angle - 30 mph - 08	1.3	-	not available	23
30° angle - 30 mph - 08	1.4	-	not available	23
30° angle - 30 mph - 08	1.5	-	not available	23

Crash Description type - speed - seq. #	scale factor	Desired Deploy Time (ms)	single-axis algorithm (ms)	multi-axes algorithm (ms)
30° angle - 30 mph - 09	0.1	-	not available	NT
30° angle - 30 mph - 09	0.2	-	not available	NT
30° angle - 30 mph - 09	0.3	-	not available	NT
30° angle - 30 mph - 09	0.4	-	not available	NT
30° angle - 30 mph - 09	0.5	-	not available	NT
30° angle - 30 mph - 09	0.6	-	not available	31
30° angle - 30 mph - 09	0.7	-	46	26
30° angle - 30 mph - 09	0.8	-	42	22
30° angle - 30 mph - 09	0.9	-	33	22
30° angle - 30 mph - 09	1.0	36	28	22
30° angle - 30 mph - 09	1.1	-	not available	22
30° angle - 30 mph - 09	1.2	-	not available	19
30° angle - 30 mph - 09	1.3	-	not available	19
30° angle - 30 mph - 09	1.4	-	not available	18
30° angle - 30 mph - 09	1.5	-	not available	18
30° angle - 20 mph - 01	0.1	-	not available	NT
30° angle - 20 mph - 01	0.2	-	not available	NT
30° angle - 20 mph - 01	0.3	-	not available	NT
30° angle - 20 mph - 01	0.4	-	not available	NT
30° angle - 20 mph - 01	0.5	-	not available	NT
30° angle - 20 mph - 01	0.6	-	not available	NT
30° angle - 20 mph - 01	0.7	-	49	33
30° angle - 20 mph - 01	0.8	-	44	33
30° angle - 20 mph - 01	0.9	-	39	30
30° angle - 20 mph - 01	1.0	44	34	30
30° angle - 20 mph - 01	1.1	-	not available	30
30° angle - 20 mph - 01	1.2	-	not available	29
30° angle - 20 mph - 01	1.3	-	not available	29
30° angle - 20 mph - 01	1.4	-	not available	28
30° angle - 20 mph - 01	1.5	-	not available	28

Crash Description type - speed - seq. #	scale factor	Desired Deploy Time (ms)	single-axis algorithm (ms)	multi-axes algorithm (ms)
30° angle - 15 mph - 01	0.1	-	not available	NT
30° angle - 15 mph - 01	0.2	-	not available	NT
30° angle - 15 mph - 01	0.3	-	not available	NT
30° angle - 15 mph - 01	0.4	-	not available	NT
30° angle - 15 mph - 01	0.5	-	not available	NT
30° angle - 15 mph - 01	0.6	-	not available	NT
30° angle - 15 mph - 01	0.7	-	not available	NT
30° angle - 15 mph - 01	0.8	-	not available	NT
30° angle - 15 mph - 01	0.9	-	not available	NT
30° angle - 15 mph - 01	1.0	NT	NT	NT
30° angle - 15 mph - 01	1.1	-	80	NT
30° angle - 15 mph - 01	1.2	-	33	NT
30° angle - 15 mph - 01	1.3	-	33	NT
30° angle - 15 mph - 01	1.4	-	33	NT
30° angle - 15 mph - 01	1.5	-	32	NT
30° angle - 12 mph - 01	0.1	-	not available	NT
30° angle - 12 mph - 01	0.2	-	not available	NT
30° angle - 12 mph - 01	0.3	-	not available	NT
30° angle - 12 mph - 01	0.4	-	not available	NT
30° angle - 12 mph - 01	0.5	-	not available	NT
30° angle - 12 mph - 01	0.6	-	not available	NT
30° angle - 12 mph - 01	0.7	-	not available	NT
30° angle - 12 mph - 01	0.8	-	not available	NT
30° angle - 12 mph - 01	0.9	-	not available	NT
30° angle - 12 mph - 01	1.0	NT	NT	NT
30° angle - 12 mph - 01	1.1	-	NT	NT
30° angle - 12 mph - 01	1.2	-	NT	NT
30° angle - 12 mph - 01	1.3	-	NT	NT
30° angle - 12 mph - 01	1.4	-	NT	NT
30° angle - 12 mph - 01	1.5	-	69	NT
30° angle - 10 mph - 01	0.1	-	not available	NT
30° angle - 10 mph - 01	0.2	-	not available	NT
30° angle - 10 mph - 01	0.3	-	not available	NT
30° angle - 10 mph - 01	0.4	-	not available	NT
30° angle - 10 mph - 01	0.5	-	not available	NT
30° angle - 10 mph - 01	0.6	-	not available	NT
30° angle - 10 mph - 01	0.7	-	not available	NT
30° angle - 10 mph - 01	0.8	-	not available	NT
30° angle - 10 mph - 01	0.9	-	not available	NT
30° angle - 10 mph - 01	1.0	NT	NT	NT
30° angle - 10 mph - 01	1.1	-	NT	NT
30° angle - 10 mph - 01	1.2	-	NT	NT
30° angle - 10 mph - 01	1.3	-	34	NT
30° angle - 10 mph - 01	1.4	-	34	NT
30° angle - 10 mph - 01	1.5	-	33	NT

Crash Description type - speed - seq. #	scale factor	Desired Deploy Time (ms)	single-axis algorithm (ms)	multi-axes algorithm (ms)
Frontal - 9 mph - 01	0.1	-	not available	NT
Frontal - 9 mph - 01	0.2	-	not available	NT
Frontal - 9 mph - 01	0.3	-	not available	NT
Frontal - 9 mph - 01	0.4	-	not available	NT
Frontal - 9 mph - 01	0.5	-	not available	NT
Frontal - 9 mph - 01	0.6	-	not available	NT
Frontal - 9 mph - 01	0.7	-	not available	NT
Frontal - 9 mph - 01	0.8	-	not available	NT
Frontal - 9 mph - 01	0.9	-	not available	NT
Frontal - 9 mph - 01	1.0	NT	NT	NT
Frontal - 9 mph - 01	1.1	-	NT	NT
Frontal - 9 mph - 01	1.2	-	NT	NT
Frontal - 9 mph - 01	1.3	-	29	NT
Frontal - 9 mph - 01	1.4	-	29	NT
Frontal - 9 mph - 01	1.5	-	28	NT
Frontal - 9 mph - 02	0.1	-	not available	NT
Frontal - 9 mph - 02	0.2	-	not available	NT
Frontal - 9 mph - 02	0.3	-	not available	NT
Frontal - 9 mph - 02	0.4	-	not available	NT
Frontal - 9 mph - 02	0.5	-	not available	NT
Frontal - 9 mph - 02	0.6	-	not available	NT
Frontal - 9 mph - 02	0.7	-	not available	NT
Frontal - 9 mph - 02	0.8	-	not available	NT
Frontal - 9 mph - 02	0.9	-	not available	NT
Frontal - 9 mph - 02	1.0	NT	NT	NT
Frontal - 9 mph - 02	1.1	-	NT	NT
Frontal - 9 mph - 02	1.2	-	NT	NT
Frontal - 9 mph - 02	1.3	-	57	NT
Frontal - 9 mph - 02	1.4	-	56	NT
Frontal - 9 mph - 02	1.5	-	51	NT
Frontal - 9 mph - 03	0.1	-	not available	NT
Frontal - 9 mph - 03	0.2	-	not available	NT
Frontal - 9 mph - 03	0.3	-	not available	NT
Frontal - 9 mph - 03	0.4	-	not available	NT
Frontal - 9 mph - 03	0.5	-	not available	NT
Frontal - 9 mph - 03	0.6	-	not available	NT
Frontal - 9 mph - 03	0.7	-	not available	NT
Frontal - 9 mph - 03	0.8	-	not available	NT
Frontal - 9 mph - 03	0.9	-	not available	NT
Frontal - 9 mph - 03	1.0	NT	NT	NT
Frontal - 9 mph - 03	1.1	-	NT	NT
Frontal - 9 mph - 03	1.2	-	NT	NT
Frontal - 9 mph - 03	1.3	-	41	NT
Frontal - 9 mph - 03	1.4	-	39	NT
Frontal - 9 mph - 03	1.5	-	39	NT

Crash Description type - speed - seq. #	scale factor	Desired Deploy Time (ms)	single-axis algorithm (ms)	multi-axes algorithm (ms)
Frontal - 9 mph - 04	0.1	-	not available	NT
Frontal - 9 mph - 04	0.2	-	not available	NT
Frontal - 9 mph - 04	0.3	-	not available	NT
Frontal - 9 mph - 04	0.4	-	not available	NT
Frontal - 9 mph - 04	0.5	-	not available	NT
Frontal - 9 mph - 04	0.6	-	not available	NT
Frontal - 9 mph - 04	0.7	-	not available	NT
Frontal - 9 mph - 04	0.8	-	not available	NT
Frontal - 9 mph - 04	0.9	-	not available	NT
Frontal - 9 mph - 04	1.0	NT	NT	NT
Frontal - 9 mph - 04	1.1	-	NT	NT
Frontal - 9 mph - 04	1.2	-	67	NT
Frontal - 9 mph - 04	1.3	-	63	NT
Frontal - 9 mph - 04	1.4	-	63	NT
Frontal - 9 mph - 04	1.5	-	63	NT
Frontal - 9 mph - 05	0.1	-	not available	NT
Frontal - 9 mph - 05	0.2	-	not available	NT
Frontal - 9 mph - 05	0.3	-	not available	NT
Frontal - 9 mph - 05	0.4	-	not available	NT
Frontal - 9 mph - 05	0.5	-	not available	NT
Frontal - 9 mph - 05	0.6	-	not available	NT
Frontal - 9 mph - 05	0.7	-	not available	NT
Frontal - 9 mph - 05	0.8	-	not available	NT
Frontal - 9 mph - 05	0.9	-	not available	NT
Frontal - 9 mph - 05	1.0	NT	NT	NT
Frontal - 9 mph - 05	1.1	-	NT	NT
Frontal - 9 mph - 05	1.2	-	NT	NT
Frontal - 9 mph - 05	1.3	-	40	NT
Frontal - 9 mph - 05	1.4	-	38	NT
Frontal - 9 mph - 05	1.5	-	37	NT

Crash Description type - speed - seq. #	scale factor	Desired Deploy Time (ms)	single-axis algorithm (ms)	multi-axes algorithm (ms)
Pole - 10 mph - 01	0.1	-	not available	NT
Pole - 10 mph - 01	0.2	-	not available	NT
Pole - 10 mph - 01	0.3	-	not available	NT
Pole - 10 mph - 01	0.4	-	not available	NT
Pole - 10 mph - 01	0.5	-	not available	NT
Pole - 10 mph - 01	0.6	-	not available	NT
Pole - 10 mph - 01	0.7	-	not available	NT
Pole - 10 mph - 01	0.8	-	not available	NT
Pole - 10 mph - 01	0.9	-	not available	NT
Pole - 10 mph - 01	1.0	NT	NT	NT
Pole - 10 mph - 01	1.1	-	NT	NT
Pole - 10 mph - 01	1.2	-	NT	NT
Pole - 10 mph - 01	1.3	-	NT	NT
Pole - 10 mph - 01	1.4	-	NT	NT
Pole - 10 mph - 01	1.5	-	NT	NT
Pole - 14 mph - 01	0.1	-	not available	NT
Pole - 14 mph - 01	0.2	-	not available	NT
Pole - 14 mph - 01	0.3	-	not available	NT
Pole - 14 mph - 01	0.4	-	not available	NT
Pole - 14 mph - 01	0.5	-	not available	NT
Pole - 14 mph - 01	0.6	-	not available	NT
Pole - 14 mph - 01	0.7	-	not available	NT
Pole - 14 mph - 01	0.8	-	not available	NT
Pole - 14 mph - 01	0.9	-	not available	NT
Pole - 14 mph - 01	1.0	NT	NT	NT
Pole - 14 mph - 01	1.1	-	NT	NT
Pole - 14 mph - 01	1.2	-	NT	NT
Pole - 14 mph - 01	1.3	-	81	NT
Pole - 14 mph - 01	1.4	-	80	NT
Pole - 14 mph - 01	1.5	-	80	NT
Pole - 14 mph - 02	0.1	-	not available	NT
Pole - 14 mph - 02	0.2	-	not available	NT
Pole - 14 mph - 02	0.3	-	not available	NT
Pole - 14 mph - 02	0.4	-	not available	NT
Pole - 14 mph - 02	0.5	-	not available	NT
Pole - 14 mph - 02	0.6	-	not available	NT
Pole - 14 mph - 02	0.7	-	not available	NT
Pole - 14 mph - 02	0.8	-	not available	NT
Pole - 14 mph - 02	0.9	-	not available	NT
Pole - 14 mph - 02	1.0	NT	NT	NT
Pole - 14 mph - 02	1.1	-	NT	NT
Pole - 14 mph - 02	1.2	-	88	NT
Pole - 14 mph - 02	1.3	-	75	NT
Pole - 14 mph - 02	1.4	-	75	NT
Pole - 14 mph - 02	1.5	-	75	NT

References

[1] Jon P. Kelley, "Sensing Considerations and Tradeoffs for Single Point Sensing", *SAE Technical Paper Series - 932916*, 1993, p. 1.

[2] Ansaf I. Alrabady, Syed M. Mahmud, "Development of a Decision Making Algorithm for Airbag Control", *IEEE Instrumentation and Measurement Technology Conference 1993*, p. 82.

[3] Stephen. Goch, Thomas. Krause, Allen Gillespie, "Inflatable Restraint System Design Considerations". *SAE International Congress and Exposition, 1990*, p. 23.

[4] Ibid, Goch et al., p. 25.

[5] Ibid, Goch et al., p. 27.

[6] Ibid, Alrabady et al., p. 83.

[7] Motomi Iyoda, "Occupant Restraint System Actuated by a Simple Operation Using a Feature Value", *European Patent - EP 0 709 255 A1*, May 1, 1996, p. 2.

[8] Jung-Woo Ohm, "Method for Judging Collision with Three Directional Accelerative Signals and Apparatus for Performing the Same", *European Patent - EP 0 709 256 A1*, May 1, 1996, p. 4.

[9] Alfons Woehrl, Peter Hora, Guenter Fendt, "Apparatus for Triggering a Passive Safety Device", *U.S. Patent - 5,173,614*, December 22, 1992, p. 1.

[10] Ibid, Iyoda, Motomi. p. 2.

[11] Kyeong-Seon Chae, "Vehicle Airbag Deployment Control Apparatus and Method", *European Patent - EP 0 709 257 A1*, May 1, 1996, P. 3.

[12] Ibid, Iyoda, Motomi. p. 13.

[13] Ibid, Ohm, Jung-Woo. P. 7.

[14] K. H. Yang, B. K. Latouf, A. I. King, "Computer Simulation of Occupant Neck Response to Airbag Deployment in Frontal Impacts", *Journal of Biomechanical Engineering, Transactions of the ASME Vol. 114 issue 3*, August, 1992, p. 329.

[15] Hans C. Ohanian, *Physics:Conservation of Energy*, 2nd Edition (New York, W. W. Norton & Company: 1989) p. 186.

[16] Ibid, Yang. K. H., p. 327.

[17] Adrian K. Lund, Susan A. Fuerguson, Michael R. Powell, "Injuries Sustained by Air Bag Protected Drivers", *SAE International Congress & Exposition, 1996*, p. 45.

[18] Jiamaw Doong, James C. Cheng, "Computer Simulations for Frontal Impact", *Computers in Engineering -1994 volume 2, ASME 1994*, p. 601.

[19] Hans. Spies, Peter Hora, Günter Fendt, Kenneth Francis, Helmut Steurer, "Device for Triggering a Passive Safety System", *U.S. Patent - 5,424,583*, June 13, 1995, p. 12.

[20] Ibid, Doong et al., p. 601.

[21] Ibid, Iyoda, Motomi. p. 11.

[22] Ibid, Doong et al., p. 603.

Additional Readings

Aboud, G.M., Repp, J.H., Strola, C.L., Husby, H.S., "Testing for Inadvertent Airbag Deployment", *Automotive Engineering, Vol. 102 n 3*, March, 1994.

Allen, Jace L. "Power-Rate Crash Sensing Method for Safety Device Actuation", *SAE International Congress and Exposition, SAE Technical Paper Series - 920478*, 1992.

Alrabady, Ansaf I., Mahmud, Syed M. "New Decision Making Algorithm for Airbag Control". *IEEE Transactions on Vehicle Technology, Vol 44 n 3*, August 1995.

Bergfried, Dietrich., Nitschke, Werner., Rutz, Martin. "Airbag Control Modules - Performance and Reliability". *Proceedings - Society of Automotive Engineers issue P-260 - 92C054*, 1992.

Breed, David S., Sanders, Thomas W., Castelli, Vittorio. "Critique of Single Point Sensing". *SAE International Congress and Exposition, SAE Technical Paper Series - 920124*, 1992.

Breed, David S., Sanders, Thomas W., Castelli, Vittorio. "Complete Frontal Crach Sensor System - 1". *Frontal Impact Protection: Seat Belts and Airbags SAE Special Publications n 947*, 1993

Diller, Robert W. "Electronic Sensing of Automobile Crashes for Airbag Deployment", *SAE International Congress and Exposition*, 1991.

Gioutsos, Tony. "A Predictive Based Algorithm for Actuation of an Airbag". *SAE International Congress and Exposition, SAE Technical Paper Series - 920479*, 1992.

Haertl, Alfons., Vogt, Richard., Huber, Anton S. "Airbag System - Their Permanent Monitoring and Its Meaning to the User". *SAE Transactions Vol. 99*, September 6, 1990.

Liu, John Kuo-Hsiao. "SIR Sensor Closure Time Prediction For Frontal Impact Using Full Vehicle Finite Element Analysis". *Frontal Impact Protection: Seat Belts and Airbags SAE Special Publications n 947*, 1993.

Mahon, Geoffrey L., Hensler, Ralph L. "Tradeoffs Encountered in Evaluating Crash Sensing Systems". *SAE International Congress and Exposition*, 1993.

Acknowledgement

I would like to thank my parents for all of their support and encouragement.

I would also like to thank my supervisor Jon P. Kelley for his help and guidance. In addition, the engineers from the SIR team including Bill Galles, Shyam Potti, and Chris Caruso devoted both their time and energy to help me complete the project.

I would like to thank Professor Martin Schmidt, my academic thesis advisor, for his feedback, encouragement, and patience.

Lastly, I like to thank Marilyn Shen for her support and faith.